



HAL
open science

A deterministic approximation method in shape optimization under random uncertainties

Grégoire Allaire, Charles Dapogny

► **To cite this version:**

Grégoire Allaire, Charles Dapogny. A deterministic approximation method in shape optimization under random uncertainties. *SMAI Journal of Computational Mathematics*, 2015, 1, pp.83-143. 10.5802/smai-jcm.5 . hal-01160256

HAL Id: hal-01160256

<https://hal.science/hal-01160256>

Submitted on 9 Jun 2015

HAL is a multi-disciplinary open access archive for the deposit and dissemination of scientific research documents, whether they are published or not. The documents may come from teaching and research institutions in France or abroad, or from public or private research centers.

L'archive ouverte pluridisciplinaire **HAL**, est destinée au dépôt et à la diffusion de documents scientifiques de niveau recherche, publiés ou non, émanant des établissements d'enseignement et de recherche français ou étrangers, des laboratoires publics ou privés.

A DETERMINISTIC APPROXIMATION METHOD IN SHAPE OPTIMIZATION UNDER RANDOM UNCERTAINTIES

G. ALLAIRE¹, C. DAPOGNY²

ABSTRACT. This paper is concerned with the treatment of uncertainties in shape optimization. We consider uncertainties in the loadings, the material properties, the geometry and the vibration frequency, both in the parametric and geometric optimization setting. We minimize objective functions which are mean values, variances or failure probabilities of standard cost functions under random uncertainties. By assuming that the uncertainties are small and generated by a finite number N of random variables, and using first- or second-order Taylor expansions, we propose a deterministic approach to optimize approximate objective functions. The computational cost is similar to that of a multiple load problems where the number of loads is N . We demonstrate the effectiveness of our approach on various parametric and geometric optimization problems in two space dimensions.

¹ *Centre de Mathématiques Appliquées (UMR 7641), École Polytechnique 91128 Palaiseau, France.*

² *Laboratoire Jean Kuntzmann, CNRS, Université Joseph Fourier, Grenoble INP, Université Pierre Mendès France, BP 53, 38041 Grenoble Cedex 9, France.*

CONTENTS

1. Introduction	2
2. Formal presentation of the main ideas	4
2.1. Minimization of the mean value, or of a higher-order moment, of the cost function	5
2.2. Minimization of the failure probability	7
2.3. Computational cost and the possible use of adjoint states	8
2.4. A few words on the finite-sum structure for perturbations	8
3. Random parametric optimization	9
3.1. A model problem	9
3.2. Uncertainty over the body forces in parametric optimization	10
3.3. Uncertainties over the elastic material's properties	18
4. Random geometric optimization	22
4.1. Description of the setting	22
4.2. Random perturbations over the body forces in shape optimization	24
4.3. Random perturbations over the material's properties in shape optimization	27
4.4. Random optimization in frequency response	28
4.5. Shape optimization under random geometric uncertainties	29
5. Numerical Illustrations	34
5.1. Examples in parametric optimization	34
5.2. Examples in geometric optimization	36
Appendix A. On second-order shape derivatives	48
A.1. Second-order shape derivatives	48
A.2. Proof of Theorem 18	48
References	51

1. INTRODUCTION

Over the last decades, shape and topology optimization has proved to be a reliable tool in the design of mechanical structures, using only very general specifications like design space, applied loads, material properties, etc... Unfortunately, in most concrete situations, these data are imperfectly known, and optimal shapes may exhibit a dramatic dependence on these parameters. Here are two manifestations of this phenomenon.

- It is a well-known result from Michell truss theory [39] that, for a given applied load, the optimal truss exhibit two orthogonal systems of bars which are aligned with the principal stress directions. Variations in the imposed loads may have a strong impact on these directions, thus on the geometry of the optimal design (see also [27] for a recent contribution on this problem).
- Many optimal compliant mechanisms feature very small hinges [43], [5] that could be broken during their manufacturing process. Therefore, small variations in the final manufactured design can completely ruined their optimality.

For these reasons, it seems necessary to take into account the effects of ‘small’ uncertainties plaguing the physical data (and by this, we include the geometry of shapes itself) in the formulation of structural optimization problems. Depending on the available informations, two main classes of methods can be considered to achieve this purpose.

- When no information is available on the uncertainties but for a maximum bound on their amplitude, several authors worked out a ‘worst-case’ design approach [2, 7, 15, 26] and references therein. In a nutshell, the idea is to minimize the worst or maximal value of the cost function over all potential perturbations. The main drawback of this approach is that it may be too pessimistic, leading to structures with poor nominal performances.
- When some statistical information is available for the uncertain data (for instance, moments of the perturbations have been reconstructed from a set of sample data, or more complicated information has been obtained by statistical inference), one may use a probabilistic description of the uncertain data. Then, it is possible to minimize the mean value and the variance of the resulting perturbed cost function. The main drawback of this approach is its high computational cost in most situations.

In this paper we focus on the latter point of view, contrary to our previous work [2] which was devoted to the worst-case design approach. Nevertheless, both works are linked by our quest of computationally cheap algorithms using approximations based on an assumption of ‘small’ uncertainties. Both works share a similar mechanical setting, namely that of mechanical structures submitted to the linear elasticity regime. The considered shapes are optimized with respect to a given cost criterion (e.g. the compliance), which depends on their geometry, and on small, uncertain parameters. In the sequel, the uncertain parameters will be either the applied loads, the material elasticity coefficients, the geometry of shapes itself, or the imposed frequency of the vibrating loads.

In this context, we study the minimization of two classes of objective functions: on the one hand, moments of the cost function evaluating the performances of shapes are considered - e.g. its mean value or its standard deviation. On the other hand, we investigate failure probabilities - that is, the probability that the cost exceeds a given threshold, above which the situation is deemed unsafe.

We derive *deterministic* approximations to these functionals, which are also computationally tractable. Our approximations rely on two key ingredients. First, assuming that the uncertainties are ‘small’, we perform a first- or second-order Taylor expansion of the cost criterion with respect to these uncertainties. This truncated Taylor expansion has moments or excess probabilities that can be computed explicitly. Second, we systematically assume that the uncertain data show up as finite sums of deterministic data functions weighted by random variables. This is clearly a natural assumption that arises, for example, by spatial discretization of a distributed random field (see Section 2.4 for more details). But in many practical cases it is not a restriction as, for example, the imposed loads are very often a finite sum of point forces.

The proposed approximations are proved to be consistent with their exact counterparts in most situations. The resulting deterministic functionals can then be minimized owing to standard tools from shape optimization, for a moderate computational cost. More precisely, the number of instances of the state equation to be solved is of the order of the number of independent random variables in the definition of uncertainties.

The question of influence of random uncertainties has already aroused much interest in the shape optimization community - see [34] for an overview. In [19], the authors consider uncertain loads, and assume cost functions that are sum of linear and quadratic terms functions of the elastic displacement. They rely on the hypothesis of multiple load scenarii, which are combinations of a given set of individual loads. In [25], uncertain loads are modelled as sums of deterministic loads, whose coefficients are uncorrelated random variables. The mean value and standard deviation of the compliance are considered as objective functions, and the authors take advantage of the quadratic structure of the compliance as a function of loads to derive explicit and deterministic objective functions. This approach is generalized in [21] to the case of quadratic cost functions of the elastic displacement, and uncertain loads described as general random fields. In particular, it turns out that, in such case, the mean value of the cost function depends solely on the correlation function of the loads.

In [8], stochastic finite element methods are introduced for the numerical simulation of partial differential equations involving random coefficients. These methods are used in [33] to deal with a diffusion problem with random coefficients and source terms in a purely probabilistic setting. Let us also mention the recent work [16] which provides an efficient and low-cost methodology for computing solutions of parametric equations in high dimensions.

In [13], the authors deal with shape optimization in the context of linear elasticity, under uncertain loads and material parameters. A Karhunen-Loève expansion of the uncertain data is performed; the objective function whose minimization is at stake, which is a moment of the cost function (mean value, standard deviation), is discretized by using Gauss-type quadrature formulae, which essentially transform it into a weighted average of the cost function under several fixed, deterministic sets of data. In [14], the authors elaborate on this idea to address the problem of shape optimization under geometric uncertainties. The geometric uncertainties acting on a shape Ω are represented by normal vector fields of ‘small amplitude’, defined on the boundary $\partial\Omega$, and the correlation matrix of these uncertainties is assumed to be known. The additional complexity is that, in this case, the objective function is a weighted sum of the cost function taken at different shapes, which are perturbations of the actual one. This induces some difficulties in the derivation of the shape sensitivities which are evaluated on perturbed shapes but have to be pulled backed to the reference shape.

The technique proposed in [40] is rather similar and is applied in the context of geometric uncertainties in aerodynamic design. Here also, the authors discretize the objective function at stake, which is a probabilistic integral of the cost function, by using Gauss-type quadrature formulae. In this work, the calculation of the shape gradient of the objective function is easier than in [14], since the geometry of shapes is parameterized by a rather small number of physical parameters. On the other hand, the authors improve the accuracy and computational efficiency of their strategy with a ‘smart’ construction procedure of the Karhunen-Loève expansion of the uncertain data and an adaptive-grid method for the evaluation of the probabilistic integrals. In [41], the same authors consider failure probability constraints by using the First-Order Reliability Method (see the description in Section 2.2 below).

Eventually, let us mention the work [30] which also deals with geometric uncertainties in the context of the SIMP method. The problem of modeling the uncertainties is formulated in terms of the filtering technology, and moments of cost functions are considered as objective functions, which are approximated by performing Taylor approximations of the cost function and of the state with respect to the uncertain variables - an idea which has a lot to do with the method at stake in the present paper.

This paper is organized as follows. In Section 2 we present our main ideas in an abstract, simplified and formal setting. As mentioned above, there are two key ingredients. First, a second-order Taylor expansion of the cost function is performed, under a smallness assumption on the uncertainties. Second, the uncertainties are restricted to a finite sum of N uncorrelated random variables. Thanks to these assumptions, we deduce approximate functionals for the mean value, the variance or the failure probability of general cost functions. The cost of evaluating these approximate functionals is of the order of N solutions of the state equation, or even independent of N in the case of the failure probability. Then, this abstract setting is applied in more details and with mathematical rigor in the next two sections. Section 3 is devoted to parametric optimization, a framework which is simple enough so that all proofs can be done completely without too much technical complexity. We also give the formulas for the derivatives of these approximate functionals in terms of additional adjoints. The computational cost for these derivatives is at most $2(N + 1)$ solutions

of a partial differential equation. Section 4 is concerned with geometric optimization, which is much more involved from a technical point of view. The results are very similar to those of the previous section so we can take advantage of this prior work to be more sketchy in the proofs and avoid too many technicalities (some of them can be found in the Appendix). Eventually, many numerical experiments are displayed in Section 5, in order to demonstrate the effectiveness of the proposed approach. In particular we make comparisons with our linearized worst case design approach as proposed in [2] (see Remark 19).

2. FORMAL PRESENTATION OF THE MAIN IDEAS

The purpose of this section is to present the main ideas of this paper in a common, simplified and formal abstract framework. Sections 3 and 4 will apply in a rigorous mathematical framework this rough sketch to the thickness optimization setting and the geometric one, respectively.

Let \mathcal{H} be a set of *admissible designs*, among which the ‘best’ element is sought, and \mathcal{P} be a Banach space of *data* characterizing the situation under consideration. The performance of a design $h \in \mathcal{H}$ under data $f \in \mathcal{P}$ is evaluated in terms of a *cost function* $\mathcal{C}(f, u_{h,f})$, which depends on h via the solution $u_{h,f}$ of the state equation:

$$(2.1) \quad \mathcal{A}(h)u_{h,f} = b(f).$$

In our applications, h stands for the thickness of a plate of given cross-section or for the shape of a mechanical domain, $\mathcal{A}(h)$ is the (design-dependent) linearized elasticity operator (a system of partial differential equations) and the data f are typically (yet not exclusively) applied body forces or surface loads. The typical problem of optimal design is to minimize the cost function over all admissible designs

$$\inf_{h \in \mathcal{H}} \mathcal{C}(f, u_{h,f}).$$

We are interested in the case when f is not known with great precision. Typically, it is the sum of a known mean value $f_0 \in \mathcal{P}$ and of ‘small’, uncertain perturbations \hat{f} , i.e. is of the form:

$$(2.2) \quad f(\omega) = f_0 + \hat{f}(\omega),$$

where ω is an event, i.e. an element of an abstract probability space $(\mathcal{O}, \mathcal{F}, \mathbb{P})$, and $\hat{f}: \mathcal{O} \rightarrow \mathcal{P}$ is ‘small’ in a sense to be made precise later on. There are several modelling issues about the uncertainties \hat{f} .

- In the first place, we assume that the uncertainties \hat{f} are independent of the design h itself. This is not always the case in some physical situations. For example, in the context of linear elastic structures, the random body forces \hat{f} may be caused by random thermal fluctuations which by thermal expansion induce design-dependent uncertain loads. For simplicity we ignore such influence of the design on \hat{f} , although it could be taken into account in our theoretical framework without any additional difficulty (except more tedious calculations).
- On a different note, there are several ways of understanding the ‘smallness’ of perturbations. From this point of view the choice of an adequate functional space for \hat{f} is crucial. The simplest and most intuitive possibility is to consider \hat{f} as an element in $L^\infty(\mathcal{O}, \mathcal{P})$. Assuming that \hat{f} is small in the norm of this space (i.e. that $\|\hat{f}\|_{L^\infty(\mathcal{O}, \mathcal{P})} < \varepsilon$ for small $\varepsilon > 0$) amounts to enforce that every realization $\hat{f}(\omega)$ of \hat{f} is small in \mathcal{P} (i.e. $\|\hat{f}(\omega)\|_{\mathcal{P}} < \varepsilon$ almost surely). Another choice is to assume that \hat{f} belongs to $L^p(\mathcal{O}, \mathcal{P})$ for a given $p < \infty$. Being small in this space does not impose that (almost) every realization is small but that, in ‘average’, ‘most’ of the realizations $\hat{f}(\omega)$ are small. This last setting is interesting in practice if one is interested in large but rare enough perturbations (see Remark 13 for further comments on this issue). Furthermore, the mathematical analysis may require different choices of the functional spaces for different type of results (see Remark 1 for some hints in this direction).

For practical purposes, we shall assume that \hat{f} can be written as a finite sum

$$(2.3) \quad \forall \omega \in \mathcal{O}, \quad \hat{f}(\omega) = \sum_{i=1}^N f_i \xi_i(\omega),$$

where $f_1, \dots, f_N \in \mathcal{P}$ are ‘small’, deterministic data functions, and ξ_1, \dots, ξ_N are random variables, whose joint first and second order statistics are known. Without loss of generality, we will often assume that the ξ_i are uncorrelated, centered and normalized, i.e.

$$(2.4) \quad \int_{\mathcal{O}} \xi_i \mathbb{P}(d\omega) = 0, \quad \int_{\mathcal{O}} \xi_i \xi_j \mathbb{P}(d\omega) = \delta_{i,j}, \quad i, j = 1, \dots, N,$$

where $\delta_{i,j}$ stands for the Kronecker delta function. This assumption is admittedly restrictive, and the reasons legitimating it - or the mathematical tools involved to approximate the actual perturbation \widehat{f} by one of the type (2.3) - may vary from one situation to another; see Section 2.4, and the examples in Section 5 for more comments on this issue.

The main goal of this paper is to study deterministic approximations of two classes of objective functions of the design h .

- The first category is concerned with averaged objective functions, where the outputs of the random uncertainties are averaged with respect to the probability measure \mathbb{P} . For example, given a cost function $\mathcal{C}(f, u_{h,f})$, we optimize its mean value or *expectation* $\mathcal{M}(h)$, defined by

$$(2.5) \quad \mathcal{M}(h) = \int_{\mathcal{O}} \mathcal{C}(f(\omega), u_{h,f(\omega)}) \mathbb{P}(d\omega),$$

or a higher-order moment of \mathcal{C} such as its *variance* $\mathcal{V}(h)$:

$$(2.6) \quad \mathcal{V}(h) = \int_{\mathcal{O}} \left(\mathcal{C}(f(\omega), u_{h,f(\omega)}) - \mathcal{M}(h) \right)^2 \mathbb{P}(d\omega).$$

- The second category falls into the framework of *reliability analysis*: one is interested in minimizing a so-called *failure probability*. For instance, assuming that $\alpha \in \mathbb{R}$ is the largest ‘safe’ value of the cost $\mathcal{C}(h, u_{h,f})$ of a design h , we minimize the functional $\mathcal{P}(h)$, defined as

$$\mathcal{P}(h) = \mathbb{P} \left(\{ \omega \in \mathcal{O}, \text{ such that } \mathcal{C}(f(\omega), u_{h,f(\omega)}) > \alpha \} \right).$$

Minimizing directly these objective functions, $\mathcal{M}(h)$, $\mathcal{V}(h)$, or $\mathcal{P}(h)$, is usually too expensive from a computational point of view. Therefore we propose an approximation process which is based on two key ingredients.

- (1) First, taking advantage of a smallness assumption on the uncertainties \widehat{f} , we perform a Taylor expansion of the considered cost functions with respect to the perturbed parameters (second-order for $\mathcal{M}(h)$ and $\mathcal{V}(h)$, first-order for $\mathcal{P}(h)$).
- (2) Inserting the particular structure (2.3) of the uncertain data \widehat{f} in this truncation yields approximate cost functions which depend linearly or quadratically on the random variables ξ_1, \dots, ξ_N . This leads to a simple, deterministic approximation of the objective functions.

The next two subsections explain this approach for the two classes of objective functions.

2.1. Minimization of the mean value, or of a higher-order moment, of the cost function.

Notations. For a smooth function $J(f)$, we write its second-order Taylor expansion

$$J(f_0 + \widehat{f}) \approx J(f_0) + J^1(f_0)(\widehat{f}) + \frac{1}{2} J^2(f_0)(\widehat{f}, \widehat{f}),$$

where $J^1(f_0) = J'(f_0)$ is the first-order derivative and $J^2(f_0) = J''(f_0)$ the second-order one, evaluated at f_0 . Furthermore, the map $\widehat{f} \rightarrow J^1(f_0)(\widehat{f})$ is linear and $\widehat{f} \rightarrow J^2(f_0)(\widehat{f}, \widehat{f})$ is quadratic.

Let us focus first on the problem of minimizing the mean value $\mathcal{M}(h)$ of the cost function \mathcal{C} over the uncertainties $\omega \in \mathcal{O}$. As previously said, the first step is to perform a second-order Taylor expansion of the cost function $f \mapsto \mathcal{C}(f, u_{h,f})$ around the mean value f_0 of f . A second-order approximation of the solution of the state equation (2.1) is

$$u_{h,f_0+\widehat{f}} \approx u_h + u_h^1(\widehat{f}) + \frac{1}{2} u_h^2(\widehat{f}, \widehat{f}),$$

where the first- and second-order derivatives $u_h^1(\hat{f}) := \frac{\partial u_{h,f}}{\partial f} \Big|_{f=f_0}(\hat{f})$ and $u_h^2(\hat{f}, \hat{f}) := \frac{\partial^2 u_{h,f}}{\partial f^2} \Big|_{f=f_0}(\hat{f}, \hat{f})$ of the state function are respectively solution to:

$$\mathcal{A}(h)u_h^1(\hat{f}) = \frac{\partial b}{\partial f}(f_0)(\hat{f}), \quad \mathcal{A}(h)u_h^2(\hat{f}, \hat{f}) = \frac{\partial^2 b}{\partial f^2}(f_0)(\hat{f}, \hat{f}).$$

Then, by the chain-rule lemma we deduce

$$(2.7) \quad \mathcal{C}(f_0 + \hat{f}, u_{h, f_0 + \hat{f}}) \approx \mathcal{C}(f_0, u_h) + \frac{\partial \mathcal{C}}{\partial f}(f_0, u_h)(\hat{f}) + \frac{\partial \mathcal{C}}{\partial u}(f_0, u_h)(u_h^1(\hat{f})) \\ + \frac{1}{2} \left(\frac{\partial^2 \mathcal{C}}{\partial f^2}(f_0, u_h)(\hat{f}, \hat{f}) + 2 \frac{\partial^2 \mathcal{C}}{\partial f \partial u}(f_0, u_h)(\hat{f}, u_h^1(\hat{f})) + \frac{\partial^2 \mathcal{C}}{\partial u^2}(f_0, u_h)(u_h^1(\hat{f}), u_h^1(\hat{f})) + \frac{\partial \mathcal{C}}{\partial u}(f_0, u_h)(u_h^2(\hat{f}, \hat{f})) \right),$$

where $u_h = u_{h, f_0}$ denotes the unperturbed state.

The second step is to replace $\mathcal{C}(f, u_{h,f})$ by its approximation in the expected value (2.5) and to use the finite-sum assumption (2.4) on the uncertainties \hat{f} . Taking the mean value of both sides in (2.7), and using the fact that \hat{f} depends on N uncorrelated, centered and normalized random variables $\xi = (\xi_1, \dots, \xi_N)$, we obtain the *approximate mean value function* $\widetilde{\mathcal{M}}(h)$ defined by:

$$(2.8) \quad \mathcal{M}(h) \approx \widetilde{\mathcal{M}}(h) = \mathcal{C}(f_0, u_h) + \frac{1}{2} \sum_{i=1}^N \frac{\partial^2 \mathcal{C}}{\partial f^2}(f_0, u_h)(f_i, f_i) + \sum_{i=1}^N \frac{\partial^2 \mathcal{C}}{\partial f \partial u}(f_0, u_h)(f_i, u_{h,i}^1) \\ + \frac{1}{2} \sum_{i=1}^N \frac{\partial^2 \mathcal{C}}{\partial u^2}(f_0, u_h)(u_{h,i}^1, u_{h,i}^1) + \frac{1}{2} \frac{\partial \mathcal{C}}{\partial u}(f_0, u_h)(u_h^2),$$

where the reduced sensitivities $u_{h,i}^1$, for $i = 1, \dots, N$, and u_h^2 are the solutions to the respective systems:

$$\mathcal{A}(h)u_{h,i}^1 = \frac{\partial b}{\partial f}(f_0)(f_i), \quad \mathcal{A}(h)u_h^2 = \sum_{i=1}^N \frac{\partial^2 b}{\partial f^2}(f_0)(f_i, f_i).$$

Note that u_h^2 is different from $u_h^2(\hat{f}, \hat{f})$ and that we do not need to evaluate the $N \times N$ entries $u_{h,i,j}^2 = \frac{\partial^2 b}{\partial f^2}(f_0)(f_i, f_j)$.

The approximate mean value $\widetilde{\mathcal{M}}(h)$ is a deterministic objective function of the design h , and can be differentiated owing to classical techniques from optimal control theory. The resulting derivative can then be exploited in a minimization algorithm (e.g. a gradient algorithm).

A similar approximation procedure can be applied to higher-order moments of the cost function \mathcal{C} , e.g. its variance $\mathcal{V}(h)$, defined by (2.6) (see for example Subsection 3.2.4).

Remark 1. This process of approximating $\mathcal{M}(h)$ with $\widetilde{\mathcal{M}}(h)$ can be made rigorous if one assumes enough smoothness of the cost function \mathcal{C} and carefully chooses the functional space for perturbations. Typically, if ε measures the smallness of perturbations (in some well-chosen norm), then, for a given design $h \in \mathcal{U}_{ad}$, the error is $|\mathcal{M}(h) - \widetilde{\mathcal{M}}(h)| = \mathcal{O}(\varepsilon^3)$, which can be uniform with respect to h .

Note that the proof of the above error estimate requires some level of regularity for the functional space of the perturbations \hat{f} . However, lesser regularity is usually sufficient for properly defining $\widetilde{\mathcal{M}}(h)$, irrespective of its closeness to $\mathcal{M}(h)$.

Remark 2. In the above discussion, we relied on a second-order Taylor expansion of the cost $f \mapsto \mathcal{C}(h, u_{h,f})$ to devise a second-order approximation $\widetilde{\mathcal{M}}(h)$ of the mean-value $\mathcal{M}(h)$ (i.e., the discrepancy between the two is of order $\mathcal{O}(\varepsilon^3)$, where ε measures the smallness of perturbations). The calculation of $\widetilde{\mathcal{M}}(h)$ demands those of the unperturbed state u_h and of the $(N+1)$ reduced sensitivities $u_{h,i}^1$, $i = 1, \dots, N$ and u_h^2 .

Obviously, the same argument can be applied to higher-order Taylor expansions of the cost to produce higher-order approximate mean-value functionals $\widetilde{\mathcal{M}}(h)$, provided higher-order statistics of the random variables ξ_i are known. However, the cost of calculating $\widetilde{\mathcal{M}}(h)$ increases dramatically. For instance, if the fourth-order expansion of \mathcal{C} is used, even in the very favorable situation where the ξ_i are independent, the evaluation of $\widetilde{\mathcal{M}}(h)$ requires a number of reduced sensitivities of the order of N^2 .

2.2. Minimization of the failure probability.

We now turn to the minimization of a failure probability $\mathcal{P}(h)$, defined in terms of the cost function $\mathcal{C}(f, u_{h,f})$. More precisely, let $\alpha \in \mathbb{R}$ be a parameter accounting for the tolerance of the considered design in the sense that it is assumed to fail when $\mathcal{C}(f, u_{h,f}) > \alpha$. The function $\mathcal{P}(h)$ whose minimization is under scrutiny reads:

$$(2.9) \quad \mathcal{P}(h) = \mathbb{P}(\{\omega \in \mathcal{O}, \mathcal{C}(f(\omega), u_{h,f(\omega)}) > \alpha\}) = \int_{\{\omega \in \mathcal{O}, \mathcal{C}(f(\omega), u_{h,f(\omega)}) > \alpha\}} \mathbb{P}(d\omega).$$

We proposed an approximate failure probability function $\tilde{\mathcal{P}}(h)$, which is very much inspired by the so-called First-Order Reliability Method (FORM) in the context of reliability-based optimization (see e.g. [17]). We need an additional assumption on the random variables ξ_i which are now independent and Gaussian, that is, their common cumulative distribution function Φ reads:

$$(2.10) \quad \forall \alpha \in \mathbb{R}, \quad \Phi(\alpha) := \mathbb{P}(\{\omega \in \mathcal{O}, \xi_i(\omega) < \alpha\}) = \frac{1}{\sqrt{2\pi}} \int_{-\infty}^{\alpha} e^{-\xi^2/2} d\xi.$$

The main idea is then to replace the *failure region* $\{\omega \in \mathcal{O}, \mathcal{C}(f(\omega), u_{h,f(\omega)}) > \alpha\}$ with a half-space, obtained by linearizing the cost function \mathcal{C} . In other words, we replace $\mathcal{C}(f, u_{h,f})$ by its first-order Taylor approximation with respect to f around f_0 . Together with the particular structure (2.2)-(2.3) of the perturbations, it yields

$$(2.11) \quad \mathcal{C}(f_0 + \hat{f}(\omega), u_{h,f_0+\hat{f}(\omega)}) \approx \mathcal{C}(f_0, u_h) + \sum_{i=1}^N \frac{\partial \mathcal{C}}{\partial f}(f_0, u_h)(f_i) \xi_i(\omega) + \sum_{i=1}^N \frac{\partial \mathcal{C}}{\partial u}(f_0, u_h)(u_{h,i}^1) \xi_i(\omega),$$

with the same notations as in the previous subsection. This identity can be rewritten in more compact form as:

$$\mathcal{C}(f_0 + \hat{f}(\omega), u_{h,f_0+\hat{f}(\omega)}) \approx b(h) + a(h) \cdot \xi(\omega),$$

with obvious notations. Now, under the additional assumption that the random variables ξ_i are independent, we approximate $\mathcal{P}(h)$ by the function $\tilde{\mathcal{P}}(h)$ defined as:

$$\tilde{\mathcal{P}}(h) = \mathbb{P}(\{\omega \in \mathcal{O}, b(h) + a(h) \cdot \xi(\omega) > \alpha\}) = \frac{1}{(2\pi)^{N/2}} \int_{\{\xi \in \mathbb{R}^N, b(h) + a(h) \cdot \xi > \alpha\}} e^{-|\xi|^2/2} d\xi.$$

If $a(h) = 0$ (a rare case, corresponding to the fact that the cost function is insensitive to the random perturbations, at first order), then either $\tilde{\mathcal{P}}(h) = 0$ or $\tilde{\mathcal{P}}(h) = 1$, depending whether $b(h) > \alpha$ or not. For such a discrete objective function (taking only two values), there is no point in optimizing it.

However, in the generic case when $a(h) \neq 0$, the last integral can be explicitly computed thanks to a change of variables. Let indeed A be any orthogonal isomorphism of \mathbb{R}^N whose matrix in the canonical basis fulfills:

$$Ae_1 = \frac{a(h)}{|a(h)|}.$$

Then, a simple calculation produces:

$$(2.12) \quad \begin{aligned} \tilde{\mathcal{P}}(h) &= \frac{1}{(2\pi)^{\frac{N}{2}}} \int_{A^{-1}(\{\xi \in \mathbb{R}^N, b(h) + a(h) \cdot \xi > \alpha\})} |\det(A)| e^{-\frac{|A\xi|^2}{2}} d\xi \\ &= \frac{1}{(2\pi)^{\frac{N}{2}}} \int_{\{\xi \in \mathbb{R}^N, \frac{b(h)}{|a(h)|} + \xi_1 > \frac{\alpha}{|a(h)|}\}} e^{-\frac{|\xi|^2}{2}} d\xi \\ &= \frac{1}{\sqrt{2\pi}} \int_{\{\xi_1 \in \mathbb{R}, \frac{b(h)}{|a(h)|} + \xi_1 > \frac{\alpha}{|a(h)|}\}} e^{-\frac{\xi_1^2}{2}} d\xi_1 \\ &= \Phi\left(-\frac{\alpha - b(h)}{|a(h)|}\right), \end{aligned}$$

where Φ stands for the cumulative distribution function (2.10) of the centered normalized Gaussian law. This last expression is a deterministic and explicit function of the design h .

Remark 3. The above analysis also covers the case when the threshold parameter is $\alpha = \beta\mathcal{C}(f_0, u_h)$ where $\beta > 1$ is the maximal authorized deviation of a perturbed state with respect to the unperturbed situation. The only difference is that this threshold depends on the design h , which will have an impact when computing the derivative of $\tilde{\mathcal{P}}(h)$.

Remark 4. This approximation as well can be justified in some particular cases; see notably Proposition 7. As we shall see in Section 5, it turns out to be true to intuition in some cases, and may be rough on other ones, pleading for higher-order approximations of $\mathcal{P}(h)$.

2.3. Computational cost and the possible use of adjoint states.

We claim that the evaluation of the approximate objective functions $\tilde{\mathcal{M}}(h)$, defined by (2.8), and $\tilde{\mathcal{P}}(h)$, defined by (2.12), is much more economical, from a computational point of view, than those of their counterparts $\mathcal{M}(h)$ and $\mathcal{P}(h)$. Indeed, $\tilde{\mathcal{M}}(h)$ and $\tilde{\mathcal{P}}(h)$ are purely deterministic and can be evaluated exactly with a finite number of inversions of the operator $\mathcal{A}(h)$ (by inversion we mean solving the associated linear system, either by a direct or an iterative algorithm).

From inspection of formula (2.8), we see that computing $\tilde{\mathcal{M}}(h)$ requires to solve $(N + 2)$ equations with the same operator $\mathcal{A}(h)$ (for $u_h, u_h^2, u_{h,i}^1$ with $1 \leq i \leq N$).

On the other hand, a naive use of formula (2.12) seems to indicate that computing $\tilde{\mathcal{P}}(h)$ requires to solve $(N + 1)$ equations (for $u_h, u_{h,i}^1$ with $1 \leq i \leq N$). However, one can improve this operation count by using an adjoint approach since the coefficient $a(h)$ in the first-order expansion (2.11) is affine with respect to $u_{h,i}^1$ (the other coefficient $b(h)$ does not depend on $u_{h,i}^1$). By definition

$$a_i(h) = \frac{\partial \mathcal{C}}{\partial u}(f_0, u_h)(u_{h,i}^1).$$

Introducing a duality pairing, denoted by \cdot in the following formulas, which depends on the particular situation and that we do not make precise, we can define a gradient $\nabla_u \mathcal{C}$ by

$$\frac{\partial \mathcal{C}}{\partial u}(f_0, u_h)(u_{h,i}^1) = \nabla_u \mathcal{C}(f_0, u_h) \cdot u_{h,i}^1.$$

As is well-known in optimal control theory, the coefficient $a_i(h)$ can be rewritten as:

$$a_i(h) = \frac{\partial \mathcal{C}}{\partial f}(f_0, u_h)(f_i) - p_h \cdot f_i,$$

where p_h is an adjoint state, solution to the system:

$$\mathcal{A}(h)^T p_h = -\nabla_u \mathcal{C}(f_0, u_h).$$

Computing $a(h)$ and thus $\tilde{\mathcal{P}}(h)$ requires only to solve 2 equations for u_h and p_h . Introducing this adjoint p_h is sometimes useful too in order to obtain a simpler formula for the h -derivative of the objective function.

Unfortunately, since $\tilde{\mathcal{M}}(h)$ depends quadratically on the reduced sensitivities $u_{h,i}^1$, there is no adjoint trick in order to reduce the cost of evaluating $\tilde{\mathcal{M}}(h)$.

2.4. A few words on the finite-sum structure for perturbations.

The finite-dimensional hypothesis (2.3) around the perturbations $\hat{f}(\omega)$ is ubiquitous in the literature. Let us briefly evoke how it turns up in concrete situations.

First, there are several cases of utmost importance where it is the ‘natural’ structure for perturbations. For instance, in a situation where the data f stand for body forces or surfaces loads applied on an elastic structure, (2.3) accounts for several load scenarii f_i , weighted by a corresponding probability of occurrence.

On a different note, (2.3) can be taken as a ‘good’ approximation of the perturbations $\hat{f}(\omega)$ in many situations where they are actually a *random field* $\hat{f} \equiv \hat{f}(x, \omega)$, depending on a space variable $x \in D$ and on $\omega \in \mathcal{O}$ (e.g., \hat{f} describes the material properties associated to an elastic structure). Then, the

relevant information about the statistics of \widehat{f} is often known (or modelled) via its *correlation function* $\text{Cor}(\widehat{f}) \in L^2(D \times D)$, defined as:

$$\text{Cor}(\widehat{f})(x, y) = \int_{\mathcal{O}} \widehat{f}(x, \omega) \widehat{f}(y, \omega) \mathbb{P}(d\omega), \text{ a.e. } (x, y) \in D \times D.$$

In such a case, it can be proved (see e.g. [32] Chap. 11) that \widehat{f} admits a decomposition

$$\widehat{f}(x, \omega) = \sum_{i=1}^{\infty} \sqrt{\lambda_i} f_i(x) \xi_i(\omega),$$

where the (λ_i, f_i) are the eigenpairs of the Hilbert-Schmidt operator $\varphi \mapsto \int_D \text{Cor}(\widehat{f})(\cdot, y) \varphi(y) dy$, from $L^2(D)$ into itself, and that the convergence of the above series holds in $L^2(D \times \mathcal{O})$. This series can then be truncated to produce a finite-dimensional approximation of \widehat{f} the form (2.3). The random variables ξ_i are recovered by orthogonality of the eigenfunctions f_i

$$\xi_i(\omega) = \frac{1}{\sqrt{\lambda_i}} \int_D \widehat{f}(x, \omega) f_i(x) dx.$$

Let us eventually mention that if \widehat{f} is a Gaussian random process - a kind of random process which is ubiquitous in stochastic modelling - the random variables ξ_i turn out to be Gaussian and independent.

3. RANDOM PARAMETRIC OPTIMIZATION

3.1. A model problem.

Let us consider a linear elastic plate with fixed cross-section $\Omega \subset \mathbb{R}^d$ (in practice $d = 2$), whose thickness $h \in L^\infty(\Omega)$ is subject to optimization. The plate is in plane stress situation: it is clamped on a part of its boundary accounted for by $\Gamma_D \subset \partial\Omega$, and submitted to both body forces $f \in L^2(\Omega)^d$ and surface loads $g \in L^2(\Gamma_N)^d$, applied on the complementary part $\Gamma_N := \partial\Omega \setminus \overline{\Gamma_D}$ to Γ_D in $\partial\Omega$ (see Figure 1).

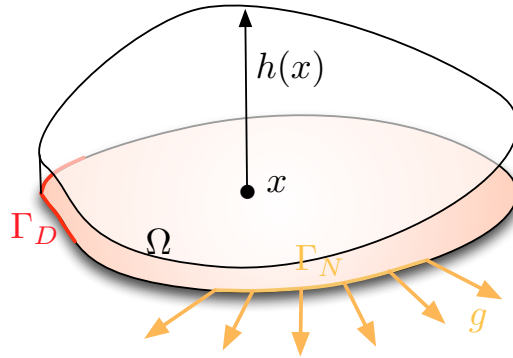


FIGURE 1. *Setting of the model parametric optimization problem.*

In this situation, the in-plane displacement $u_h \in H^1(\Omega)^d$ of the plate arises as the unique solution to the linear elasticity system:

$$(3.1) \quad \begin{cases} -\text{div}(hAe(u)) = f & \text{in } \Omega \\ u = 0 & \text{on } \Gamma_D \\ hAe(u)n = g & \text{on } \Gamma_N \end{cases},$$

where $e(u) = (\nabla u^T + \nabla u)/2$ is the strain tensor, $n : \partial\Omega \rightarrow \mathbb{S}^{d-1}$ is the unit outer normal vector field to Ω , and A is the material Hooke's law, defined for any $e \in \mathcal{S}(\mathbb{R}^d)$ (the set of $d \times d$ real symmetric matrices) by

$$(3.2) \quad Ae = 2\mu e + \lambda \text{tr}(e)I,$$

with the Lamé coefficients λ, μ , satisfying $\mu > 0$ and $\lambda + 2\mu/d > 0$. Introducing the functional space

$$(3.3) \quad H_{\Gamma_D}^1(\Omega) := \{v \in H^1(\Omega), v = 0 \text{ on } \Gamma_D\},$$

u_h can be equivalently seen as the unique solution in $H_{\Gamma_D}^1(\Omega)^d$ to the following variational problem:

$$(3.4) \quad \forall v \in H_{\Gamma_D}^1(\Omega)^d, \quad \int_{\Omega} h A e(u_h) : e(v) dx = \int_{\Omega} f \cdot v dx + \int_{\Gamma_N} g \cdot v ds.$$

The thickness h of such a plate must belong to a set \mathcal{U}_{ad} of *admissible designs*:

$$\mathcal{U}_{ad} = \{h \in L^\infty(\Omega), \forall x \in \Omega, h_{min} \leq h(x) \leq h_{max}\},$$

where h_{min} and h_{max} are imposed lower and upper bounds for the thickness. Admittedly, in most relevant situations, additional constraints should be imposed for the optimization problem. Yet, to keep notations as general as possible, we chose not to incorporate them in the modeling of the present section (see Section 5 as regards the numerical treatment of those constraints). The goal of parametric optimization is to minimize the following *cost function*

$$\inf_{h \in \mathcal{H}} \left\{ \mathcal{C}(h) = \int_{\Omega} j(u_h) dx \right\},$$

where u_h is the solution of the state equation (3.1) for the thickness h and j is some given integrand.

Remark 5. The above setting of thickness optimization for a plate is completely equivalent to that of the so-called SIMP method for topology optimization [9]. The thickness h becomes the material density ρ (with $\rho_{min} = 0$ and $\rho_{max} = 1$), possibly penalized as ρ^p for some integer $p \geq 1$. This considerably extends the scope and applicability of the present framework of parametric optimization.

3.2. Uncertainty over the body forces in parametric optimization.

In this subsection, we focus on a fairly simple setting - that of the optimization of the thickness h of the elastic plate described in Section 3.1, in a context where random body forces are expected. Our purpose is here to exemplify how the framework of Section 2 translates in a more realistic situation, and how its general ideas can be applied. The next sections will involve similar techniques, in more sophisticated situations.

For a given thickness function $h \in L^\infty(\Omega)$ and body forces $f \in L^2(\Omega)^d$, let us denote as $u_{h,f} \in H_{\Gamma_D}^1(\Omega)^d$ the displacement of the plate, unique solution to (3.1) using this set of data (for simplicity, we omit surface loads: $g = 0$).

The *cost function* $\mathcal{C}(h, f)$ at stake in this section is of the form:

$$(3.5) \quad \mathcal{C}(h, f) = \int_{\Omega} j(f, u_{h,f}) dx,$$

where $j : \mathbb{R}^d \times \mathbb{R}^d \rightarrow \mathbb{R}$ is a function of class \mathcal{C}^3 , satisfying the growth conditions:

$$(3.6) \quad \forall f \in \mathbb{R}^d, \forall u \in \mathbb{R}^d, \quad \begin{cases} |j(f, u)| \leq C(1 + |f|^2 + |u|^2), \\ |\nabla_f j(f, u)| + |\nabla_u j(f, u)| \leq C(1 + |f| + |u|), \\ \text{all the partial derivatives of } j \text{ of order 2 and 3 are bounded by } C, \end{cases}$$

for some constant $C > 0$. We explicitly indicate the dependence with respect to f since it is the uncertain variable which will be averaged in the sequel. Note that j could as well depend explicitly on the space variable $x \in \mathbb{R}^d$, with the following results being unchanged; so to keep notations compact insofar as possible, this dependence is omitted. More general cost functions could also be considered, e.g. cost functions involving quantities related to the values of $u_{h,f}$ on (a part of) $\partial\Omega$, without any conceptual change in the developments ahead.

3.2.1. Second-order asymptotic expansion of the cost function with respect to perturbations.

Let us introduce perturbations \widehat{f} over the body forces $f = f_0 + \widehat{f}$, around a particular value f_0 . The natural choice of a functional space for f_0 and \widehat{f} (thus f) is $L^2(\Omega)^d$. However, as evoked in Remark 1, our approximation results (Propositions 2 and 3 below) can be rigorously justified if we ask for slightly more integrability of the forces, namely $f_0, \widehat{f} \in L^3(\Omega)^d$, which is now our standing assumption.

We shall focus on approximations of the objective functions obtained by a first- or second-order Taylor expansion of the cost function $f \mapsto \mathcal{C}(h, f)$ around f_0 . In this perspective, let us recall the following result about the regularity of the mapping $(h, f) \mapsto u_{h,f}$, which will be used implicitly and repeatedly in the following. Its proof relies on a use of the implicit function theorem which is rather classical in optimal control theory; see e.g. [29], Chap. 5.

Lemma 1. *Let $p \geq 2$. The function $\mathcal{U}_{ad} \times L^p(\Omega)^d \ni (h, f) \mapsto u_{h,f} \in H_{\Gamma_D}^1(\Omega)^d$ is of class \mathcal{C}^∞ .*

A first calculation of interest then concerns the asymptotic expansion of the cost \mathcal{C} .

Proposition 2. *The cost function $f \mapsto \mathcal{C}(h, f)$, from $L^3(\Omega)^d$ into \mathbb{R} has the following expansion around $f_0 \in L^3(\Omega)^d$:*

$$(3.7) \quad \mathcal{C}(h, f_0 + \widehat{f}) = \int_{\Omega} j(f_0, u_h) dx + \int_{\Omega} \left(\nabla_f j(f_0, u_h) \cdot \widehat{f} + \nabla_u j(f_0, u_h) \cdot u_h^1(\widehat{f}) \right) dx \\ + \frac{1}{2} \int_{\Omega} \left(\nabla_f^2 j(f_0, u_h)(\widehat{f}, \widehat{f}) + 2 \nabla_f \nabla_u j(f_0, u_h)(\widehat{f}, u_h^1(\widehat{f})) + \nabla_u^2 j(f_0, u_h)(u_h^1(\widehat{f}), u_h^1(\widehat{f})) \right) dx + R(\widehat{f}).$$

In this formula, we have denoted as $u_h = u_{h,f_0}$ the displacement of the plate in the unperturbed situation, and the sensitivity $u_h^1(\widehat{f}) := \frac{\partial u_{h,f}}{\partial f} \Big|_{f=f_0}(\widehat{f})$ is solution to the following variational problem:

$$(3.8) \quad \forall v \in H_{\Gamma_D}^1(\Omega)^d, \quad \int_{\Omega} h A e \left(u_h^1(\widehat{f}) \right) : e(v) dx = \int_{\Omega} \widehat{f} \cdot v dx.$$

As for the residual $R(\widehat{f})$, there exists a constant $C > 0$, which is uniform with respect to $h \in \mathcal{U}_{ad}$, such that:

$$\forall \widehat{f} \in L^3(\Omega)^d, \quad |R(\widehat{f})| \leq C \|\widehat{f}\|_{L^3(\Omega)^d}^3.$$

Proof. Performing a second-order Taylor expansion of $f \mapsto \mathcal{C}(h, f)$ around f_0 (which is possible because of Lemma 1) in an arbitrary direction $\widehat{f} \in L^3(\Omega)^d$ directly yields (3.7), with a residual $R(\widehat{f})$ defined as:

$$R(\widehat{f}) = \int_{\Omega} \int_0^1 \frac{\partial^3 \mathcal{C}}{\partial f^3}(h, f_0 + t\widehat{f})(\widehat{f}, \widehat{f}, \widehat{f}) dt dx.$$

The expression of the partial derivative $\frac{\partial^3 \mathcal{C}}{\partial f^3}$ involves the various derivatives of j , up to order 3 (which can be controlled owing to (3.6)), as well as those of $f \mapsto u_{h,f}$. Writing the variational problem satisfied by the latter and deriving a priori estimates in the usual way provide the desired control on $R(\widehat{f})$. \square

Remark 6. In utter generality, the expansion (3.7) should contain an additional term, involving the second order derivative $u_h^2(\widehat{f}, \widehat{f}) := \frac{\partial^2 u_{h,f}}{\partial f^2} \Big|_{f=f_0}(\widehat{f}, \widehat{f})$ (compare with (2.7)). However, in the particular case of this section, the mapping $f \mapsto u_{h,f}$ is linear and this term vanishes.

3.2.2. Introduction of random perturbations, and approximation of the mean-value of the cost function.

Let us now assume that the perturbations \widehat{f} over the applied body forces are modelled as random fields $\widehat{f} \equiv \widehat{f}(x, \omega)$, defined for $x \in \Omega$, and $\omega \in \mathcal{O}$, where $(\mathcal{O}, \mathcal{F}, \mathbb{P})$ is an abstract probability space. Roughly speaking, an \mathbb{R}^d -valued random variable is attached to each point $x \in \Omega$ in the ‘physical space’. We assume that \widehat{f} belongs to the Böchner space $L^3(\mathcal{O}, L^3(\Omega)^d)$.

Let us consider the *mean value* $\mathcal{M}(h)$ of the cost function $\mathcal{C}(h, f(\cdot, \omega))$, that is:

$$\mathcal{M}(h) = \int_{\mathcal{O}} \mathcal{C}(h, f(\cdot, \omega)) \mathbb{P}(d\omega).$$

Replacing $\mathcal{C}(h, f(\cdot, \omega))$ with the right-hand side of (3.7) (without the error term), then integrating over $\omega \in \mathcal{O}$, gives rise to the *approximate mean-value* functional $\widetilde{\mathcal{M}}(h)$, defined as:

$$(3.9) \quad \begin{aligned} \widetilde{\mathcal{M}}(h) &= \int_{\Omega} j(f_0, u_h) dx + \int_{\mathcal{O}} \int_{\Omega} \left(\nabla_f j(f_0, u_h) \cdot \widehat{f} + \nabla_u j(f_0, u_h) \cdot u_h^1(\widehat{f}) \right) dx \mathbb{P}(d\omega) \\ &+ \frac{1}{2} \int_{\mathcal{O}} \int_{\Omega} \left(\nabla_f^2 j(f_0, u_h)(\widehat{f}, \widehat{f}) + 2\nabla_f \nabla_u j(f_0, u_h)(\widehat{f}, u_h^1(\widehat{f})) + \nabla_u^2 j(f_0, u_h)(u_h^1(\widehat{f}), u_h^1(\widehat{f})) \right) dx \mathbb{P}(d\omega). \end{aligned}$$

Using Proposition 2, we easily deduce an estimate on the error entailed by replacing $\mathcal{M}(h)$ with $\widetilde{\mathcal{M}}(h)$:

Proposition 3. *Assume that the random field \widehat{f} belongs to $L^3(\mathcal{O}, L^3(\Omega)^d)$. Then there exists a constant $C > 0$ (uniform in $h \in \mathcal{U}_{ad}$) such that:*

$$|\widetilde{\mathcal{M}}(h) - \mathcal{M}(h)| \leq C \|\widehat{f}\|_{L^3(\mathcal{O}, L^3(\Omega)^d)}^3.$$

We now consider the minimization of $\widetilde{\mathcal{M}}(h)$ instead of that of $\mathcal{M}(h)$, since it features a simpler dependence (at most quadratic) in terms of the perturbations \widehat{f} .

In this context, let us observe that the definition (3.9) of $\widetilde{\mathcal{M}}(h)$ actually makes sense under less restrictive assumptions than $\widehat{f} \in L^3(\mathcal{O}, L^3(\Omega)^d)$. It is indeed tantalizing to consider the minimization of $\widetilde{\mathcal{M}}(h)$ in situations where \widehat{f} belongs to a more intuitive functional space (even though it is then not clear whether it is a rigorous approximation of $\mathcal{M}(h)$). As such, one could for instance ask that \widehat{f} belong to the Böchner space $L^\infty(\mathcal{O}, L^2(\Omega)^d)$, with the meaning that each realization of a small perturbation \widehat{f} in this space is a small function (in $L^2(\Omega)^d$ -norm). One could alternatively ask that $\widehat{f} \in L^2(\mathcal{O}, L^2(\Omega)^d)$, thus authorizing \widehat{f} to have large (but unlikely) realizations. We retain this last idea in the remainder of this section.

As explained in Section 2, we rely on the hypothesis that \widehat{f} is a finite sum of deterministic functions $f_i \in L^2(\Omega)^d$, $i = 1, \dots, N$, weighted by uncorrelated, normalized random variables ξ_i (i.e. (2.4) holds):

$$(3.10) \quad \widehat{f}(x, \omega) = \sum_{i=1}^N f_i(x) \xi_i(\omega).$$

Notice that the assumption that \widehat{f} be ‘small’ in $L^2(\mathcal{O}, L^2(\Omega)^d)$ -norm implies that each of the functions f_i is ‘small’ in $L^2(\Omega)^d$ -norm, since

$$\|\widehat{f}\|_{L^2(\mathcal{O}, L^2(\Omega)^d)}^2 = \sum_{i=1}^N \|f_i\|_{L^2(\Omega)^d}^2,$$

as a consequence of the ξ_i being uncorrelated. Inserting (3.10) into (3.7) yields a simpler expression of $\widetilde{\mathcal{M}}(h)$:

$$(3.11) \quad \begin{aligned} \widetilde{\mathcal{M}}(h) &= \int_{\Omega} j(f_0, u_h) dx + \frac{1}{2} \int_{\Omega} \sum_{i=1}^N \nabla_f^2 j(f_0, u_h)(f_i, f_i) dx \\ &+ \sum_{i=1}^N \int_{\Omega} \nabla_f \nabla_u j(f_0, u_h)(f_i, u_{h,i}^1) dx + \frac{1}{2} \sum_{i=1}^N \int_{\Omega} \nabla_u^2 j(f_0, u_h)(u_{h,i}^1, u_{h,i}^1) dx, \end{aligned}$$

where we have introduced the reduced sensitivities $u_{h,i}^1 := u_h^1(f_i)$, $i = 1, \dots, n$, as the unique solutions in $H_{\Gamma_D}^1(\Omega)^d$ of

$$(3.12) \quad \begin{cases} -\operatorname{div}(hAe(u_{h,i}^1)) = f_i & \text{in } \Omega, \\ u_{h,i}^1 = 0 & \text{on } \Gamma_D, \\ hAe(u_{h,i}^1)n = 0 & \text{on } \Gamma_N. \end{cases}$$

3.2.3. Differentiation of the approximate mean value function.

We now compute the Fréchet derivative $\widetilde{\mathcal{M}}'(h)$ of the approximate mean value function $\widetilde{\mathcal{M}}(h)$ given by (3.11).

Theorem 4. *The functional $\widetilde{\mathcal{M}}(h)$ is Fréchet-differentiable at any $h \in \mathcal{U}_{ad}$, and its derivative reads:*

$$(3.13) \quad \forall \widehat{h} \in L^\infty(\Omega), \quad \widetilde{\mathcal{M}}'(h)(\widehat{h}) = \int_{\Omega} \widehat{h} \left(Ae(u_h) : e(p_h^0) + \sum_{i=1}^N Ae(u_{h,i}^1) : e(p_{h,i}^1) \right) dx,$$

where p_h^0 , and $p_{h,i}^1$ for $i = 1, \dots, N$ are $(N+1)$ adjoint states, defined as the unique solutions in $H_{\Gamma_D}^1(\Omega)^d$ to the respective variational problems:

$$(3.14) \quad \forall v \in H_{\Gamma_D}^1(\Omega)^d, \quad \int_{\Omega} h Ae(p_h^0) : e(v) dx = - \int_{\Omega} \nabla_u j(f_0, u_h) \cdot v dx - \frac{1}{2} \int_{\Omega} \sum_{i=1}^N \nabla_f^2 \nabla_u j(f_0, u_h) (f_i, f_i, v) dx \\ - \sum_{i=1}^N \int_{\Omega} \left(\nabla_f \nabla_u^2 j(f_0, u_h) (f_i, u_{h,i}^1, v) + \frac{1}{2} \nabla_u^3 j(f_0, u_h) (u_{h,i}^1, u_{h,i}^1, v) \right) dx,$$

$$(3.15) \quad \forall v \in H_{\Gamma_D}^1(\Omega)^d, \quad \int_{\Omega} h Ae(p_{h,i}^1) : e(v) dx = - \int_{\Omega} (\nabla_f \nabla_u j(f_0, u_h) (f_i, v) + \nabla_u^2 j(f_0, u_h) (u_{h,i}^1, v)) dx.$$

Proof. The differentiability of $\widetilde{\mathcal{M}}(h)$ is a straightforward consequence of Lemma 1. Taking the derivative with respect to h in (3.4) and (3.8) yields, for any $\widehat{h} \in L^\infty(\Omega)$:

$$(3.16) \quad \forall v \in H_{\Gamma_D}^1(\Omega)^d, \quad \int_{\Omega} h Ae \left(\frac{\partial u_h}{\partial h}(\widehat{h}) \right) : e(v) dx = - \int_{\Omega} \widehat{h} Ae(u_h) : e(v) dx,$$

$$(3.17) \quad \forall v \in H_{\Gamma_D}^1(\Omega)^d, \quad \int_{\Omega} h Ae \left(\frac{\partial u_{h,i}^1}{\partial h}(\widehat{h}) \right) : e(v) dx = - \int_{\Omega} \widehat{h} Ae(u_{h,i}^1) : e(v) dx,$$

Hence, for any $\widehat{h} \in L^\infty(\Omega)$, we obtain:

$$(3.18) \quad \widetilde{\mathcal{M}}'(h)(\widehat{h}) = \int_{\Omega} \nabla_u j(f_0, u_h) \cdot \frac{\partial u_h}{\partial h}(\widehat{h}) dx + \frac{1}{2} \int_{\Omega} \sum_{i=1}^N \nabla_f^2 \nabla_u j(f_0, u_h) \left(f_i, f_i, \frac{\partial u_h}{\partial h}(\widehat{h}) \right) dx \\ + \sum_{i=1}^N \int_{\Omega} \left(\nabla_f \nabla_u^2 j(f_0, u_h) \left(f_i, u_{h,i}^1, \frac{\partial u_h}{\partial h}(\widehat{h}) \right) + \frac{1}{2} \nabla_u^3 j(f_0, u_h) \left(u_{h,i}^1, u_{h,i}^1, \frac{\partial u_h}{\partial h}(\widehat{h}) \right) \right) dx \\ + \sum_{i=1}^N \int_{\Omega} \left(\nabla_f \nabla_u j(f_0, u_h) \left(f_i, \frac{\partial u_{h,i}^1}{\partial h}(\widehat{h}) \right) + \nabla_u^2 j(f_0, u_h) \left(u_{h,i}^1, \frac{\partial u_{h,i}^1}{\partial h}(\widehat{h}) \right) \right) dx.$$

Let us now bring into play the adjoint states p_h^0 , and $p_{h,i}^1$ ($i = 1, \dots, n$), defined by (3.14), and (3.15) respectively. The first three terms in the right-hand side of (3.18) rewrite:

$$\int_{\Omega} \nabla_u j(f_0, u_h) \cdot \frac{\partial u_h}{\partial h}(\widehat{h}) dx + \frac{1}{2} \int_{\Omega} \sum_{i=1}^N \nabla_f^2 \nabla_u j(f_0, u_h) \left(f_i, f_i, \frac{\partial u_h}{\partial h}(\widehat{h}) \right) dx \\ + \sum_{i=1}^N \int_{\Omega} \left(\nabla_f \nabla_u^2 j(f_0, u_h) \left(f_i, u_{h,i}^1, \frac{\partial u_h}{\partial h}(\widehat{h}) \right) + \frac{1}{2} \nabla_u^3 j(f_0, u_h) \left(u_{h,i}^1, u_{h,i}^1, \frac{\partial u_h}{\partial h}(\widehat{h}) \right) \right) dx \\ = - \int_{\Omega} h Ae(p_h^0) : e \left(\frac{\partial u_h}{\partial h}(\widehat{h}) \right) = \int_{\Omega} \widehat{h} Ae(u_h) : e(p_h^0) dx,$$

where the last line is a consequence of (3.16). Using similar rearrangements for the remaining terms in (3.18), we end up with the desired formula (3.13). \square

Remark 7. Alternatively, we could have used C ea's method for the calculation of the above derivative (see e.g. [1, 12]). The formula for the derivative of $\widetilde{\mathcal{M}}(h)$ requires to solve $2(N+1)$ equations to obtain the solutions u_h , $u_{h,i}$, p_h^0 and $p_{h,i}$, for $i = 1, \dots, N$. All equations share the same partial differential operator as (3.1) with merely different right-hand sides. Thus, from a practical point of view, the attached finite element

matrix needs only be inverted once. Or, if using an iterative solver, all these independent computations could be carried out in parallel.

Remark 8. Let us recall that, in the definitions (3.14) and (3.15) of the adjoints, the right hand sides feature terms of the type $\nabla_f \nabla_u j(f_0, u_h)(f_i, v)$ which are bilinear in (f_i, v) (namely the matrix $\nabla_f \nabla_u j(f_0, u_h)$ contracted with the two vectors f_i and v) and of the type $\nabla_f^2 \nabla_u j(f_0, u_h)(f_i, f_i, v)$ which are trilinear in (f_i, f_i, v) .

When there are no uncertainties, i.e. $f_i = 0$ for $i = 1, \dots, N$, then $p_{h,i} = 0$ and $p_h^0 = p_h$ where p_h is the usual adjoint, solution of

$$\begin{cases} -\operatorname{div}(hAe(p_h)) = -\nabla_u j(f_0, u_h) & \text{in } \Omega, \\ p_h = 0 & \text{on } \Gamma_D, \\ hAe(p_h)n = 0 & \text{on } \Gamma_N. \end{cases}$$

Example 1. Let us consider the compliance of the plate as an objective function, namely $j(f, u) = f \cdot u$. The various derivatives of j needed to perform the calculation of $\widetilde{\mathcal{M}}(h)$ and its derivative are:

$$\nabla_u j(f_0, u) = f_0, \quad \nabla_f \nabla_u j(f_0, u)(\widehat{f}, v) = \widehat{f} \cdot v, \quad \nabla_u^2 j(f_0, u) = 0, \quad \text{and} \quad \nabla_f^2 j(f_0, u) = 0.$$

Then, $p_h^0 = -u_h$ and $p_h^i = -u_h^i$, while $\widetilde{\mathcal{M}}(h)$ and its directional derivative $\widetilde{\mathcal{M}}'(h)(\widehat{h})$ read:

$$\widetilde{\mathcal{M}}(h) = \int_{\Omega} \left(f_0 \cdot u_h + \sum_{i=1}^N f_i \cdot u_{h,i} \right) dx \quad \text{and} \quad \widetilde{\mathcal{M}}'(h)(\widehat{h}) = - \int_{\Omega} \widehat{h} \left(Ae(u_h) : e(u_h) + \sum_{i=1}^N Ae(u_{h,i}) : e(u_{h,i}) \right) dx.$$

Interestingly, $\widetilde{\mathcal{M}}(h)$ is nothing but the multi-load objective functional studied, e.g. in [4].

3.2.4. Approximation of the variance.

The ideas presented above can be elaborated upon to produce an approximation of the *variance* \mathcal{V} of the considered cost \mathcal{C} , defined by

$$\mathcal{V}(h) = \int_{\mathcal{O}} (\mathcal{C}(h, f(\cdot, \omega)) - \mathcal{M}(h))^2 \mathbb{P}(d\omega).$$

We introduce the following approximate variance

$$(3.19) \quad \widetilde{\mathcal{V}}(h) = \int_{\mathcal{O}} \left(\int_{\Omega} \left(\nabla_f j(f_0, u_h) \cdot \widehat{f}(\cdot, \omega) + \nabla_u j(f_0, u_h) \cdot u_h^1(\widehat{f}(\cdot, \omega)) \right) dx \right)^2 \mathbb{P}(d\omega).$$

Proposition 5. *Assume that the perturbations \widehat{f} belong to $L^4(\mathcal{O}, L^2(\Omega)^d)$, and that $\int_{\mathcal{O}} \widehat{f} \mathbb{P}(d\omega) = 0$. Then, there exists a constant C (uniform with respect to $h \in \mathcal{U}_{ad}$) such that:*

$$|\widetilde{\mathcal{V}}(h) - \mathcal{V}(h)| \leq C \|\widehat{f}\|_{L^4(\mathcal{O}, L^2(\Omega)^d)}^3.$$

Proof. Arguing as in Sections 3.2.1 and 3.2.2, the following asymptotic expansions are easily derived, for a given $h \in \mathcal{U}_{ad}$:

$$\mathcal{M}(h) = \int_{\Omega} j(f_0, u_h) dx + \mathcal{O}(\|\widehat{f}\|_{L^2(\mathcal{O}, L^2(\Omega)^d)}^2),$$

and for a.e. event $\omega \in \mathcal{O}$:

$$\mathcal{C}(h, f(\cdot, \omega)) - \mathcal{M}(h) = \int_{\Omega} \left(\nabla_f j(f_0, u_h) \cdot \widehat{f}(\cdot, \omega) + \nabla_u j(f_0, u_h) \cdot u_h^1(\widehat{f}(\cdot, \omega)) \right) dx + R(\widehat{f}(\cdot, \omega)) + \mathcal{O}(\|\widehat{f}\|_{L^2(\mathcal{O}, L^2(\Omega)^d)}^2),$$

where u_h^1 is defined in (3.8), and the remainder function satisfies

$$|R(\widehat{f}(\cdot, \omega))| \leq C \|\widehat{f}(\cdot, \omega)\|_{L^2(\Omega)^d}^2,$$

for a constant $C > 0$, independent of h . Note that $L^4(\mathcal{O}, L^2(\Omega)^d)$ is embedded in $L^2(\mathcal{O}, L^2(\Omega)^d)$. Squaring the difference $(\mathcal{C} - \mathcal{M})$, integrating over the probability space \mathcal{O} , using the centering condition for \widehat{f} as well as its higher integrability yields the desired estimate. \square

Remark 9. Since the integrand in the definition of the variance $\mathcal{V}(h)$ is a square, it is enough to perform a first-order, instead of a second-order, Taylor expansion of the cost function. This greatly simplifies the analysis, avoiding the introduction of second-order terms.

Again, formula (3.19) actually makes sense for more general perturbations than $\widehat{f} \in L^4(\mathcal{O}, L^2(\Omega)^d)$. We now consider $\widehat{f} \in L^2(\mathcal{O}, L^2(\Omega)^d)$ with the particular structure (3.10), in which case $\widetilde{\mathcal{V}}(h)$ rewrites:

$$(3.20) \quad \widetilde{\mathcal{V}}(h) = \sum_{i=1}^N \left(\int_{\Omega} (\nabla_f j(f_0, u_h) \cdot f_i + \nabla_u j(f_0, u_h) \cdot u_{h,i}^1) dx \right)^2,$$

where the $u_{h,i}^1$ are given by (3.12). The derivative of (3.20) can be calculated along the lines of the proof of Theorem 4, so we omit the proof.

Theorem 6. *The approximate variance $\widetilde{\mathcal{V}}(h)$ is Fréchet-differentiable at any $h \in \mathcal{U}_{ad}$, and its derivative reads:*

$$(3.21) \quad \forall \widehat{h} \in L^\infty(\Omega), \quad \widetilde{\mathcal{V}}'(h)(\widehat{h}) = \int_{\Omega} \widehat{h} \left(Ae(u_h) : e(p_h^0) + 2 \sum_{i=1}^N a_{h,i} Ae(u_{h,i}^1) : e(p_h^1) \right) dx,$$

where, for $i = 1, \dots, N$,

$$a_{h,i} := \int_{\Omega} (\nabla_f j(f_0, u_h) \cdot f_i + \nabla_u j(f_0, u_h) \cdot u_{h,i}^1) dx,$$

and the adjoint states p_h^0 and $p_h^1 \in H_{\Gamma_D}^1(\Omega)^d$ are defined as the unique solutions to the variational problems:

$$\forall v \in H_{\Gamma_D}^1(\Omega)^d, \quad \int_{\Omega} h Ae(p_h^0) : e(v) dx = -2 \sum_{i=1}^N a_{h,i} \int_{\Omega} (\nabla_f \nabla_u j(f_0, u_h)(f_i, v) + \nabla_u^2 j(f_0, u_h)(u_{h,i}^1, v)) dx,$$

$$\forall v \in H_{\Gamma_D}^1(\Omega)^d, \quad \int_{\Omega} h Ae(p_h^1) : e(v) dx = - \int_{\Omega} \nabla_u j(f_0, u_h) \cdot v dx.$$

Remark 10. Note that, according to Section 2.3, one may get rid of the $u_{h,i}^1$ in formula (3.20) thanks to the introduction of the adjoint state p_h^1 , namely

$$\widetilde{\mathcal{V}}(h) = \sum_{i=1}^N \left(\int_{\Omega} (\nabla_f j(f_0, u_h) - p_h^1) \cdot f_i dx \right)^2.$$

Therefore, the evaluation of $\widetilde{\mathcal{V}}(h)$ requires to solve only two equations (for u_h and p_h^1). Similarly, introducing the combination $u_{h,a}^1 = \sum_{i=1}^N a_{h,i} u_{h,i}^1$, one needs to solve merely four equations (for u_h , $u_{h,a}^1$, p_h^0 and p_h^1) in order to obtain the derivative (3.21).

Remark 11. When there are no uncertainties, i.e. $f_i = 0$, then $u_{h,i}^1 = 0$ and the approximate variance vanishes, $\widetilde{\mathcal{V}}(h) = 0$, as well as its derivatives. Note in passing that, contrary to the case of Theorem 4, it is p_h^1 (and not p_h^0) which coincides with the usual adjoint p_h introduced in Remark 8.

Remark 12. The same strategy allows to derive approximate functionals for higher-order moments of \mathcal{C} (e.g. its skewness or kurtosis), provided information about higher-order moments of the tuple (ξ_1, \dots, ξ_N) is known (e.g. if the variables ξ_1, \dots, ξ_N are assumed to be independent, and not merely uncorrelated).

Example 2. In the setting of example 1, i.e. when the cost function is the compliance, the functional $\widetilde{\mathcal{V}}(h)$ and its derivative simply read:

$$\widetilde{\mathcal{V}}(h) = \sum_{i=1}^N a_{h,i}^2, \quad \widetilde{\mathcal{V}}'(h)(\widehat{h}) = -4 \sum_{i=1}^N a_{h,i} \int_{\Omega} \widehat{h} Ae(u_h) : e(u_{h,i}) dx,$$

with the coefficients $a_{h,i} = \int_{\Omega} (f_i \cdot u_h + f_0 \cdot u_{h,i}) dx$. It is possible to give an interpretation of the minimization of the approximated variance $\widetilde{\mathcal{V}}(h)$ when the cost function is the compliance.

We consider a multiple load compliance minimization for the N loads $f_0 + \delta_i f_i$ where $\delta_i > 0$ are some weighting factors to be determined. The corresponding elasticity solutions are $u_h + \delta_i u_{h,i}$ and the multiple load objective functions is a weighted sum of compliances

$$\mathcal{J}(h) = \sum_{i=1}^N c_i \int_{\Omega} (f_0 + \delta_i f_i) \cdot (u_h + \delta_i u_{h,i}) dx,$$

where $c_i > 0$ are some other weighting factors to be determined. Developing yields

$$\mathcal{J}(h) = \sum_{i=1}^N \left(c_i \int_{\Omega} (f_0 \cdot u_h + \delta_i^2 f_i \cdot u_{h,i}) dx + \delta_i c_i \int_{\Omega} (f_0 \cdot u_{h,i} + f_i \cdot u_h) dx \right).$$

We define

$$c_i = \left(\delta \int_{\Omega} (f_0 \cdot u_{h,i} + f_i \cdot u_h) dx \right)^2 \quad \text{and} \quad \delta_i = \left(\delta \int_{\Omega} (f_0 \cdot u_{h,i} + f_i \cdot u_h) dx \right)^{-1},$$

$$\text{with} \quad \delta = \left(\sum_{i=1}^N \left(\int_{\Omega} (f_0 \cdot u_{h,i} + f_i \cdot u_h) dx \right)^2 \right)^{-1/2} = \tilde{\mathcal{V}}(h)^{-1/2},$$

which implies that $\sum_{i=1}^N c_i = 1$ and $c_i \delta_i^2 = 1$. Then

$$\mathcal{J}(h) = \int_{\Omega} f_0 \cdot u_h dx + \sum_{i=1}^N \int_{\Omega} f_i \cdot u_{h,i} dx + \sqrt{\tilde{\mathcal{V}}(h)}.$$

Therefore, minimizing the approximated variance $\tilde{\mathcal{V}}(h)$ is equivalent to minimize a weighted sum of N compliances with perturbed loads $f_0 + \delta_i f_i$, while maximizing the sum of $(N + 1)$ compliances associated to the loads f_0, f_1, \dots, f_N .

3.2.5. Approximation of the failure probability.

We now come to the approximation of the failure probability, following the idea of Section 2.2, still in the context of random perturbations of the body forces. We keep the previous notations of Section 3.2. Let $\alpha \in \mathbb{R}$ be the threshold value for the cost function $\mathcal{C}(h, f)$ above which the design of thickness h , submitted to forces f , is assumed to ‘fail’. The objective function is the *failure probability*

$$\mathcal{P}(h) = \mathbb{P}(\{\omega \in \mathcal{O}, \mathcal{C}(h, f(\cdot, \omega)) > \alpha\}).$$

We first give a first-order Taylor expansion the cost $f \mapsto \mathcal{C}(h, f)$ around f_0 . It is nothing but the truncation at first order of the second-order expansion delivered by Proposition 2. However, since the remainder term is dominated by a quadratic term, it is enough to consider forces which belong to $L^2(\Omega)^d$. More precisely, for $f_0 \in L^2(\Omega)^d$ and any variation $\hat{f} \in L^2(\Omega)^d$,

$$(3.22) \quad \mathcal{C}(h, f_0 + \hat{f}) = \int_{\Omega} j(f_0, u_h) dx + \int_{\Omega} \left(\nabla_f j(f_0, u_h) \cdot \hat{f} + \nabla_u j(f_0, u_h) \cdot u_h^1(\hat{f}) \right) dx + R(\hat{f}),$$

and there exists a constant $C > 0$, uniform with respect to $h \in \mathcal{U}_{ad}$, such that the residual $R(\hat{f})$ satisfies:

$$|R(\hat{f})| \leq C \|\hat{f}\|_{L^2(\Omega)^d}^2.$$

We consider perturbations $\hat{f} \in L^2(\mathcal{O}, L^2(\mathbb{R}^d))$ which are a finite sum of the form (3.10), where the random variables $\xi = (\xi_1, \dots, \xi_N)$ are centered, normalized, but also *independent* and *Gaussian* random variables. The expansion (3.22) becomes:

$$\mathcal{C}(h, f_0 + \hat{f}) = b_h + a_h \cdot \xi + q_h(\xi),$$

where

$$b_h = \int_{\Omega} j(f_0, u_h) dx,$$

the entries of $a_h := (a_{h,1}, \dots, a_{h,N})$ are given, for $i = 1, \dots, N$, by

$$a_{h,i} = \int_{\Omega} \left(\nabla_f j(f_0, u_h) \cdot f_i + \nabla_u j(f_0, u_h) \cdot u_{h,i}^1 \right) dx,$$

where $u_{h,i}^1$ is the solution of (3.12), and the error term $q_h(\xi)$ satisfies:

$$\forall \xi \in \mathbb{R}^N, \quad |q_h(\xi)| \leq C \|\widehat{f}\|_{L^2(\mathcal{O}, L^2(\Omega)^d)}^2 |\xi|^2.$$

Notice that the constant C involved in the last estimate is uniform with respect to h according to (3.22) and Proposition 2. Similarly, uniform bounds with respect to h can be given to the coefficients b_h and a_h , using the hypothesis $h_{\min} \leq h \leq h_{\max}$ and the usual a priori estimates for u_h and $u_{h,i}^1$.

Following the discussion of Section 2.2, we consider the *approximate failure probability* $\widetilde{\mathcal{P}}(h)$, defined as:

$$(3.23) \quad \widetilde{\mathcal{P}}(h) = \Phi \left(-\frac{\alpha - b_h}{|a_h|} \right),$$

where Φ stands for the cumulative distribution function of the normal law, defined by (2.10). The next result states that it is a rigorous uniform approximation of the true failure probability.

Proposition 7. *There exists a constant C (uniform with respect to $h \in \mathcal{U}_{ad}$) such that:*

$$\|\widehat{f}\|_{L^2(\mathcal{O}, L^2(\Omega)^d)} \leq \varepsilon \Rightarrow |\widetilde{\mathcal{P}}(h) - \mathcal{P}(h)| \leq C\varepsilon^2 |\log \varepsilon|^{\frac{N+1}{2}}.$$

Proof. Denote $\varepsilon = \|\widehat{f}\|_{L^2(\mathcal{O}, L^2(\Omega)^d)}$ and consider the cube $Y_\varepsilon := \left\{ \xi \in \mathbb{R}^N, \max_i |\xi_i| < r_\varepsilon \right\}$, of size r_ε yet to be chosen. It follows from the definitions that:

$$\begin{aligned} |\widetilde{\mathcal{P}}(h) - \mathcal{P}(h)| &\leq \frac{1}{(2\pi)^{\frac{N}{2}}} \int_{\mathbb{R}^N} e^{-\frac{|\xi|^2}{2}} \left| \mathbb{1}_{\{b_h + a_h \cdot \xi > \alpha\}} - \mathbb{1}_{\{b_h + a_h \cdot \xi + q_h(\xi) > \alpha\}} \right| d\xi \\ &\leq \frac{1}{(2\pi)^{\frac{N}{2}}} \left(\int_{Y_\varepsilon} e^{-\frac{|\xi|^2}{2}} \left| \mathbb{1}_{\{b_h + a_h \cdot \xi > \alpha\}} - \mathbb{1}_{\{b_h + a_h \cdot \xi + q_h(\xi) > \alpha\}} \right| d\xi + 2 \int_{\mathbb{R}^N \setminus Y_\varepsilon} e^{-\frac{|\xi|^2}{2}} d\xi \right). \end{aligned}$$

The second integral at the right-hand side can be estimated as:

$$\int_{\mathbb{R}^N \setminus Y_\varepsilon} e^{-\frac{|\xi|^2}{2}} d\xi \leq C \int_{\mathbb{R} \setminus [-r_\varepsilon, r_\varepsilon]} e^{-\frac{t^2}{2}} dt \leq Cr_\varepsilon \int_{\mathbb{R} \setminus [-1, 1]} e^{-\frac{r_\varepsilon^2 t^2}{2}} dt \leq Cr_\varepsilon \int_{\mathbb{R} \setminus [-1, 1]} e^{-\frac{r_\varepsilon^2 t}{2}} dt \leq \frac{C}{r_\varepsilon} e^{-\frac{r_\varepsilon^2}{2}}.$$

As for the first one, we have, estimating the distance between the two hyperspaces $\{b_h + a_h \cdot \xi > \alpha\}$ and $\{b_h + a_h \cdot \xi + q_h(\xi) > \alpha\}$:

$$\begin{aligned} \int_{Y_\varepsilon} e^{-\frac{|\xi|^2}{2}} \left| \mathbb{1}_{\{b_h + a_h \cdot \xi > \alpha\}} - \mathbb{1}_{\{b_h + a_h \cdot \xi + q_h(\xi) > \alpha\}} \right| d\xi &\leq Cr_\varepsilon^{N-1} \sup_{\xi \in Y_\varepsilon} |q_h(\xi)|, \\ &\leq C\varepsilon^2 r_\varepsilon^{N+1}. \end{aligned}$$

for some constant C , where we used the fact that, for any $\xi \in Y_\varepsilon$, $|q_h(\xi)| \leq C\varepsilon^2 r_\varepsilon^2$. Combining both estimates, and optimizing with respect to r_ε , namely taking $r_\varepsilon^2 = 4|\log \varepsilon|$, the desired result follows. \square

When it comes to the differentiation of $\widetilde{\mathcal{P}}(h)$, the result of interest is the following:

Theorem 8. *The functional $\widetilde{\mathcal{P}}(h)$, defined by (3.23), is Fréchet-differentiable at any $h \in \mathcal{U}_{ad}$, and its derivative $\widetilde{\mathcal{P}}'(h)(\widehat{h})$ in a direction $\widehat{h} \in L^\infty(\Omega)$ reads:*

$$(3.24) \quad \widetilde{\mathcal{P}}'(h)(\widehat{h}) = \frac{1}{\sqrt{2\pi}} e^{-\frac{1}{2} \left(\frac{\alpha - b_h}{|a_h|} \right)^2} \int_{\Omega} \widehat{h} \left(\frac{1}{|a_h|} Ae(u_h) : e(p_h^0) + \frac{\alpha - b_h}{|a_h|^3} \left(Ae(u_h) : e(p_h^1) + \sum_{i=1}^N a_{h,i} Ae(u_{h,i}^1) : e(p_h^0) \right) \right) dx,$$

where the adjoint states $p_h^0, p_h^1 \in H_{\Gamma_D}^1(\Omega)^d$ are defined by the respective variational problems:

$$(3.25) \quad \forall v \in H_{\Gamma_D}^1(\Omega)^d, \quad \int_{\Omega} h Ae(p_h^0) : e(v) dx = - \int_{\Omega} \nabla_u j(f_0, u_h) \cdot v dx,$$

$$(3.26) \quad \forall v \in H_{\Gamma_D}^1(\Omega)^d, \int_{\Omega} h A e(p_h^1) : e(v) \, dx = \\ - \sum_{i=1}^N a_{h,i} \int_{\Omega} (\nabla_f \nabla_u j(f_0, u_h)(f_i, v) + \nabla_u^2 j(f_0, u_h)(u_{h,i}^1, v)) \, dx.$$

Proof. This is a rather straightforward calculation; a direct differentiation in (3.23) reveals:

$$\begin{aligned} \tilde{\mathcal{P}}'(h)(\hat{h}) &= \frac{1}{\sqrt{2\pi}} e^{-\frac{1}{2} \left(\frac{\alpha - b_h}{|a_h|} \right)^2} \left(\frac{1}{|a_h|} \int_{\Omega} \nabla_u j(f_0, u_h) \cdot \frac{\partial u_h}{\partial h}(\hat{h}) \, dx \right. \\ &\left. + \frac{\alpha - b_h}{|a_h|^3} \sum_{i=1}^N a_{h,i} \int_{\Omega} \left(\nabla_f \nabla_u j(f_0, u_h) \left(f_i, \frac{\partial u_h}{\partial h}(\hat{h}) \right) + \nabla_u^2 j(f_0, u_h) \left(u_{h,i}^1, \frac{\partial u_h}{\partial h}(\hat{h}) \right) + \nabla_u j(f_0, u_h) \cdot \frac{\partial u_{h,i}^1}{\partial h}(\hat{h}) \right) \, dx \right). \end{aligned}$$

Now, using the definition (3.25)-(3.26) of the adjoint states p_h^0, p_h^1 in combination with (3.16)-(3.17), we obtain the desired formula (3.24). \square

Example 3. In the situation of Example 1, namely when the cost function is the compliance, it is easily seen that $p_h^0 = -u_h$ and $p_h^1 = -\sum_{i=1}^N a_{h,i} u_{h,i}^1$. Then, formula (3.24) simply becomes:

$$\tilde{\mathcal{P}}'(h)(\hat{h}) = -\frac{1}{\sqrt{2\pi}} e^{-\frac{1}{2} \left(\frac{\alpha - b_h}{|a_h|} \right)^2} \int_{\Omega} \hat{h} \left(\frac{1}{|a_h|} A e(u_h) : e(u_h) + 2 \frac{\alpha - b_h}{|a_h|^3} \sum_{i=1}^N a_{h,i} A e(u_h) : e(u_{h,i}^1) \right) \, dx.$$

Remark 13. Overall through Section 3.2 we considered small perturbations $\hat{f} \in L^2(\mathcal{O}, L^2(\Omega)^d)$, in the sense that

$$\|\hat{f}\|_{L^2(\mathcal{O}, L^2(\Omega)^d)} \leq \varepsilon.$$

In particular, if we assume that \hat{f} is a finite sum of the form (3.10), namely $\hat{f}(x, \omega) = \sum_{i=1}^N f_i(x) \xi_i(\omega)$ with independent centered normalized random variables ξ_i , then necessarily the functions f_i are small in $L^2(\Omega)^d$: $\|f_i\|_{L^2(\Omega)^d} \leq \varepsilon$. Hence, (3.10) accounts for perturbations of small amplitude, which are distributed around 0 with respect to a normalized law.

In the case when ξ_i are centered and normalized Gaussian random variables, there is an interesting equivalent meaning of our assumption. Indeed, a simple change of variables reveals that (3.10) may be rewritten as:

$$(3.27) \quad \hat{f}(x, \omega) = \sum_{i=1}^N \frac{f_i(x)}{\varepsilon} \xi_{\varepsilon,i}(\omega),$$

where the $\xi_{\varepsilon,i}$ are centered Gaussian random variables, with standard deviation ε , i.e. with cumulative distribution function $\Phi_{\varepsilon}(x) = \frac{1}{\sqrt{2\pi\varepsilon}} \int_{-\infty}^x e^{-\frac{\xi^2}{2\varepsilon^2}} \, d\xi$. Since $\|f_i\|_{L^2(\Omega)^d} \leq \varepsilon$, under the form (3.27), \hat{f} appears as a sum of perturbations of unit amplitude, but which are ‘often’ concentrated around their mean value 0. This interpretation is valid for the whole Section 3.2.

3.3. Uncertainties over the elastic material’s properties.

We now turn to a somewhat different situation, in which the constituent material of the plate described in Section 3.1 undergoes random perturbations. For the sake of simplicity, let us assume that only its Young modulus E is prone to uncertainties, and that its Poisson ratio ν is deterministic. Under these circumstances, the Hooke’s tensor $A \equiv A(E)$ of the plate reads:

$$(3.28) \quad \forall e \in \mathcal{S}(\mathbb{R}^d), \quad A(E)e = 2\mu(E)e + \lambda(E)\text{tr}(e)I,$$

where the Lamé moduli $\lambda(E), \mu(E)$ of the material depend on E via the relations:

$$(3.29) \quad \lambda(E) = \frac{E\nu}{(1+\nu)(1-2\nu)} \quad \text{and} \quad \mu(E) = \frac{E}{2(1+\nu)}.$$

The displacement $u_{h,E}$ of the plate when the Young’s modulus is $E \in L^\infty(\Omega)$ is now the unique solution in $H_{\Gamma_D}^1(\Omega)^d$ of the system (3.1), where A is replaced by $A(E)$. To bring some variety in the model, the

mechanical performance is now assessed in terms of a cost function $\mathcal{C}(h, E)$ which is an integral on some part Γ of the boundary $\partial\Omega$ (instead of a bulk integral), i.e.

$$\mathcal{C}(h, E) = \int_{\Gamma} k(u_{h,E}) dx,$$

where $k : \mathbb{R}^d \rightarrow \mathbb{R}$ is a function of class \mathcal{C}^3 , and whose dependence on the space variable $x \in \Gamma$ is omitted. It satisfies adequate growth conditions, namely, there exists a constant $C > 0$ such that:

$$(3.30) \quad \forall u \in \mathbb{R}^d, |k(u)| \leq C(1 + |u|^2), |\nabla k(u)| \leq C(1 + |u|), |\nabla^2 k(u)| + |\nabla^3 k(u)| \leq C.$$

Again, more general cost functions could be devised, leading to similar developments.

In the following, $A = A(E_0)$ (resp. $\lambda = \lambda(E_0)$, $\mu = \mu(E_0)$, and $u_h = u_{h,E_0}$) is the Hooke's tensor (resp. the Lamé coefficients and the displacement) of the plate when no uncertainty holds. Besides, \bar{A} is the tensor defined by the relation $A(E) = E\bar{A}$, that is:

$$(3.31) \quad \forall e \in \mathcal{S}(\mathbb{R}^d), \bar{A}e = \frac{1}{2(1+\nu)}e + \frac{\nu}{(1+\nu)(1-2\nu)}\text{tr}(e)I.$$

3.3.1. Asymptotic expansion of the cost function.

We now consider 'small' perturbations over the Young modulus E around a reference configuration E_0 :

$$E(x) = E_0(x) + \hat{E}(x).$$

Both E_0 and \hat{E} are bounded functions which belong to $L^\infty(\Omega)$. We assume that E_0 is essentially bounded from below by a positive constant and we restrict ourselves to perturbations satisfying:

$$(3.32) \quad \|\hat{E}\|_{L^\infty(\Omega)} \leq \alpha, \text{ where } \alpha \text{ is a real number such that } \alpha < \inf_{x \in \Omega} E_0(x),$$

so that E is always bounded from below by a positive constant, and the system (3.1) makes sense (i.e. is coercive) as soon as (3.32) is satisfied.

Remark 14. Instead of imposing (3.32), it is customary, in particular in the engineering literature, to work with perturbed data of the form $E = E_0 + \chi(\hat{E})$, where \hat{E} may assume arbitrarily large values and χ is a cut-off function ensuring that E stays positive.

According to the general framework of Section 2, our first target is to achieve a first-, or second-order Taylor expansion of the function $\hat{E} \mapsto \mathcal{C}(h, E_0 + \hat{E})$ around 0.

Proposition 9. *The cost function $E \mapsto \mathcal{C}(h, E)$, from $L^\infty(\Omega)$ into \mathbb{R} , has the following expansion around $E_0 \in L^\infty(\Omega)$:*

$$(3.33) \quad \begin{aligned} \mathcal{C}(h, E_0 + \hat{E}) &= \int_{\Gamma} k(u_h) dx + \int_{\Gamma} \nabla k(u_h) \cdot u_h^1(\hat{E}) dx \\ &+ \frac{1}{2} \int_{\Gamma} \left(\nabla^2 k(u_h)(u_h^1(\hat{E}), u_h^1(\hat{E})) + \nabla k(u_h) \cdot u_h^2(\hat{E}, \hat{E}) \right) dx + R(\hat{E}), \end{aligned}$$

where $u_h^1(\hat{E}) := \frac{\partial u_{h,E}}{\partial E} \Big|_{E=E_0}(\hat{E})$, and $u_h^2(\hat{E}, \hat{E}) := \frac{\partial^2 u_{h,E}}{\partial E^2} \Big|_{E=E_0}(\hat{E}, \hat{E})$ are the first- and second-order sensitivities of the displacement $u_{h,E}$ with respect to the Young's modulus, and arise as the solutions to the respective variational problems:

$$\forall v \in H_{\Gamma_D}^1(\Omega)^d, \int_{\Omega} hAe(u_h^1(\hat{E})) : e(v) dx = - \int_{\Omega} h\hat{E}\bar{A}e(u_h) : e(v) dx.$$

$$\forall v \in H_{\Gamma_D}^1(\Omega)^d, \int_{\Omega} hAe(u_h^2(\hat{E}, \hat{E})) : e(v) dx = -2 \int_{\Omega} h\hat{E}\bar{A}e(u_h^1(\hat{E})) : e(v) dx.$$

There exist positive constants $\delta, C > 0$ (which do not depend on h) such that, if $\|\hat{E}\|_{L^\infty(\Omega)} \leq \delta$, then the residual $R(\hat{E})$ satisfies

$$(3.34) \quad |R(\hat{E})| \leq C\|\hat{E}\|_{L^\infty(\Omega)}^3.$$

Proof. First, let us notice that a similar result to Lemma 1 holds in the present situation (and is proved in the same way), according to which the function $\mathcal{U}_{ad} \times L^\infty(\Omega) \ni (h, E) \mapsto u_{h,E} \in H_{\Gamma_D}^1(\Omega)^d$ enjoys \mathcal{C}^∞ regularity. A Taylor expansion of the cost function $E \mapsto \mathcal{C}(h, E)$ then immediately yields (3.33), with residual:

$$R(\widehat{E}) = \int_{\Omega} \int_0^1 \frac{\partial^3 \mathcal{C}}{\partial E^3}(h, E_0 + t\widehat{E})(\widehat{E}, \widehat{E}, \widehat{E}) dt dx.$$

Eventually (3.34) follows from the hypotheses (3.30) and from the variational problems satisfied by the various partial derivatives of $E \mapsto u_{h,E}$. \square

3.3.2. Introduction of uncertainties and calculation of an approximate mean value function.

Let us now assume that the perturbation \widehat{E} is uncertain, i.e. it arises as a random field $\widehat{E} \equiv \widehat{E}(x, \omega)$, depending on the space variable $x \in \Omega$ and on an uncertainty variable $\omega \in \mathcal{O}$, where $(\mathcal{O}, \mathcal{F}, \mathbb{P})$ is an abstract probability space. The objective function of interest in this section is the mean value $\mathcal{M}(h)$ of the cost function $\mathcal{C}(h, u_{h, E_0 + \widehat{E}(\cdot, \omega)})$ over all the possible events ω :

$$\mathcal{M}(h) = \int_{\mathcal{O}} \mathcal{C}(h, E_0 + \widehat{E}(\cdot, \omega)) \mathbb{P}(d\omega).$$

To give a rigorous setting to the approximation of this functional, let us first rely on the (restrictive) assumption that $\widehat{E} \in L^\infty(\mathcal{O}, L^\infty(\Omega))$. Hence, if \widehat{E} is small for such a norm, then almost every realization $\widehat{E}(\cdot, \omega)$ is small in the $L^\infty(\Omega)$ norm.

The following proposition is now an easy consequence of Proposition 9.

Proposition 10. *The approximate mean value function $\widetilde{\mathcal{M}}(h)$, defined as:*

$$(3.35) \quad \begin{aligned} \widetilde{\mathcal{M}}(h) = & \int_{\Gamma} k(u_h) dx + \int_{\mathcal{O}} \int_{\Gamma} \nabla k(u_h) \cdot u_h^1(\widehat{E}) dx \mathbb{P}(d\omega) \\ & + \frac{1}{2} \int_{\mathcal{O}} \int_{\Gamma} \left(\nabla^2 k(u_h)(u_h^1(\widehat{E}), u_h^1(\widehat{E})) + \nabla k(u_h) \cdot u_h^2(\widehat{E}, \widehat{E}) \right) dx \mathbb{P}(d\omega), \end{aligned}$$

is a consistent approximation of $\mathcal{M}(h)$ in the sense that there exist positive constants $\delta, C > 0$ (which do not depend on h) such that, if $\|\widehat{E}\|_{L^\infty(\Omega)} \leq \delta$, then

$$\left| \mathcal{M}(h) - \widetilde{\mathcal{M}}(h) \right| \leq C \|\widehat{E}\|_{L^\infty(\mathcal{O}, L^\infty(\Omega))}^3.$$

As remarked previously, the definition of the approximate mean value $\widetilde{\mathcal{M}}(h)$ makes sense for a wider class of perturbations, and it is somehow natural to consider the case $\widehat{E} \in L^2(\mathcal{O}, L^\infty(\Omega))$ (which leaves room for perturbations of large amplitude, occurring on ‘rare’ sets of events). In line with the general framework of Section 2, we now assume that \widehat{E} is a finite sum

$$(3.36) \quad \widehat{E}(x, \omega) = \sum_{i=1}^N E_i(x) \xi_i(\omega),$$

where the $E_i \in L^\infty(\Omega)$ are deterministic functions, and the ξ_i are uncorrelated, normalized (e.g. Gaussian) random variables. Inserting (3.36) into (3.35) yields:

$$(3.37) \quad \widetilde{\mathcal{M}}(h) = \int_{\Gamma} k(u_h) dx + \frac{1}{2} \sum_{i=1}^N \int_{\Gamma} \nabla^2 k(u_h)(u_{h,i}^1, u_{h,i}^1) dx + \frac{1}{2} \int_{\Gamma} \nabla k(u_h) \cdot u_h^2 dx,$$

with the reduced sensitivities $u_{h,i}^1 := u_h^1(E_i)$ and $u_h^2 := \sum_{i=1}^N u_h^2(E_i, E_i)$, which are respectively solutions to the following variational problems:

$$(3.38) \quad \forall v \in H_{\Gamma_D}^1(\Omega)^d, \quad \int_{\Omega} h A e(u_{h,i}^1) : e(v) dx = - \int_{\Omega} h E_i \bar{A} e(u_h) : e(v) dx,$$

$$(3.39) \quad \forall v \in H_{\Gamma_D}^1(\Omega)^d, \quad \int_{\Omega} h A e(u_h^2) : e(v) \, dx = -2 \sum_{i=1}^N \int_{\Omega} h E_i \bar{A} e(u_{h,i}^1) : e(v) \, dx.$$

3.3.3. *Derivative of the approximate mean-value function.*

Let us now proceed to the calculation of the derivative of $\widetilde{\mathcal{M}}$.

Theorem 11. *The functional $\widetilde{\mathcal{M}}(h)$ defined by (3.37) is Fréchet-differentiable at any point $h \in \mathcal{U}_{ad}$, and its derivative $\widetilde{\mathcal{M}}'(h)(\widehat{h})$ in an arbitrary direction $\widehat{h} \in L^\infty(\Omega)$ reads:*

$$\begin{aligned} \widetilde{\mathcal{M}}'(h)(\widehat{h}) &= \frac{1}{2} \int_{\Omega} \widehat{h} A e(u_h^2) : e(p_h^0) \, dx + \sum_{i=1}^N \int_{\Omega} \widehat{h} E_i \bar{A} e(u_{h,i}^1) : e(p_h^0) \, dx + \sum_{i=1}^N \int_{\Omega} \widehat{h} A e(u_{h,i}^1) : e(p_{h,i}^1) \, dx \\ &\quad + \sum_{i=1}^N \int_{\Omega} \widehat{h} E_i \bar{A} e(u_h) : e(p_{h,i}^1) \, dx + \int_{\Omega} \widehat{h} A e(u_h) : e(p_h^2) \, dx. \end{aligned}$$

where the adjoint states $p_h^0, p_{h,i}^1$, for $i = 1, \dots, N$, and p_h^2 are defined as the unique solutions in $H_{\Gamma_D}^1(\Omega)^d$ to the respective variational problems:

$$(3.40) \quad \forall v \in H_{\Gamma_D}^1(\Omega)^d, \quad \int_{\Omega} h A(p_h^0) : e(v) \, dx = - \int_{\Gamma} \nabla k(u_h) \cdot v \, ds,$$

$$(3.41) \quad \forall v \in H_{\Gamma_D}^1(\Omega)^d, \quad \int_{\Omega} h A(p_{h,i}^1) : e(v) \, dx = - \int_{\Gamma} \nabla^2 k(u_h)(u_{h,i}^1, v) \, ds - \int_{\Omega} h E_i \bar{A} e(v) : e(p_h^0) \, dx,$$

$$(3.42) \quad \forall v \in H_{\Gamma_D}^1(\Omega)^d, \quad \int_{\Omega} h A(p_h^2) : e(v) \, dx = - \int_{\Gamma} \nabla k(u_h) \cdot v \, ds - \frac{1}{2} \int_{\Gamma} \nabla^2 k(u_h)(u_h^2, v) \, ds \\ - \frac{1}{2} \int_{\Gamma} \sum_{i=1}^N \nabla^3 k(u_h)(u_{h,i}^1, u_{h,i}^1, v) \, ds - \sum_{i=1}^N \int_{\Omega} h E_i \bar{A} e(v) : e(p_{h,i}^1) \, dx.$$

Proof. Take $\widehat{h} \in L^\infty(\Omega)$. A direct differentiation in (3.37) and some reordering lead to:

$$(3.43) \quad \begin{aligned} \widetilde{\mathcal{M}}'(h)(\widehat{h}) &= \int_{\Gamma} \nabla k(u_h) \cdot \frac{\partial u_h}{\partial h}(\widehat{h}) \, ds + \frac{1}{2} \int_{\Gamma} \nabla^2 k(u_h) \left(u_h^2, \frac{\partial u_h}{\partial h}(\widehat{h}) \right) \, ds \\ &+ \frac{1}{2} \int_{\Gamma} \sum_{i=1}^N \nabla^3 k(u_h) \left(u_{h,i}^1, u_{h,i}^1, \frac{\partial u_h}{\partial h}(\widehat{h}) \right) \, ds + \int_{\Gamma} \sum_{i=1}^N \nabla^2 k(u_h) \left(u_{h,i}^1, \frac{\partial u_{h,i}^1}{\partial h}(\widehat{h}) \right) \, ds + \frac{1}{2} \int_{\Gamma} \nabla k(u_h) \cdot \frac{\partial u_h^2}{\partial h}(\widehat{h}) \, ds. \end{aligned}$$

Furthermore, differentiating with respect to h in the variational formulations (3.4), (3.38), (3.39) produces, for arbitrary test function $v \in H_{\Gamma_D}^1(\Omega)^d$,

$$(3.44) \quad \int_{\Omega} h A e \left(\frac{\partial u_h}{\partial h}(\widehat{h}) \right) : e(v) \, dx = - \int_{\Omega} \widehat{h} A e(u_h) : e(v) \, dx,$$

$$(3.45) \quad \int_{\Omega} h A e \left(\frac{\partial u_{h,i}^1}{\partial h}(\widehat{h}) \right) : e(v) \, dx = - \int_{\Omega} \widehat{h} A e(u_{h,i}^1) : e(v) \, dx - \int_{\Omega} \widehat{h} E_i \bar{A} e(u_h) : e(v) \, dx \\ - \int_{\Omega} h E_i \bar{A} e \left(\frac{\partial u_h}{\partial h}(\widehat{h}) \right) : e(v) \, dx,$$

$$(3.46) \quad \int_{\Omega} h A e \left(\frac{\partial u_h^2}{\partial h}(\hat{h}) \right) : e(v) \, dx = - \int_{\Omega} \hat{h} A e(u_h^2) : e(v) \, dx - 2 \sum_{i=1}^N \int_{\Omega} \hat{h} E_i \bar{A} e(u_{h,i}^1) : e(v) \, dx \\ - 2 \sum_{i=1}^N \int_{\Omega} h E_i \bar{A} e \left(\frac{\partial u_{h,i}^1}{\partial h}(\hat{h}) \right) : e(v) \, dx.$$

Combining (3.46) with (3.40) and inserting in (3.43) yield:

$$\begin{aligned} \widetilde{\mathcal{M}}'(h)(\hat{h}) &= \frac{1}{2} \int_{\Omega} \hat{h} A e(u_h^2) : e(p_h^0) \, dx + \sum_{i=1}^N \int_{\Omega} \hat{h} E_i \bar{A} e(u_{h,i}^1) : e(v) \, dx + \int_{\Gamma} \nabla k(u_h) \cdot \frac{\partial u_h}{\partial h}(\hat{h}) \, ds \\ &+ \frac{1}{2} \int_{\Gamma} \nabla^2 k(u_h) \left(u_h^2, \frac{\partial u_h}{\partial h}(\hat{h}) \right) \, ds + \frac{1}{2} \int_{\Gamma} \sum_{i=1}^N \nabla^3 k(u_h) \left(u_{h,i}^1, u_{h,i}^1, \frac{\partial u_h}{\partial h}(\hat{h}) \right) \, ds + \int_{\Gamma} \sum_{i=1}^N \nabla^2 k(u_h) \left(u_{h,i}^1, \frac{\partial u_{h,i}^1}{\partial h}(\hat{h}) \right) \, ds \\ &+ \sum_{i=1}^N \int_{\Omega} h E_i \bar{A} e \left(\frac{\partial u_{h,i}^1}{\partial h}(\hat{h}) \right) : e(p_h^0) \, dx. \end{aligned}$$

Now using (3.45) together with the definition (3.41) makes it possible to eliminate the sensitivities $\frac{\partial u_{h,i}^1}{\partial h}$ from the last expression:

$$\begin{aligned} \widetilde{\mathcal{M}}'(h)(\hat{h}) &= \frac{1}{2} \int_{\Omega} \hat{h} A e(u_h^2) : e(p_h^0) \, dx + \sum_{i=1}^N \int_{\Omega} \hat{h} E_i \bar{A} e(u_{h,i}^1) : e(v) \, dx + \sum_{i=1}^N \int_{\Omega} \hat{h} A e(u_{h,i}^1) : e(p_{h,i}^1) \, dx \\ &+ \sum_{i=1}^N \int_{\Omega} \hat{h} E_i \bar{A} e(u_h) : e(p_{h,i}^1) \, dx + \int_{\Gamma} \nabla k(u_h) \cdot \frac{\partial u_h}{\partial h}(\hat{h}) \, ds + \frac{1}{2} \int_{\Gamma} \nabla^2 k(u_h) \left(u_h^2, \frac{\partial u_h}{\partial h}(\hat{h}) \right) \, ds \\ &+ \frac{1}{2} \int_{\Gamma} \sum_{i=1}^N \nabla^3 k(u_h) \left(u_{h,i}^1, u_{h,i}^1, \frac{\partial u_h}{\partial h}(\hat{h}) \right) \, ds + \sum_{i=1}^N \int_{\Omega} h E_i \bar{A} e \left(\frac{\partial u_{h,i}^1}{\partial h}(\hat{h}) \right) : e(p_{h,i}^1) \, dx. \end{aligned}$$

Eventually, using the definition (3.42) of p_h^2 and (3.44) yields the desired formula. \square

Example 4. To obtain a context similar to that of Example 1, namely if we want to consider the compliance as the cost function, we have to assume that $f = 0$, $\Gamma = \Gamma_N$ and $k(u) = g \cdot u$. Then, it is easily seen that $\nabla k(u) = g$ and $\nabla^2 k(u) = \nabla^3 k(u) = 0$, which implies $p_h^0 = -u_h$, $p_{h,i}^1 = -u_{h,i}^1$ and $p_h^2 = -u_h^0 - \frac{1}{2} u_h^2$. This implies some simplifications in the formula for the derivative $\widetilde{\mathcal{M}}'(h)(\hat{h})$.

4. RANDOM GEOMETRIC OPTIMIZATION

4.1. Description of the setting.

We now turn to the framework of geometric optimization, still in the context of linear elastic structures. A *shape* is a bounded, Lipschitz domain $\Omega \subset \mathbb{R}^d$, filled with a linear elastic material with Hooke's law A , defined by (3.2) (we shall often assume more regularity for the shapes). Every such shape is clamped on a part Γ_D of its boundary, submitted to body forces $f \in H^1(\mathbb{R}^d)^d$ and surface loads $g \in H^2(\mathbb{R}^d)^d$, applied on a subset $\Gamma_N \subset \partial\Omega$ disjoint from Γ_D , and only its *free boundary* $\Gamma := \partial\Omega \setminus (\Gamma_D \cup \Gamma_N)$ is subject to optimization (see Figure 2 for an illustration).

Recalling definition (3.3) of the space $H_{\Gamma_D}^1(\Omega)^d$, the displacement u_{Ω} of a shape Ω under these circumstances is the unique solution in $H_{\Gamma_D}^1(\Omega)^d$ of the linear elasticity system:

$$(4.1) \quad \begin{cases} -\operatorname{div}(Ae(u)) = f & \text{in } \Omega \\ u = 0 & \text{on } \Gamma_D \\ Ae(u)n = g & \text{on } \Gamma_N \\ Ae(u)n = 0 & \text{on } \Gamma \end{cases}.$$

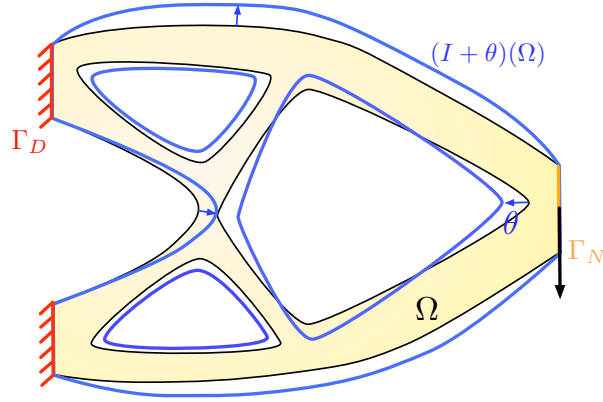


FIGURE 2. *Setting of the geometric optimization problems.*

For some objective function $J(\Omega)$ we consider the optimization problem

$$\inf_{\Omega \in \mathcal{U}_{ad}} J(\Omega),$$

with the set of admissible shapes

$$(4.2) \quad \mathcal{U}_{ad} := \{\Omega \subset \mathbb{R}^d \text{ is open, bounded and Lipschitz, } \Gamma_D \cup \Gamma_N \subset \partial\Omega\}.$$

When it comes to evaluating the sensitivity of such functionals, we rely on *Hadamard's boundary variation* method - see e.g. [29, 35, 45]. In a nutshell, variations of a shape Ω of the form:

$$\Omega_\theta := (I + \theta)(\Omega), \quad \theta \in W^{1,\infty}(\mathbb{R}^d, \mathbb{R}^d), \quad \|\theta\|_{W^{1,\infty}(\mathbb{R}^d, \mathbb{R}^d)} < 1$$

are considered, thus leading to the following notion of differentiation with respect to the domain:

Definition 1. *A functional $J(\Omega)$ of the domain is shape differentiable at Ω provided the underlying function $\theta \mapsto J((I + \theta)(\Omega))$, from $W^{1,\infty}(\mathbb{R}^d, \mathbb{R}^d)$ into \mathbb{R} is Fréchet differentiable at $\theta = 0$. The shape derivative $J'(\Omega)$ of J at Ω is the corresponding Fréchet differential, and the following asymptotic expansion holds in the vicinity of $0 \in W^{1,\infty}(\mathbb{R}^d, \mathbb{R}^d)$:*

$$(4.3) \quad J(\Omega_\theta) = J(\Omega) + J'(\Omega)(\theta) + o(\theta), \quad \text{where } \lim_{\theta \rightarrow 0} \frac{|o(\theta)|}{\|\theta\|_{W^{1,\infty}(\mathbb{R}^d, \mathbb{R}^d)}} = 0.$$

In practice, so as to ensure that the considered variations of shapes $\Omega \in \mathcal{U}_{ad}$ stay admissible, we have to restrict the set of considered deformations to:

$$(4.4) \quad \Theta_{ad} := \{\theta \in W^{1,\infty}(\mathbb{R}^d, \mathbb{R}^d), \text{ such that } \theta = 0 \text{ on } \Gamma_D \cup \Gamma_N\}.$$

Remark 15. The various approximations and shape differentiability results discussed in the sequel require some additional smoothness of solutions to linear elasticity systems of the form (4.1). Such smoothness is a classical result in the linear elasticity theory [18] and in the shape optimization literature [1, 29, 35, 45], provided the featured data (notably f, g , and the domain Ω itself) are smooth enough. In the following developments, we will implicitly and systematically assume that the data at hand are smooth enough, and that the sets \mathcal{U}_{ad} and Θ_{ad} encompass additional regularity requirements, so that all our calculations are legitimate.

Remark 16. In most cases the proposed approximate objective functionals can be proved to be uniformly close from the original objective functionals. Since the analysis of this issue is identical to that of its parametric counterpart in Section 3, for the sake of brevity we shall not dwell on it.

4.2. Random perturbations over the body forces in shape optimization.

This section is the mirror of Section 3.2, in the context of shape optimization. Here again, our purpose is not to achieve utter generality, but rather to investigate a simple situation, in which the ideas of Section 2 can be conveniently illustrated.

Let us denote as $u_{\Omega, f} \in H_{\Gamma_D}^1(\Omega)^d$ the displacement of a shape $\Omega \in \mathcal{U}_{ad}$, unique solution to the system (4.1), when body forces f are applied but surface loads are neglected (i.e. $g = 0$). The performance of such a shape Ω is evaluated in terms of a *cost function* $\mathcal{C}(\Omega, f)$ of the form:

$$\mathcal{C}(\Omega, f) = \int_{\Omega} j(f, u_{\Omega, f}) \, dx,$$

where $j : \mathbb{R}^d \times \mathbb{R}^d \rightarrow \mathbb{R}$ is smooth of class \mathcal{C}^3 , and satisfies the growth conditions (3.6). The body forces f are of the form:

$$f = f_0 + \widehat{f},$$

where f_0 is a mean value and \widehat{f} are expected perturbations, which will soon be assumed to be random.

4.2.1. Second-order expansion of the cost function and introduction of random perturbations.

As we have seen previously, a first step is to obtain a Taylor expansion of the mapping $f \mapsto \mathcal{C}(\Omega, f)$ around f_0 . As in Proposition 2 (for parametric optimization) we assume some higher integrability of the forces in $L^3(\mathbb{R}^d)^d$ in order to justify the following result (the proof of which is safely left to the reader).

Proposition 12. *The cost function $f \mapsto \mathcal{C}(\Omega, f)$, from $L^3(\mathbb{R}^d)^d$ into \mathbb{R} has the following expansion around $f_0 \in L^3(\mathbb{R}^d)^d$:*

$$(4.5) \quad \begin{aligned} \mathcal{C}(\Omega, f_0 + \widehat{f}) &= \int_{\Omega} j(f_0, u_{\Omega}) \, dx + \int_{\Omega} \left(\nabla_f j(f_0, u_{\Omega}) \cdot \widehat{f} + \nabla_u j(f_0, u_{\Omega}) \cdot u_{\Omega}^1(\widehat{f}) \right) \, dx \\ &+ \frac{1}{2} \int_{\Omega} \left(\nabla_f^2 j(f_0, u_{\Omega})(\widehat{f}, \widehat{f}) + 2 \nabla_f \nabla_u j(f_0, u_{\Omega})(\widehat{f}, u_{\Omega}^1(\widehat{f})) + \nabla_u^2 j(f_0, u_{\Omega})(u_{\Omega}^1(\widehat{f}), u_{\Omega}^1(\widehat{f})) \right) \, dx + R(\widehat{f}), \end{aligned}$$

where u_{Ω} stands for the unperturbed state u_{Ω, f_0} , and $u_{\Omega}^1(\widehat{f})$ is the first-order derivative $u_{\Omega}^1(\widehat{f}) = \left. \frac{\partial u_{\Omega, f}}{\partial f} \right|_{f=f_0}(\widehat{f})$, unique solution in $H_{\Gamma_D}^1(\Omega)^d$ of the variational problem:

$$\forall v \in H_{\Gamma_D}^1(\Omega)^d, \quad \int_{\Omega} Ae(u_{\Omega}^1(\widehat{f})) : e(v) \, dx = \int_{\Omega} \widehat{f} \cdot v \, dx.$$

There exists a constant $C > 0$ (depending on Ω) such that the residual $R(\widehat{f})$ is controlled as:

$$\forall \widehat{f} \in L^3(\mathbb{R}^d)^d, \quad |R(\widehat{f})| \leq C \|\widehat{f}\|_{L^3(\mathbb{R}^d)^d}^3.$$

4.2.2. Study of the mean-value of the considered cost function.

Let us now assume that the considered perturbations are described as random fields $\widehat{f} \equiv \widehat{f}(x, \omega)$, where ω is an event lying in the probability space $(\mathcal{O}, \mathcal{F}, \mathbb{P})$. As in Section 3.2, in order to achieve rigorous approximation results, we assume at first that $\widehat{f} \in L^3(\mathcal{O}, L^3(\mathbb{R}^d)^d)$.

The objective function of interest is the mean value $\mathcal{M}(\Omega)$ of \mathcal{C} :

$$\mathcal{M}(\Omega) = \int_{\mathcal{O}} \mathcal{C}(\Omega, f(\cdot, \omega)) \, \mathbb{P}(d\omega),$$

which we approximate along the lines of the following result:

Proposition 13. *The approximate mean value function $\widetilde{\mathcal{M}}(\Omega)$, defined as:*

$$(4.6) \quad \begin{aligned} \widetilde{\mathcal{M}}(\Omega) &= \int_{\Omega} j(f_0, u_{\Omega}) dx + \int_{\mathcal{O}} \int_{\Omega} \left(\nabla_f j(f_0, u_{\Omega}) \cdot \widehat{f} + \nabla_u j(f_0, u_{\Omega}) \cdot u_{\Omega}^1(\widehat{f}) \right) dx \mathbb{P}(d\omega) \\ &+ \frac{1}{2} \int_{\mathcal{O}} \int_{\Omega} \left(\nabla_f^2 j(f_0, u_{\Omega})(\widehat{f}, \widehat{f}) + 2\nabla_f \nabla_u j(f_0, u_{\Omega})(\widehat{f}, u_{\Omega}^1(\widehat{f})) + \nabla_u^2 j(f_0, u_{\Omega})(u_{\Omega}^1(\widehat{f}), u_{\Omega}^1(\widehat{f})) \right) dx \mathbb{P}(d\omega), \end{aligned}$$

approximates $\mathcal{M}(\Omega)$ in the sense that there exists a constant $C > 0$ (depending on Ω) such that:

$$|\widetilde{\mathcal{M}}(\Omega) - \mathcal{M}(\Omega)| \leq C \|\widehat{f}\|_{L^3(\mathcal{O}, L^3(\mathbb{R}^d))}^3.$$

As usual, we notice that the definition (4.6) makes sense for more general perturbations than $\widehat{f} \in L^3(\mathcal{O}, L^3(\mathbb{R}^d))$; henceforth, we assume that it belongs to $L^2(\mathcal{O}, L^2(\mathbb{R}^d))$, and enjoys the particular structure:

$$\widehat{f}(x, \omega) = \sum_{i=1}^N f_i(x) \xi_i(\omega),$$

where the functions $f_i \in L^2(\mathbb{R}^d)$ are deterministic, and the ξ_i are centered, normalized and uncorrelated random variables (i.e. (2.4) holds). In this context, $\widetilde{\mathcal{M}}(\Omega)$ rewrites:

$$(4.7) \quad \begin{aligned} \widetilde{\mathcal{M}}(\Omega) &= \int_{\Omega} j(f_0, u_{\Omega}) dx + \frac{1}{2} \sum_{i=1}^N \int_{\Omega} \nabla_f^2 j(f_0, u_{\Omega})(f_i, f_i) dx \\ &+ \sum_{i=1}^N \int_{\Omega} \nabla_f \nabla_u j(f_0, u_{\Omega})(f_i, u_{\Omega,i}^1) dx + \frac{1}{2} \sum_{i=1}^N \int_{\Omega} \nabla_u^2 j(f_0, u_{\Omega})(u_{\Omega,i}^1, u_{\Omega,i}^1) dx, \end{aligned}$$

with $u_{\Omega,i} := u_{\Omega}^1(f_i)$. When it comes to differentiating this functional, the result of interest is the following, whose proof is almost identical to that of Theorem 4 and thus omitted.

Theorem 14. *Assume that the functions f_i enjoy additional regularity (typically, $f_i \in H^1(\mathbb{R}^d)$); the function $\widetilde{\mathcal{M}}(\Omega)$ given by (4.7) is shape differentiable at any $\Omega \in \mathcal{U}_{ad}$, and its derivative reads:*

$$\forall \theta \in \Theta_{ad}, \quad \widetilde{\mathcal{M}}'(\Omega)(\theta) = \int_{\Gamma} \mathcal{D}(u_{\Omega}, p_{\Omega}^0, u_{\Omega,1}^1, \dots, u_{\Omega,N}^1, p_{\Omega,1}^1, \dots, p_{\Omega,N}^1) \theta \cdot n ds,$$

where the integrand is:

$$\begin{aligned} \mathcal{D}(u_{\Omega}, p_{\Omega}^0, u_{\Omega,1}^1, \dots, u_{\Omega,N}^1, p_{\Omega,1}^1, \dots, p_{\Omega,N}^1) &= j(f_0, u_{\Omega}) + \frac{1}{2} \sum_{i=1}^N \nabla_f^2 j(f_0, u_{\Omega})(f_i, f_i) + \sum_{i=1}^N \nabla_f \nabla_u j(f_0, u_{\Omega})(f_i, u_{\Omega,i}^1) \\ &+ \frac{1}{2} \sum_{i=1}^N \nabla_u^2 j(f_0, u_{\Omega})(u_{\Omega,i}^1, u_{\Omega,i}^1) + Ae(u_{\Omega}) : e(p_{\Omega}^0) + \sum_{i=1}^N Ae(u_{\Omega,i}^1) : e(p_{\Omega,i}^1) - f_0 \cdot p_{\Omega}^0 - \sum_{i=1}^N f_i \cdot p_{\Omega,i}^1, \end{aligned}$$

and $p_{\Omega}^0, p_{\Omega,i}^1$ ($i = 1, \dots, N$) are $(N+1)$ adjoint states, defined as the unique solutions in $H_{\Gamma_D}^1(\Omega)^d$ of the variational problems:

$$\begin{aligned} \forall v \in H_{\Gamma_D}^1(\Omega)^d, \quad \int_{\Omega} Ae(p_{\Omega}^0) : e(v) dx &= - \int_{\Omega} \nabla_u j(f_0, u_{\Omega}) \cdot v dx - \frac{1}{2} \sum_{i=1}^N \int_{\Omega} \nabla_f^2 \nabla_u j(f_0, u_{\Omega})(f_i, f_i, v) dx \\ &- \sum_{i=1}^N \int_{\Omega} \nabla_f \nabla_u^2 j(f_0, u_{\Omega})(f_i, u_{\Omega,i}^1, v) dx - \frac{1}{2} \sum_{i=1}^N \int_{\Omega} \nabla_u^3 j(f_0, u_{\Omega})(u_{\Omega,i}^1, u_{\Omega,i}^1, v) dx, \\ \forall v \in H_{\Gamma_D}^1(\Omega)^d, \quad \int_{\Omega} Ae(p_{\Omega,i}^1) : e(v) dx &= - \int_{\Omega} (\nabla_f \nabla_u j(f_0, u_{\Omega})(f_i, v) + \nabla_u^2 j(f_0, u_{\Omega})(u_{\Omega,i}^1, v)) dx. \end{aligned}$$

Example 5. Let us specialize the above theorem in the case of the *compliance* as a cost function, that is: $j(f, u) = f \cdot u$. The relevant non-zero derivatives of j are:

$$\nabla_f j(f, u) = u, \quad \nabla_u j(f, u) = f, \quad \nabla_f \nabla_u j(f, u) = I,$$

and the approximate mean value function simplifies into:

$$\widetilde{\mathcal{M}}(\Omega) = \int_{\Omega} f_0 \cdot u_{\Omega} \, dx + \sum_{i=1}^N \int_{\Omega} f_i \cdot u_{\Omega,i}^1 \, dx.$$

The adjoint states then read: $p_{\Omega}^0 = -u_{\Omega}$, $p_{\Omega,i}^1 = -u_{\Omega,i}^1$, and the shape derivative of $\widetilde{\mathcal{M}}(\Omega)$ is, for any $\theta \in \Theta_{ad}$,

$$\widetilde{\mathcal{M}}'(\Omega)(\theta) = \int_{\Gamma} \left(2f_0 \cdot u_{\Omega} + 2 \sum_{i=1}^N f_i \cdot u_{\Omega,i}^1 - Ae(u_{\Omega}) : e(u_{\Omega}) - \sum_{i=1}^N Ae(u_{\Omega,i}^1) : e(u_{\Omega,i}^1) \right) \theta \cdot n \, ds.$$

Again, $\mathcal{M}(\Omega)$ comes down to the multiple load objective function of [4].

Remark 17. When the cost function $\mathcal{C}(\Omega, f)$ is the compliance (which is a quadratic functional of f), its second-order Taylor expansion is exact. More precisely, we find that $\widetilde{\mathcal{M}}(\Omega) = \mathcal{M}(\Omega)$, which, as explained in the above example, coincides with the multiple load objective function. The special character of quadratic functionals for computing exactly mean values without any details of the uncertainty distribution has already been recognized by many authors, including [21] and [25].

4.2.3. Minimization of a failure probability associated to the cost $\mathcal{C}(\Omega, f)$.

We are now interested in the minimization of the failure probability:

$$\mathcal{P}(\Omega) = \mathbb{P}(\{\omega \in \mathcal{O}, \mathcal{C}(\Omega, f(\cdot, \omega)) > \alpha\}),$$

where α is the authorized tolerance over the values of \mathcal{C} . As suggested in Section 2 (see also Section 3.2.5), the approximate functional $\widetilde{\mathcal{P}}(\Omega)$ of interest is:

$$(4.8) \quad \widetilde{\mathcal{P}}(\Omega) = \Phi \left(-\frac{\alpha - b_{\Omega}}{|a_{\Omega}|} \right),$$

where $b_{\Omega} = \int_{\Omega} j(f_0, u_{\Omega}) \, dx$ and

$$a_{\Omega} := (a_{\Omega,1}, \dots, a_{\Omega,N}), \quad a_{\Omega,i} = \int_{\Omega} (\nabla_f j(f_0, u_{\Omega}) \cdot f_i + \nabla_u j(f_0, u_{\Omega}) \cdot u_{\Omega,i}^1) \, dx$$

are the coefficients involved in the first-order truncation of (4.5) (recall also that these coefficients may be rewritten by introducing an adjoint state; see Section 2.3). We assume that the f_i enjoy additional regularity, and that $a_{\Omega} \neq 0$, otherwise the function $\widetilde{\mathcal{P}}(\Omega)$ takes only the two values 0 and 1 (see Subsection 2.2).

Theorem 15. *The functional $\widetilde{\mathcal{P}}(\Omega)$ defined by (4.8) is shape differentiable at any $\Omega \in \mathcal{U}_{ad}$, and its shape derivative reads, for any $\theta \in \Theta_{ad}$,*

$$\widetilde{\mathcal{P}}(\Omega)'(\theta) = \frac{1}{\sqrt{2\pi}} e^{-\left(\frac{\alpha - b_{\Omega}}{|a_{\Omega}|}\right)^2} \int_{\Gamma} \mathcal{D}(u_{\Omega}, p_{\Omega}^0, u_{\Omega,1}, \dots, u_{\Omega,N}, p_{\Omega}^1) \theta \cdot n \, ds,$$

where the integrand is defined by:

$$\begin{aligned} \mathcal{D}(u_{\Omega}, p_{\Omega}^0, u_{\Omega,1}, \dots, u_{\Omega,N}, p_{\Omega}^1) &= \frac{1}{|a_{\Omega}|} j(f_0, u_{\Omega}) + \frac{\alpha - b_{\Omega}}{|a_{\Omega}|^3} \sum_{i=1}^N a_{\Omega,i} (\nabla_f j(f_0, u_{\Omega}) \cdot f_i + \nabla_u j(f_0, u_{\Omega}) \cdot u_{\Omega,i}) \\ &+ \frac{1}{|a_{\Omega}|} (Ae(u_{\Omega}) : e(p_{\Omega}^0) - f \cdot p_{\Omega}^0) + \frac{\alpha - b_{\Omega}}{|a_{\Omega}|^3} (Ae(u_{\Omega}) : e(p_{\Omega}^1) - f \cdot p_{\Omega}^1) \\ &+ \frac{\alpha - b_{\Omega}}{|a_{\Omega}|^3} \sum_{i=1}^N a_{\Omega,i} (Ae(u_{\Omega,i}^1) : e(p_{\Omega}^0) - f_i \cdot p_{\Omega}^0), \end{aligned}$$

and p_{Ω}^0 and $p_{\Omega}^1 \in H_{\Gamma_D}^1(\Omega)^d$ are two adjoint states, defined as the solutions to the following respective variational problems:

$$\forall v \in H_{\Gamma_D}^1(\Omega)^d, \quad \int_{\Omega} Ae(p_{\Omega}^0) : e(v) \, dx = - \int_{\Omega} \nabla_u j(f_0, u_{\Omega}) \cdot v \, dx,$$

$$\forall v \in H_{\Gamma_D}^1(\Omega)^d, \quad \int_{\Omega} Ae(p_{\Omega}^1) : e(v) \, dx = - \sum_{i=1}^N a_{\Omega,i} \int_{\Omega} (\nabla_f \nabla_u j(f_0, u_{\Omega})(f_i, v) + \nabla_u^2 j(f_0, u_{\Omega})(u_{\Omega,i}^1, v)) \, dx.$$

4.3. Random perturbations over the material's properties in shape optimization.

In this section, we briefly explain how the ideas of Section 3.3 readily extend to the shape optimization context. The developments being very similar, we solely outline the main results. Let us suppose that the Young's modulus E of the constituent material of the shapes Ω is subject to uncertainties, and consider the cost function $\mathcal{C}(\Omega, E)$ defined by:

$$\mathcal{C}(\Omega, E) = \int_{\Omega} j(u_{\Omega, E}) \, dx,$$

where the function $j : \mathbb{R}^d \rightarrow \mathbb{R}$ is smooth enough and satisfies adequate growth conditions, like (3.6) and (3.30). In this formula, $u_{\Omega, E}$ is the linear elastic displacement of Ω , solution of (4.1) when the Hooke's tensor A equals that $A(E)$ given by (3.28)-(3.29). As in Section 3.3, we assume 'small' random perturbations \widehat{E} around a reference Young's modulus E_0 , namely

$$E = E_0 + \widehat{E} \quad \text{with} \quad \widehat{E}(x, \omega) = \sum_{i=1}^N E_i(x) \xi_i(\omega),$$

where the $E_i \in L^\infty(\mathbb{R}^d)$ and the ξ_i are centered, normalized and uncorrelated random variables. In the following we use the shortcuts $A \equiv A(E_0)$, $\lambda \equiv \lambda(E_0)$, $\mu \equiv \mu(E_0)$, and $u_\Omega \equiv u_{\Omega, E_0}$ for quantities attached to the unperturbed situation.

The objective function of interest is the mean value $\mathcal{M}(\Omega)$ of the cost \mathcal{C} :

$$\mathcal{M}(\Omega) = \int_{\mathcal{O}} \mathcal{C}(\Omega, E_0 + \widehat{E}(\cdot, \omega)) \, \mathbb{P}(d\omega).$$

Following the steps of Section 3.3 gives rise to the approximate functional $\widetilde{\mathcal{M}}(\Omega)$ defined by:

$$(4.9) \quad \widetilde{\mathcal{M}}(\Omega) = \int_{\Omega} j(u_\Omega) \, dx + \frac{1}{2} \sum_{i=1}^N \int_{\Omega} \nabla^2 j(u_\Omega)(u_{\Omega, i}^1, u_{\Omega, i}^1) \, dx + \frac{1}{2} \int_{\Omega} \nabla j(u_\Omega) \cdot u_\Omega^2 \, dx,$$

where the sensitivities $u_{\Omega, i}^1$, $i = 1, \dots, N$ and u_Ω^2 are the solutions in $H_{\Gamma_D}^1(\Omega)^d$ to the variational problems:

$$\begin{aligned} \forall v \in H_{\Gamma_D}^1(\Omega)^d, \quad \int_{\Omega} A e(u_{\Omega, i}^1) : e(v) \, dx &= - \int_{\Omega} E_i \bar{A} e(u_\Omega) : e(v) \, dx, \\ \forall v \in H_{\Gamma_D}^1(\Omega)^d, \quad \int_{\Omega} A e(u_\Omega^2) : e(v) \, dx &= -2 \sum_{i=1}^N \int_{\Omega} E_i \bar{A} e(u_{\Omega, i}^1) : e(v) \, dx, \end{aligned}$$

where \bar{A} is defined in (3.31). Notice that, as in Sections 3.2, 3.3 and 4.2, a rigorous framework can be given to this approximation, which we do not insist on. The shape derivative is given by the following result.

Theorem 16. *Assume the functions E_i to be smooth. The functional $\widetilde{\mathcal{M}}(\Omega)$, defined by (4.9), is shape differentiable at any shape $\Omega \in \mathcal{U}_{ad}$, and its shape derivative reads, for any $\theta \in \Theta_{ad}$,*

$$\widetilde{\mathcal{M}}'(\Omega)(\theta) = \int_{\Gamma} \mathcal{D}(u_\Omega, u_{\Omega, 1}^1, p_{\Omega, 1}^1, \dots, u_{\Omega, N}^1, p_{\Omega, N}^1, u_\Omega^2, p_\Omega^2) \theta \cdot n \, dx,$$

where the integrand factor is defined by:

$$\begin{aligned} \mathcal{D}(u_\Omega, u_{\Omega, 1}^1, p_{\Omega, 1}^1, \dots, u_{\Omega, N}^1, p_{\Omega, N}^1, u_\Omega^2, p_\Omega^2) &= \left(j(u_\Omega) + \frac{1}{2} \sum_{i=1}^N \nabla^2 j(u_\Omega)(u_{\Omega, i}^1, u_{\Omega, i}^1) + \frac{1}{2} \nabla j(u_\Omega) \cdot u_\Omega^2 \right) \\ &+ A e(u_\Omega^2) : e(p_\Omega^0) + A e(u_\Omega) : e(p_\Omega^2) + \sum_{i=1}^N (E_i \bar{A} e(u_{\Omega, i}^1) : e(p_\Omega^0) + A e(u_{\Omega, i}^1) : e(p_{\Omega, i}^1) + E_i \bar{A} e(u_\Omega) : e(p_{\Omega, i}^1)), \end{aligned}$$

and the adjoint states p_Ω^0 , $p_{\Omega, i}^1$, $i = 1, \dots, N$, and p_Ω^2 are the unique solutions in $H_{\Gamma_D}^1(\Omega)^d$ to the respective variational problems:

$$\forall v \in H_{\Gamma_D}^1(\Omega)^d, \quad \int_{\Omega} A(p_\Omega^0) : e(v) \, dx = - \int_{\Omega} \nabla j(u_\Omega) \cdot v \, dx,$$

$$\forall v \in H_{\Gamma_D}^1(\Omega)^d, \int_{\Omega} A(p_{\Omega,i}^1) : e(v) dx = - \int_{\Gamma} \nabla^2 j(u_{\Omega}) (u_{\Omega,i}^1, v) dx - \int_{\Omega} E_i \bar{A} e(p_{\Omega}^0) : e(v) dx,$$

$$\begin{aligned} \forall v \in H_{\Gamma_D}^1(\Omega)^d, \int_{\Omega} A(p_{\Omega}^2) : e(v) dx &= - \int_{\Omega} \nabla j(u_{\Omega}) \cdot v dx - \frac{1}{2} \int_{\Omega} \nabla^2 j(u_{\Omega}) (u_{\Omega}^2, v) dx \\ &\quad - \frac{1}{2} \int_{\Omega} \sum_{i=1}^N \nabla^3 j(u_{\Omega}) (u_{\Omega,i}^1, u_{\Omega,i}^1, v) dx - \sum_{i=1}^N \int_{\Omega} E_i \bar{A} e(p_{\Omega,i}^1) : e(v) dx. \end{aligned}$$

4.4. Random optimization in frequency response.

Let us now outline an application of the proposed framework in the setting of frequency response problems. The shapes Ω under consideration are submitted to time-harmonic surface loads with frequency $\xi \in \mathbb{R}^+$, whose amplitude $g \in H^2(\mathbb{R}^d)^d$ is assumed to be independent of ξ for simplicity. Omitting body forces (i.e. $f = 0$), the displacement $u_{\Omega,\xi} \in H_{\Gamma_D}^1(\Omega)^d$ is then the solution of the system:

$$(4.10) \quad \begin{cases} -\operatorname{div}(Ae(u)) - \xi^2 u = 0 & \text{in } \Omega \\ u = 0 & \text{on } \Gamma_D \\ Ae(u)n = g & \text{on } \Gamma_N \\ Ae(u)n = 0 & \text{on } \Gamma \end{cases}.$$

This system has a unique solution, provided ξ^2 is not an eigenvalue of the linear elasticity operator featured in (4.1). Without loss of generality we consider the cost function:

$$\mathcal{C}(\Omega, \xi) = \int_{\Gamma_N} k(u_{\Omega,\xi}) ds,$$

where $k : \mathbb{R}^d \rightarrow \mathbb{R}$ is a smooth function, satisfying the growth conditions (3.30).

The frequency ξ is prone to perturbations in the sense that it is of the form $\xi = \xi_0 + \hat{\xi}$, where ξ_0 is a reference frequency, such that ξ_0^2 is not an eigenvalue for the system (4.1), and $\hat{\xi}$ is ‘small’. Under these circumstances, the cost function \mathcal{C} defined above has the following expansion:

$$(4.11) \quad \begin{aligned} \mathcal{C}(\Omega, \xi_0 + \hat{\xi}) &= \int_{\Gamma_N} k(u_{\Omega}) ds + \int_{\Gamma_N} \nabla k(u_{\Omega}) \cdot u_{\Omega}^1(\hat{\xi}) ds \\ &\quad + \frac{1}{2} \int_{\Gamma_N} \left(\nabla^2 k(u_{\Omega})(u_{\Omega}^1(\hat{\xi}), u_{\Omega}^1(\hat{\xi})) + \nabla k(u_{\Omega}) \cdot u_{\Omega}^2(\hat{\xi}, \hat{\xi}) \right) ds + \mathcal{O}(\hat{\xi}^3), \end{aligned}$$

a formula in which u_{Ω} stands for the unperturbed state u_{Ω,ξ_0} , and the sensitivities $u_{\Omega}^1(\hat{\xi}) := \left. \frac{\partial u_{\Omega,\xi}}{\partial \xi} \right|_{\xi=\xi_0}(\hat{\xi})$ and $u_{\Omega}^2(\hat{\xi}, \hat{\xi}) := \left. \frac{\partial^2 u_{\Omega,\xi}}{\partial \xi^2} \right|_{\xi=\xi_0}(\hat{\xi}, \hat{\xi})$ are respectively solution to:

$$\forall v \in H_{\Gamma_D}^1(\Omega)^d, \int_{\Omega} Ae(u_{\Omega}^1(\hat{\xi})) : e(v) dx - \xi_0^2 \int_{\Omega} u_{\Omega}^1(\hat{\xi}) \cdot v dx = 2\xi_0 \hat{\xi} \int_{\Omega} u_{\Omega} \cdot v dx,$$

$$\forall v \in H_{\Gamma_D}^1(\Omega)^d, \int_{\Omega} Ae(u_{\Omega}^2(\hat{\xi}, \hat{\xi})) : e(v) dx - \xi_0^2 \int_{\Omega} u_{\Omega}^2(\hat{\xi}, \hat{\xi}) \cdot v dx = 2\hat{\xi}^2 \int_{\Omega} u_{\Omega} \cdot v dx + 4\xi_0 \hat{\xi} \int_{\Omega} u_{\Omega}^1(\hat{\xi}) \cdot v dx.$$

We now assume that the perturbation $\hat{\xi}$ is uncertain, i.e. it arises as a random variable $\hat{\xi} \equiv \hat{\xi}(\omega) \in L^\infty(\mathcal{O}, \mathbb{R})$, defined over the probability space $(\mathcal{O}, \mathcal{F}, \mathbb{P})$, and is distributed according to the uniform law over the interval $(-m, m)$, where $m > 0$ is the ‘small’ amplitude of perturbations. In other words, the cumulative distribution function of $\hat{\xi}$ is:

$$\forall \bar{\xi} \in \mathbb{R}, \mathbb{P} \left(\left\{ \omega \in \mathcal{O}, \hat{\xi}(\omega) < \bar{\xi} \right\} \right) = \int_{-\infty}^{\bar{\xi}} \mathbf{1}_{(-m,m)}(t) dt;$$

its mean value is 0, and its variance equals $m^2/3$. We are interested in the minimization of the mean value functional

$$\mathcal{M}(\Omega) = \int_{\mathcal{O}} \mathcal{C}(\Omega, \xi_0 + \hat{\xi}(\omega)) \mathbb{P}(d\omega).$$

Integrating both sides of (4.11) over the space \mathcal{O} of events immediately leads to:

$$\mathcal{M}(\Omega) = \widetilde{\mathcal{M}}(\Omega) + \mathcal{O}(m^3).$$

In this formula, the approximate mean value function $\widetilde{\mathcal{M}}(\Omega)$ is defined by:

$$(4.12) \quad \widetilde{\mathcal{M}}(\Omega) = \int_{\Gamma_N} k(u_\Omega) ds + \frac{m^2}{6} \int_{\Gamma_N} (\nabla^2 k(u_\Omega)(u_\Omega^1, u_\Omega^1) + \nabla k(u_\Omega) \cdot u_\Omega^2) ds,$$

where we have introduced the reduced sensitivities $u_\Omega^1 := u_\Omega^1(1)$ and $u_\Omega^2 := u_\Omega^2(1,1)$. In the spirit of the previous Theorems 14 and 16 it is easy to obtain the following result.

Proposition 17. *Under the assumption that ξ_0^2 is not an eigenvalue of the system (4.1) for $\Omega \in \mathcal{U}_{ad}$, the functional $\widetilde{\mathcal{M}}(\Omega)$ is shape differentiable at Ω , and:*

$$(4.13) \quad \forall \theta \in \Theta_{ad}, \quad \widetilde{\mathcal{M}}'(\Omega)(\theta) = \int_{\Gamma} \mathcal{D}(u_\Omega, p_\Omega^0, u_\Omega^1, p_\Omega^1, u_\Omega^2, p_\Omega^2) \theta \cdot n ds,$$

where the integrand factor reads:

$$\begin{aligned} \mathcal{D}(u_\Omega, p_\Omega^0, u_\Omega^1, p_\Omega^1, u_\Omega^2, p_\Omega^2) &= Ae(u_\Omega) : e(p_\Omega^2) - \xi_0^2 u_\Omega \cdot p_\Omega^2 + \frac{m^2}{3} (Ae(u_\Omega^1) : e(p_\Omega^1) - \xi_0^2 u_\Omega^1 \cdot p_\Omega^1) \\ &\quad + \frac{m^2}{6} (Ae(u_\Omega^2) : e(p_\Omega^0) - \xi_0^2 u_\Omega^2 \cdot p_\Omega^0) - \frac{m^2}{3} (2\xi_0 u_\Omega \cdot p_\Omega^1 + 2\xi_0 u_\Omega^1 \cdot p_\Omega^0 + u_\Omega \cdot p_\Omega^0), \end{aligned}$$

and the adjoint states p_Ω^0 , p_Ω^1 and p_Ω^2 are the solutions to the respective problems:

$$\begin{aligned} \forall v \in H_{\Gamma_D}^1(\Omega)^d, \quad &\int_{\Omega} Ae(p_\Omega^0) : e(v) dx - \xi_0^2 \int_{\Omega} p_\Omega^0 \cdot v dx = - \int_{\Gamma_N} \nabla k(u_\Omega) \cdot v ds, \\ \forall v \in H_{\Gamma_D}^1(\Omega)^d, \quad &\int_{\Omega} Ae(p_\Omega^1) : e(v) dx - \xi_0^2 \int_{\Omega} p_\Omega^1 \cdot v dx = - \int_{\Gamma_N} \nabla^2 k(u_\Omega)(u_\Omega^1, v) ds + 2\xi_0 \int_{\Omega} p_\Omega^0 \cdot v dx, \\ \forall v \in H_{\Gamma_D}^1(\Omega)^d, \quad &\int_{\Omega} Ae(p_\Omega^2) : e(v) dx - \xi_0^2 \int_{\Omega} p_\Omega^2 \cdot v dx = - \int_{\Gamma_N} \nabla k(u_\Omega) \cdot v ds \\ &- \frac{m^2}{6} \int_{\Gamma_N} (\nabla^3 k(u_\Omega)(u_\Omega^1, u_\Omega^1, v) + \nabla^2 k(u_\Omega)(u_\Omega^2, v)) ds + \frac{m^2}{3} \int_{\Omega} p_\Omega^0 \cdot v dx + \frac{2\xi_0 m^2}{3} \int_{\Omega} p_\Omega^1 \cdot v dx. \end{aligned}$$

Example 6. Let us consider the compliance of shapes as a cost function, that is $k(u) = g \cdot u$. Straightforward calculations lead to the identifications:

$$p_\Omega^0 = -u_\Omega, \quad p_\Omega^1 = -u_\Omega^1, \quad \text{and} \quad p_\Omega^2 = -u_\Omega - \frac{m^2}{6} u_\Omega^2.$$

Then, the approximate functional $\widetilde{\mathcal{M}}(\Omega)$ reads:

$$\widetilde{\mathcal{M}}(\Omega) = \int_{\Gamma_N} g \cdot u_\Omega ds + \frac{m^2}{6} \int_{\Gamma_N} g \cdot u_\Omega^2 ds,$$

and the formula (4.13) for its shape derivative simplifies into:

$$\forall \theta \in \Theta_{ad}, \quad \widetilde{\mathcal{M}}'(\Omega)(\theta) = \int_{\Gamma} \mathcal{D}(u_\Omega, u_\Omega^1, u_\Omega^2) \theta \cdot n ds,$$

where:

$$\begin{aligned} \mathcal{D}(u_\Omega, u_\Omega^1, u_\Omega^2) &= -(Ae(u_\Omega) : e(u_\Omega) - \xi_0^2 u_\Omega \cdot u_\Omega) - \frac{m^2}{3} (Ae(u_\Omega) : e(u_\Omega^2) - \xi_0^2 u_\Omega \cdot u_\Omega^2) \\ &\quad - \frac{m^2}{3} ((Ae(u_\Omega^1) : e(u_\Omega^1) - \xi_0^2 u_\Omega^1 \cdot u_\Omega^1)) + \frac{m^2}{3} (4\xi_0 u_\Omega \cdot u_\Omega^1 + u_\Omega \cdot u_\Omega). \end{aligned}$$

4.5. Shape optimization under random geometric uncertainties.

4.5.1. A foreword about the modeling of random geometric uncertainties.

The definition of random perturbations over the geometry of shapes adopted in this note follows the most prevalent approach in the literature [14, 20, 41] - see however [30] for another idea in the framework of density-based topology optimization methods, relying on the so-called filtering technology.

Let $\Omega \in \mathcal{U}_{ad}$ be an admissible shape. We introduce two fixed open neighborhoods $U_1 \Subset U_2$ of the region $\Gamma_D \cup \Gamma_N$, and a smooth ‘cut-off’ function $\eta : \mathbb{R}^d \rightarrow \mathbb{R}$, taking its values in $[0, 1]$, enjoying the properties:

$$\eta \equiv 0 \text{ in } U_1, \text{ and } \eta \equiv 1 \text{ in } {}^c\overline{U_2}.$$

Perturbations of a shape $\Omega \in \mathcal{U}_{ad}$ are assumed of the form $(I + V)(\Omega)$, where V is a vector field with the structure:

$$(4.14) \quad \forall x \in \mathbb{R}^d, \quad V(x) = \eta(x)v(x)n_\Omega(x).$$

The scalar function $v : \mathbb{R}^d \rightarrow \mathbb{R}$ appearing in (4.14) is smooth enough, and n_Ω stands for an extension of the normal vector to Ω to the whole ambient space \mathbb{R}^d . We assume that the fixed parts Γ_D and Γ_N are not prone to uncertainties and the role of the cut-off function η is also to avoid any singularity due to the change of boundary conditions on Γ , Γ_N , Γ_D .

At this point, let us hint at the minimal regularity we should impose on shapes and their perturbations so that the developments ahead make sense. As we should now anticipate, deriving approximate mean value, variance functionals of some (smooth) cost criterion $\mathcal{C}(\Omega)$ require to differentiate it *twice* with respect to the domain. Hence, we need to assume at least that the shapes at hand are of class \mathcal{C}^3 , and that the scalar perturbation functions v are of class \mathcal{C}^2 . Doing so, there exists an extension of n_Ω to \mathbb{R}^d which is also of class \mathcal{C}^2 (see e.g. [24], chapter 7, Thm. 3.1, 3.3 and [29], §5.4.4 for a proof), so that the vector V is of class \mathcal{C}^2 . These hypotheses are precisely those required for second-order shape calculus (see e.g. [29], §5.9).

Let us now evoke the context where the perturbation function v is uncertain - i.e. it arises as a random field $v \equiv v(x, \omega)$, the event variable ω lying in the probability space $(\mathcal{O}, \mathcal{F}, \mathbb{P})$. The ‘natural’ functional space as for v when it comes to performing rigorous approximation analyses will obviously turn out to be $L^\infty(\mathcal{O}, \mathcal{C}^{2,\infty}(\mathbb{R}^d))$, so that (4.14) defines smooth enough perturbed shapes for a.e. event $\omega \in \mathcal{O}$ as soon as v is ‘small enough’. However, as a second step, in the same spirit as before, the derived approximate functionals will turn out to be well-defined for a wider class of perturbations.

4.5.2. Some definitions in tangential calculus.

The calculations of second-order shape derivatives ahead will involve several concepts of tangential calculus, which we now briefly outline. A more thorough reminder may be found in Section 2 in [3].

Definition 2. Let $\Gamma \subset \mathbb{R}^d$ be an oriented \mathcal{C}^2 submanifold of \mathbb{R}^d , of dimension $(d - 1)$.

- Let $V \in \mathcal{C}(\Gamma, \mathbb{R}^d)$ be a d -dimensional vector field defined on Γ . The tangential part V_Γ of V is the tangential vector field defined as:

$$V_\Gamma = V - (V \cdot n)n.$$

- Let $f \in \mathcal{C}^1(\Gamma, \mathbb{R})$ be a function, and, for an arbitrary point $x \in \Gamma$, let $df(x) : T_x\Gamma \rightarrow \mathbb{R}$ be its differential. The tangential gradient $\nabla_\Gamma f$ of f is the (unique) vector field on Γ defined by the following identity:

$$\forall x \in \Gamma, \quad \forall v \in T_x\Gamma, \quad df(x)(v) = \langle \nabla_\Gamma f(x), v \rangle,$$

where $\langle \cdot, \cdot \rangle$ stands for the Euclidean scalar product on \mathbb{R}^d . Alternatively, $\nabla_\Gamma f$ may be defined as:

$$\nabla_\Gamma f = (\nabla \tilde{f})_\Gamma = \nabla \tilde{f} - (\nabla \tilde{f} \cdot n)n,$$

where \tilde{f} is any \mathcal{C}^1 extension of f to a neighborhood of Γ .

- The tangential divergence $\text{div}_\Gamma(V) : \Gamma \rightarrow \mathbb{R}$ of a vector field $V \in \mathcal{C}^1(\Gamma, \mathbb{R}^d)$ is the function:

$$\text{div}_\Gamma(V) = \text{div}(\tilde{V}) - \nabla \tilde{V} n \cdot n,$$

where \tilde{V} is any \mathcal{C}^1 extension of V to a neighborhood of Γ .

- Let $\sigma : \Gamma \rightarrow \mathcal{S}(\mathbb{R}^d)$ be a tensor field defined on Γ . The tangential part $\sigma_{\tau\tau}$ of σ is the symmetric bilinear form on the tangent bundle $T\Gamma$ satisfying:

$$\forall x \in \Gamma, \forall v, w \in T_x\Gamma, \sigma_{\tau\tau}(x)(v, w) = \sigma(x)(v, w).$$

In a local orthonormal basis (τ, n) of \mathbb{R}^d obtained by gathering $(d-1)$ unit tangent vectors to Γ (collectively denoted by τ) and the normal vector n , σ may be expressed as:

$$\sigma = \begin{pmatrix} \sigma_{\tau\tau} & \sigma_{\tau n} \\ \sigma_{n\tau} & \sigma_{nn} \end{pmatrix}$$

Under the additional assumption that $\sigma \in \mathcal{C}^1(\Gamma, \mathcal{S}(\mathbb{R}^d))$, the tangential divergence $\operatorname{div}_\Gamma(\sigma) : \Gamma \rightarrow \mathbb{R}^d$ of σ is the vector field whose coordinates read:

$$(\operatorname{div}_\Gamma(\sigma))_i = (\operatorname{div}((\sigma_{i,j})_{j=1,\dots,d}))_\Gamma, \quad i = 1, \dots, d.$$

Let us also mention that integration by parts formula involving these operators exist, which are very much alike their more classical ‘volumetric’ counterparts - see e.g. [29] (Prop. 5.4.9) and [22] (Prop. 5.3 and 5.4) for statements and proofs.

4.5.3. Second-order asymptotic expansion of the cost function with respect to the perturbations.

Let us start by computing a second-order approximation of the mean value of random perturbations of a cost functions of the type:

$$(4.15) \quad \mathcal{C}(\Omega) = \int_\Omega j(u_\Omega) dx,$$

where $j : \mathbb{R}^d \rightarrow \mathbb{R}$ is a smooth function satisfying the growth conditions (3.6), and u_Ω is the elastic displacement of the shape Ω , solution of (4.1).

From the previous sections, we anticipate that the approximation of the mean-value of (4.15) will involve the second-order shape derivative as defined in Definition 3. This involves quite tedious computations as shown in the following result, the proof of which is given in the Appendix.

Theorem 18. *The functional $\mathcal{C}(\Omega)$, defined by (4.15) is twice shape differentiable and the following asymptotic expansion holds, for any $\theta \in \Theta_{ad}$,*

$$\mathcal{C}((I + \theta)(\Omega)) = \mathcal{C}(\Omega) + \mathcal{C}'(\Omega)(\theta) + \frac{1}{2}\mathcal{C}''(\Omega)(\theta, \theta) + R(\theta),$$

where the residual $R(\theta)$ satisfies:

$$\exists \delta, C > 0 \text{ such that } \forall \theta \in \Theta_{ad}, \|\theta\|_{\mathcal{C}^{2,\infty}(\mathbb{R}^d, \mathbb{R}^d)} \leq \delta \Rightarrow |R(\theta)| \leq C\|\theta\|_{\mathcal{C}^{2,\infty}(\mathbb{R}^d, \mathbb{R}^d)}^3.$$

The shape derivative of \mathcal{C} appearing in the above formula reads:

$$\mathcal{C}'(\Omega)(\theta) = \int_\Gamma (j(u_\Omega) + Ae(u_\Omega) : e(p_\Omega) - f \cdot p_\Omega) \theta \cdot n ds,$$

where p_Ω is the adjoint state, defined as the unique solution in $H_{\Gamma_D}^1(\Omega)^d$ of the system:

$$(4.16) \quad \begin{cases} -\operatorname{div}(Ae(p)) = -\nabla j(u_\Omega) & \text{in } \Omega \\ p = 0 & \text{on } \Gamma_D \\ Ae(p)n = 0 & \text{on } \Gamma_N \cup \Gamma \end{cases}.$$

The shape Hessian of \mathcal{C} reads:

$$(4.17) \quad \mathcal{C}''(\Omega)(\theta, \xi) = \mathcal{B}_\Omega(\theta, \xi) - \mathcal{C}'(\Omega)(Z(\theta, \xi)),$$

where

$$\begin{aligned} \mathcal{B}_\Omega(\theta, \xi) &= \int_\Gamma \left(\frac{\partial}{\partial n} + \kappa \right) (j(u_\Omega) + Ae(u_\Omega) : e(p_\Omega) - f \cdot p_\Omega) (\theta \cdot n)(\xi \cdot n) ds - \int_\Omega \nabla^2 j(u_\Omega)(q_\Omega(\theta \cdot n), q_\Omega(\xi \cdot n)) dx \\ &\quad - \int_\Omega (Ae(q_\Omega(\theta \cdot n)) : e(z_\Omega(\xi \cdot n)) + Ae(q_\Omega(\xi \cdot n)) : e(z_\Omega(\theta \cdot n))) dx \end{aligned}$$

and

$$Z(\theta, \xi) := (\nabla n^T \theta_\Gamma) \cdot \xi_\Gamma - \xi_\Gamma \cdot \nabla_\Gamma(\theta \cdot n) - \theta_\Gamma \cdot \nabla_\Gamma(\xi \cdot n).$$

In these formulae, the adjoint states $q_\Omega(w)$ and $z_\Omega(w)$ are defined as the unique solutions in $H_{\Gamma_D}^1(\Omega)^d$ of

$$(4.18) \quad \begin{cases} -\operatorname{div}(Ae(q)) = 0 & \text{in } \Omega \\ q = 0 & \text{on } \Gamma_D \\ Ae(q)n = 0 & \text{on } \Gamma_N \\ Ae(q)n = fw + \operatorname{div}_\Gamma(w(Ae(u_\Omega))_{\tau\tau}) & \text{on } \Gamma \end{cases},$$

$$(4.19) \quad \begin{cases} -\operatorname{div}(Ae(z)) = -\nabla^2 j(u_\Omega)q_\Omega(w) & \text{in } \Omega \\ z = 0 & \text{on } \Gamma_D \\ Ae(z)n = 0 & \text{on } \Gamma_N \\ Ae(z)n = -j'(u_\Omega)w + \operatorname{div}_\Gamma(w(Ae(p_\Omega))_{\tau\tau}) & \text{on } \Gamma \end{cases}.$$

Remark 18. The shape Hessian (4.17) agrees with the general structure theorem 5.9.2 in [29] for shape Hessians of smooth functionals of the domain. In particular, it is symmetric and $\mathcal{B}_\Omega(\theta, \xi)$ is a symmetric bilinear form of θ and ξ which only depends on their normal components $\theta \cdot n$ and $\xi \cdot n$. Furthermore, the adjoint states $q_\Omega(w)$ and $z_\Omega(w)$ depend linearly on w , a function defined on Γ .

We now assume uncertain perturbations on shapes of the form (4.14), parameterized via a random field $v \in L^\infty(\mathcal{O}, \mathcal{C}^{2,\infty}(\mathbb{R}^d))$. We consider the mean-value functional:

$$(4.20) \quad \mathcal{M}(\Omega) = \int_{\mathcal{O}} \mathcal{C}((I + \eta v(\cdot, \omega)n_\Omega)(\Omega)) \mathbb{P}(d\omega),$$

and a simple consequence of Theorem 18 is the following result.

Corollary 19. *The approximate mean value function $\widetilde{\mathcal{M}}(\Omega)$, defined as:*

$$\widetilde{\mathcal{M}}(\Omega) = \mathcal{C}(\Omega) + \int_{\mathcal{O}} \mathcal{C}'(\Omega)(\eta v(\cdot, \omega)n_\Omega) \mathbb{P}(d\omega) + \int_{\mathcal{O}} \mathcal{C}''(\Omega)(\eta v(\cdot, \omega)n_\Omega, \eta v(\cdot, \omega)n_\Omega) \mathbb{P}(d\omega),$$

approximates $\mathcal{M}(\Omega)$ in the sense that there exists a constant $C > 0$ (depending on Ω) such that:

$$|\widetilde{\mathcal{M}}(\Omega) - \mathcal{M}(\Omega)| \leq C \|v\|_{L^\infty(\mathcal{O}, \mathcal{C}^{2,\infty}(\mathbb{R}^d))}^3.$$

We now specialize the random field $v(x, \omega)$ to be of the form

$$(4.21) \quad v(x, \omega) = \sum_{i=1}^N v_i(x) \xi_i(\omega),$$

where the functions v_i are in $\mathcal{C}^{2,\infty}(\mathbb{R}^d, \mathbb{R}^d)$, and the ξ_i are uncorrelated, centered and normalized random variables.

Taking advantage of (4.21), $\widetilde{\mathcal{M}}(\Omega)$ rewrites in this context:

$$(4.22) \quad \begin{aligned} \widetilde{\mathcal{M}}(\Omega) &= \int_{\Omega} j(u_\Omega) dx + \sum_{i=1}^N \int_{\Gamma} \left(\frac{\partial}{\partial n} + \kappa \right) (j(u_\Omega) + Ae(u_\Omega) : e(p_\Omega) - f \cdot p_\Omega) v_i^2 ds \\ &\quad - \sum_{i=1}^N \int_{\Omega} \nabla^2 j(u_\Omega)(q_\Omega(v_i), q_\Omega(v_i)) dx - 2 \sum_{i=1}^N \int_{\Omega} Ae(q_\Omega(v_i)) : e(z_\Omega(v_i)) dx, \end{aligned}$$

where the adjoint state p_Ω , q_Ω and z_Ω are defined in (4.16), (4.18) and (4.19) respectively.

To devise a gradient-based minimization algorithm for $\widetilde{\mathcal{M}}(\Omega)$ requires the calculation of its shape derivative, which corresponds, in light of Corollary 19, to the evaluation of the third-order shape derivative of the cost function $\mathcal{C}(\Omega)$. In theory, this can be done but it is a formidable and tedious computation and, in numerical practice we doubt that the resulting formulae could be tractable, insofar as they involve third-order geometric quantities attached to $\partial\Omega$ (the derivative of curvatures); see for instance the formulas of Lemma 5 in the supplementary material [3]. For this reason, we do not proceed further in the study of the minimization of $\widetilde{\mathcal{M}}(\Omega)$, and, in the sequel, we deal instead with the case of functionals involving only first-order shape derivatives of \mathcal{C} .

If, instead of the mean value $\mathcal{M}(\Omega)$, we consider the variance $\mathcal{V}(\Omega)$ of some cost function $\mathcal{C}(\Omega)$, then it is possible to compute the shape derivative of its approximation since it will require at most a second-order shape derivative (instead of a third-order one for $\mathcal{M}(\Omega)$). This is precisely what we are investigating in the sequel. To vary the range of applications we change the previous cost function (4.15) to a stress-based cost function of the form

$$\mathcal{C}(\Omega) = \int_{\Omega} j(\sigma(u_{\Omega})) dx,$$

where $j : \mathcal{S}(\mathbb{R}^d) \rightarrow \mathbb{R}$ is a smooth function satisfying adequate growth conditions, u_{Ω} is the elastic displacement of the shape Ω , solution of (4.1) and $\sigma(u_{\Omega})$ is the corresponding stress tensor. Since the technical details are very similar, we limit ourselves with stating the results. The variance $\mathcal{V}(\Omega)$, associated to \mathcal{C} , is

$$\mathcal{V}(\Omega) = \int_{\mathcal{O}} \left(\mathcal{C}((I + \eta v(\cdot, \omega) n_{\Omega})(\Omega)) - \mathcal{M}(\Omega) \right)^2 \mathbb{P}(d\omega),$$

where $\mathcal{M}(\Omega)$ is the mean value defined by (4.20). Following the same line of thought, we obtain the second-order approximate variance functional $\tilde{\mathcal{V}}(\Omega)$, defined by

$$(4.23) \quad \tilde{\mathcal{V}}(\Omega) = \sum_{i=1}^N a_{\Omega,i}^2 \quad \text{with} \quad a_{\Omega,i} = \int_{\Gamma} (j(\sigma(u_{\Omega})) + Ae(u_{\Omega}) : e(p_{\Omega}) - f \cdot p_{\Omega}) v_i ds,$$

and the adjoint state $p_{\Omega} \in H_{\Gamma_D}^1(\Omega)^d$ is the solution of:

$$\begin{cases} -\operatorname{div}(Ae(p)) = \operatorname{div}(A \frac{\partial j}{\partial \sigma}(\sigma(u_{\Omega}))) & \text{in } \Omega, \\ p = 0 & \text{on } \Gamma_D, \\ Ae(p)n = -A \frac{\partial j}{\partial \sigma}(\sigma(u_{\Omega}))n & \text{on } \Gamma \cup \Gamma_N. \end{cases}$$

In the spirit of Theorem 18 one can obtain the following result.

Proposition 20. *The functional $\tilde{\mathcal{V}}(\Omega)$ is shape differentiable at any $\Omega \in \mathcal{U}_{ad}$, and its shape derivative reads:*

$$\forall \theta \in \Theta_{ad}, \quad \tilde{\mathcal{V}}'(\Omega)(\theta) = 2 \int_{\Gamma} \mathcal{D}(u_{\Omega}, p_{\Omega}, q_{\Omega}, z_{\Omega}) \theta \cdot n ds,$$

where the integrand factor is given by:

$$\begin{aligned} \mathcal{D}(u_{\Omega}, p_{\Omega}, q_{\Omega}, z_{\Omega}) &= \left(\frac{\partial}{\partial n} + \kappa \right) \left((j(\sigma(u_{\Omega})) + Ae(u_{\Omega}) : e(p_{\Omega}) - f \cdot p_{\Omega}) \left(\sum_{i=1}^N a_{\Omega,i} v_i \right) \right) \\ &\quad + \left(Ae(u_{\Omega}) : e(z_{\Omega}) + Ae(p_{\Omega}) : e(q_{\Omega}) - f \cdot z_{\Omega} + \frac{\partial j}{\partial \sigma}(u_{\Omega}) : q_{\Omega} \right), \end{aligned}$$

and the adjoint states are $q_{\Omega} = q \left(\sum_{i=1}^N a_{\Omega,i} v_i \right)$, with $q(w)$ the solution of (4.18), and z_{Ω} the solution of

$$\begin{cases} -\operatorname{div}(Ae(z)) = \operatorname{div} \left(A \frac{\partial^2 j}{\partial \sigma^2}(\sigma(u_{\Omega})) \sigma(q_{\Omega}) \right) & \text{in } \Omega, \\ z = 0 & \text{on } \Gamma_D, \\ Ae(z)n = 0 & \text{on } \Gamma_N, \\ Ae(z)n = \operatorname{div}_{\Gamma} \left(A \frac{\partial j}{\partial \sigma}(\sigma(u_{\Omega})) \left(\sum_{i=1}^N a_{\Omega,i} v_i \right) \right) + \operatorname{div}_{\Gamma} \left(\left(\sum_{i=1}^N a_{\Omega,i} v_i \right) (Ae(p_{\Omega}))_{\tau\tau} \right) & \text{on } \Gamma. \end{cases}$$

4.5.4. Approximation of the failure probability.

Similarly, an approximate failure probability function may be devised as:

$$(4.24) \quad \tilde{\mathcal{P}}(\Omega) = \Phi \left(-\frac{\alpha - b_{\Omega}}{|a_{\Omega}|} \right),$$

where

$$b_{\Omega} = \int_{\Omega} j(u_{\Omega}) dx \quad \text{and} \quad a_{\Omega,i} = \int_{\Gamma} (j(u_{\Omega}) + Ae(u_{\Omega}) : e(p_{\Omega}) - f \cdot p_{\Omega}) v_i ds.$$

In the spirit of Theorem 18 one can obtain the following result.

Proposition 21. *The functional $\tilde{\mathcal{P}}(\Omega)$ is shape differentiable at any $\Omega \in \mathcal{U}_{ad}$, and its shape derivative reads:*

$$\forall \theta \in \Theta_{ad}, \quad \tilde{\mathcal{P}}'(\Omega)(\theta) = \frac{1}{\sqrt{2\pi}} e^{-\left(\frac{\alpha-b\Omega}{|a\Omega|}\right)^2} \int_{\Gamma} \mathcal{D}(u_{\Omega}, p_{\Omega}, q_{\Omega}, z_{\Omega}) \theta \cdot n \, ds,$$

where the integrand factor is given by:

$$\begin{aligned} \mathcal{D}(u_{\Omega}, p_{\Omega}, q_{\Omega}, z_{\Omega}) &= \frac{1}{|a\Omega|} (j(u_{\Omega}) + Ae(u_{\Omega}) : e(p_{\Omega}) - f \cdot p_{\Omega}) \\ &+ \frac{\alpha-b\Omega}{|a\Omega|^3} \left(\frac{\partial}{\partial n} + \kappa \right) \left((j(u_{\Omega}) + Ae(u_{\Omega}) : e(p_{\Omega}) - f \cdot p_{\Omega}) \left(\sum_{i=1}^N a_{\Omega,i} v_i \right) \right), \\ &+ \frac{\alpha-b\Omega}{|a\Omega|^3} (Ae(u_{\Omega}) : e(z_{\Omega}) + Ae(p_{\Omega}) : e(q_{\Omega}) - f \cdot z_{\Omega} + \nabla j(u_{\Omega}) \cdot q_{\Omega}), \end{aligned}$$

and the adjoint states q_{Ω}, z_{Ω} are defined by

$$q_{\Omega} = q \left(\sum_{i=1}^N a_{\Omega,i} v_i \right) \quad \text{and} \quad z_{\Omega} = z \left(\sum_{i=1}^N a_{\Omega,i} v_i \right),$$

where $q(w)$ is the solution of (4.18) and $z(w)$ is the solution of (4.19).

5. NUMERICAL ILLUSTRATIONS

All computations are performed within the **FreeFem++** software [28, 38], except otherwise mentioned. Even though no particular effort has been put in optimizing the performance of the implementation, we give approximate CPU times for several test cases, which are executed on a MacBook Air, 1.8 GHz Intel Core i5 with 4 Go of RAM. Additional examples are presented in Section 1 of the supplementary material [3].

5.1. Examples in parametric optimization.

5.1.1. Brief description of the numerical implementation.

This first series of examples is aimed at illustrating the material presented in Section 3. The optimization variable is the thickness $h \in L^{\infty}(\Omega)$ of a plate with cross-section $\Omega \subset \mathbb{R}^2$. The objective function $\mathcal{J}(h)$ is a moment (mean, variance) of a probabilistic cost function $\mathcal{C}(h, \omega)$, or a failure probability.

We rely on a standard steepest-descent algorithm, taking advantage of the general structure of the derivative of $\mathcal{J}(h)$:

$$\forall \hat{h} \in L^{\infty}(\Omega), \quad \mathcal{J}'(h)(\hat{h}) = \int_{\Omega} \mathcal{D}_h \hat{h} \, dx,$$

where \mathcal{D}_h is a scalar quantity depending on the problem at stake (see its various expressions in Theorems 4, 6, 8 and 11). More precisely, either we use a classical (projected) gradient algorithm, or an Augmented Lagrangian algorithm (see [36], §17.4) when it comes to imposing an equality constraint on the volume $\text{Vol}(h) = \int_{\Omega} h \, dx$ of shapes. In addition, we systematically impose lower and upper bounds $h_{min} = 0.1$ and $h_{max} = 1$ on h . The thickness is consistently initialized with the constant value $h_{ini} = 0.5$. The Young's modulus and Poisson ratio of the elastic material are respectively set to $E = 100$ and $\nu = 0.3$.

5.1.2. Minimization of a weighted sum of the mean value and the standard deviation of the compliance.

Let us first investigate the case of perturbations over the body forces f , as described in Section 3.2, neglecting surface loads (i.e. $g = 0$). The situation is as depicted on Figure 3 (left): body forces $f_0 = (0, -10)$ apply on the middle of the lower part of the plate (red spot on Figure 3) in the unperturbed state, and two perturbations f_1, f_2 , both equal to $(0, -10/3)$, are localized on two disjoint regions of this lower part (blue spots on Figure 3). The total body force $f(x, \omega)$ is thus

$$f(x, \omega) = f_0(x) + \sum_{i=1}^2 f_i(x) \xi_i(\omega),$$

where ξ_1, ξ_2 are uncorrelated, centered and normalized random variables.

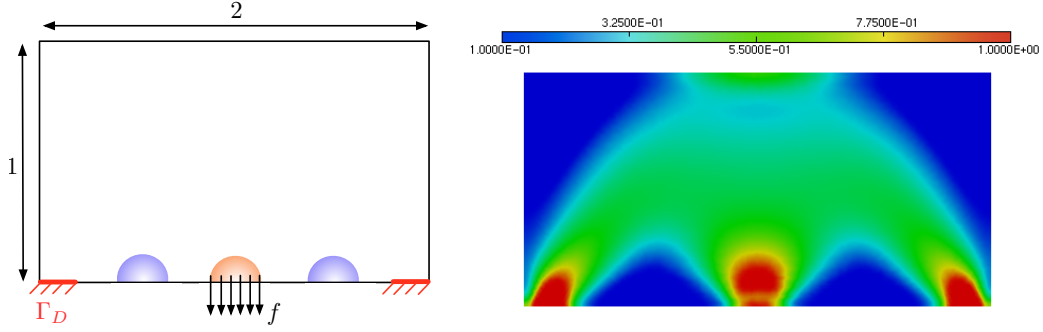


FIGURE 3. (Left) Description of the test-case of Section 5.1.2, (right) optimal shape without uncertainties.

The cost function of interest is the compliance of the plate, $\mathcal{C}(h, f) = \int_{\Omega} f \cdot u_h \, dx$, where u_h is the solution to the linear elasticity system (3.1). We minimize a weighted sum $\mathcal{J}(h)$ of the mean value and of the standard deviation of \mathcal{C} :

$$(5.1) \quad \mathcal{J}(h) = \widetilde{\mathcal{M}}(h) + \delta \sqrt{\widetilde{\mathcal{V}}(h)},$$

where the functions $\widetilde{\mathcal{M}}(h)$ and $\widetilde{\mathcal{V}}(h)$ are respectively defined by (3.11) and (3.20), and $\delta \geq 0$ is a weighting parameter. To minimize $\mathcal{J}(h)$ while imposing (at convergence) a volume constraint $\text{Vol}(h) = V_T$ (here, $V_T = 0.7$), we use an Augmented Lagrangian algorithm. The formula for the gradient can be found in Theorems 4, 6, and in Example 1. This optimization is carried out for several values of the parameter δ , on a triangular mesh of Ω composed of 10,128 vertices (about twice as many triangles). Each computation is achieved within 150 iterations of the algorithm and takes about 7 min.

As a reference, the optimal design of the plate without uncertainties is displayed on Figure 3 (right). In comparison, the resulting optimal designs from the optimization of (5.1) in the perturbed situation, associated to several values of δ are reported on Figure 4, and the corresponding convergence histories are displayed on Figure 5. Remember that the case $\delta = 0$ is equivalent to the multi-load case.

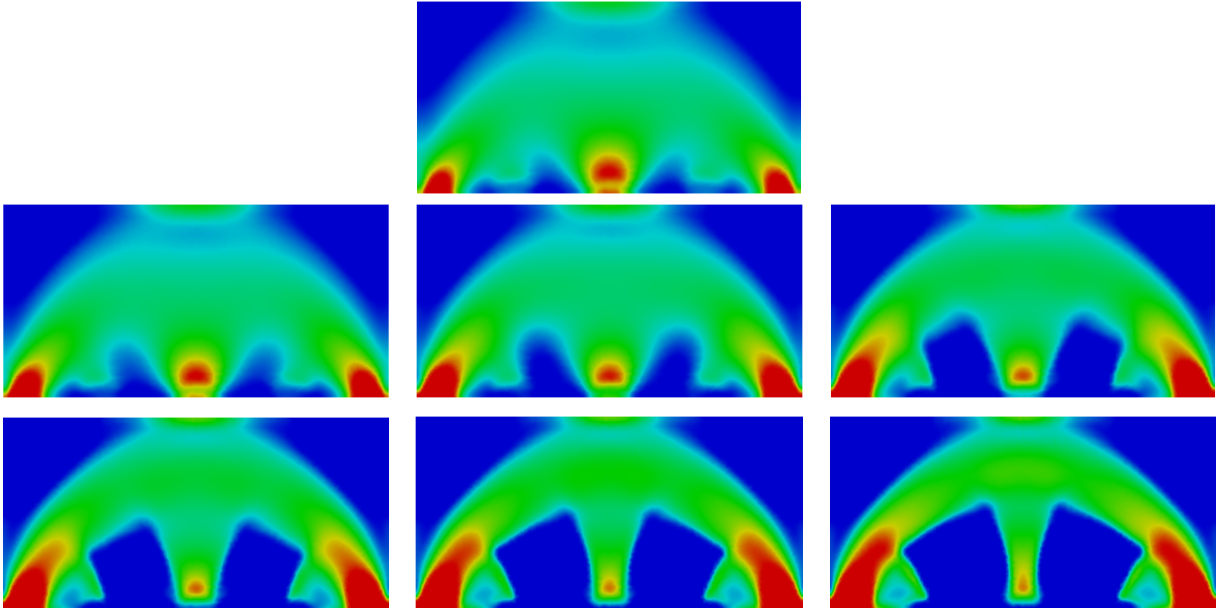


FIGURE 4. Test-case of Section 5.1.2: optimal shapes obtained in the minimization of (5.1); from left to right, top to bottom, $\delta = 0, 1, 3, 7, 10, 15, 20$.

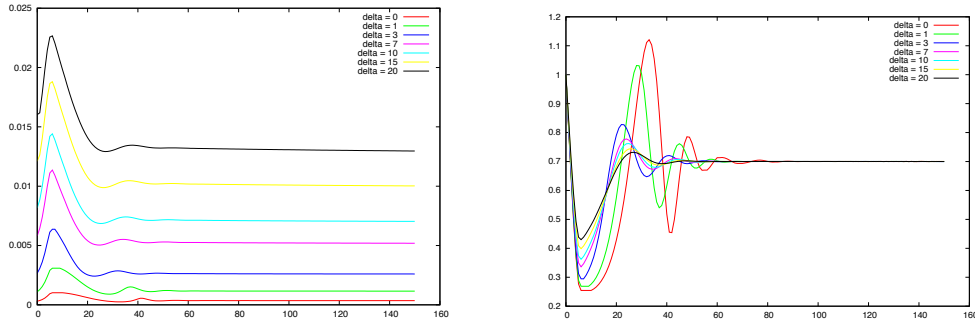


FIGURE 5. *Test-case of Section 5.1.2: convergence histories for the objective function (5.1) (left), and the volume (right).*

5.1.3. Minimization of a failure probability based on the compliance of the plate.

We now minimize the approximate failure probability $\tilde{\mathcal{P}}(h)$, defined by (3.23) in Section 3.2.5, for the same geometry and loading condition as in the previous Subsection 5.1.2 (see Figure 3 for details).

In order to guess a relevant values of the threshold parameter α , we first minimize the compliance in the unperturbed situation (i.e. when only the force f_0 is applied), with a volume constraint $V_T = 0.7$ (see the result in Figure 6, top). We call h^* the resulting optimal thickness and its compliance is $\mathcal{C}(h^*, f_0) = 0.001729$.

In a second step, always starting from the constant thickness function h_{ini} , we perform several examples of minimization of $\tilde{\mathcal{P}}(h)$, associated to different values of the maximum tolerance parameter $\alpha = 0.0017, 0.0018, 0.0019, 0.002, 0.0025, 0.003$, while imposing the target volume V_T . Results are displayed on Figure 6 and the convergence histories are reported on Figure 7.

5.2. Examples in geometric optimization.

5.2.1. Description of the numerical algorithm.

We now turn to geometric optimization and, for its ease of implementation, as well as its ability to change topology, we rely on the Level Set method, introduced by Osher and Sethian in [37] (see [6, 46] for details concerning its implementation in the shape optimization context). The basic idea is to consider a shape $\Omega \subset \mathbb{R}^d$ as the negative subdomain of an auxiliary *level set function* $\phi : \mathbb{R}^d \rightarrow \mathbb{R}$, i.e.

$$\forall x \in \mathbb{R}^d, \begin{cases} \phi(x) < 0 & \text{if } x \in \Omega, \\ \phi(x) = 0 & \text{if } x \in \partial\Omega, \\ \phi(x) > 0 & \text{if } x \in {}^c\Omega. \end{cases}$$

The motion of a domain $\Omega(t)$, $t \in [0, T]$, according to a normal velocity field $V(t, x)$ translates into an *Hamilton-Jacobi* equation for the associated level set function $\phi(t, \cdot)$:

$$(5.2) \quad \frac{\partial \phi}{\partial t} + V|\nabla \phi| = 0, \quad t \in (0, T), \quad x \in \mathbb{R}^d.$$

In shape optimization, t is a pseudo-time corresponding to a descent step and V stems from the analytical formulae for the shape derivatives of the considered objective functions $\mathcal{J}(\Omega)$, which enjoy the common structure:

$$\forall \theta \in \Theta_{ad}, \quad \mathcal{J}'(\Omega)(\theta) = \int_{\Gamma} \mathcal{D}_{\Omega} \theta \cdot n \, ds,$$

where \mathcal{D}_{Ω} is a scalar function. Instead of taking $V = -\mathcal{D}_{\Omega}$ (which is a typical descent direction), we rely on a regularization and extension process for \mathcal{D}_{Ω} based on the Laplacian as in [6].

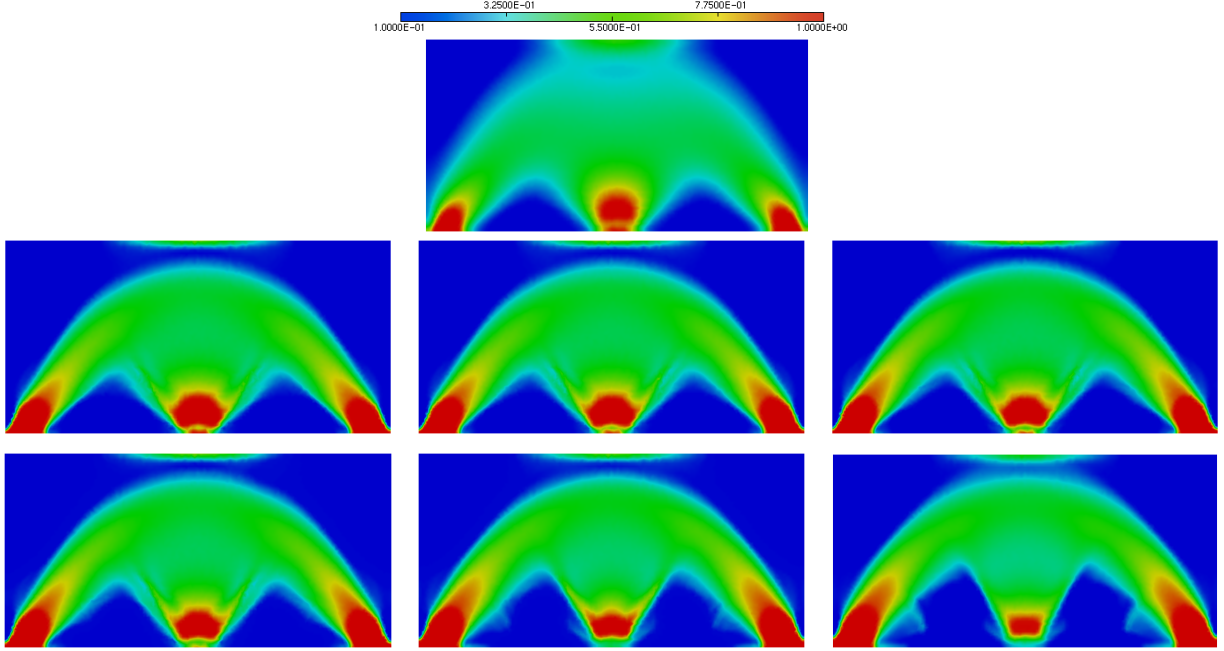


FIGURE 6. *Test-case of Section 5.1.3: minimization of the failure probability (3.23); from left to right, top to bottom, unperturbed design, and optimal thicknesses associated to the values $\alpha = 0.0017, 0.0018, 0.0019, 0.002, 0.0025, 0.003$.*

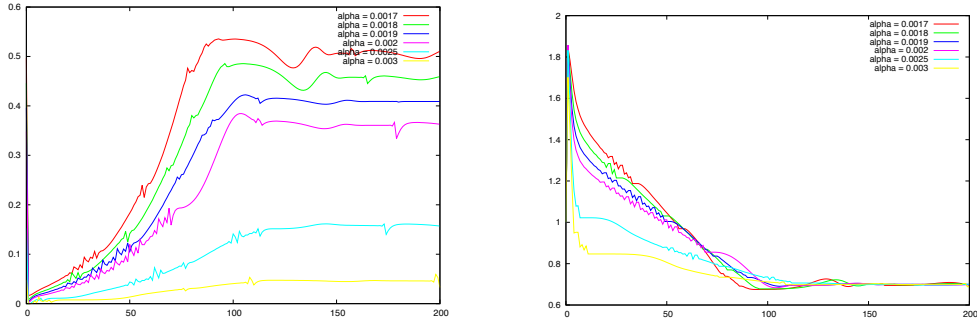


FIGURE 7. *Test-case of Section 5.1.3: convergence histories for the objective function (left), and the volume (right).*

In numerical practice, any shape Ω is constrained to belong to a large computational box D , equipped with a fixed triangular mesh \mathcal{T} . A shape $\Omega \subset D$ is represented by a level set function ϕ , discretized at the vertices of \mathcal{T} . The elastic displacement u_Ω , solution to the linear elasticity system (4.1), or the adjoint states involved in the computation of \mathcal{D}_Ω , cannot be calculated exactly since no mesh of Ω is available, and we rely on the Ersatz material approach [6] to achieve this calculation approximately: the problem (4.1) is transferred to a problem on D by filling the void part $D \setminus \bar{\Omega}$ with a very soft material, whose Hooke's law is εA , $\varepsilon = 10^{-3}$.

All finite element computations are performed within the **FreeFem++** software, and we rely on algorithms from our previous works [11, 23], based on the method of characteristics for a triangular mesh, when it comes to solve the Hamilton-Jacobi equation (5.2) or to reinitialize the level set function as the signed

distance function to the boundary $\partial\Omega$. When we display shapes, we plot the level set function (and not the interpolated material density).

5.2.2. Compliance minimization with force uncertainties.

Our first two examples in the setting of shape optimization illustrate Section 4.2 about random perturbations of the forces, and deal with the compliance of shapes as a cost function:

$$(5.3) \quad \mathcal{C}(\Omega, f) = \int_{\Omega} Ae(u_{\Omega, f}) : e(u_{\Omega, f}) dx = \int_{\Omega} f \cdot u_{\Omega, f} dx.$$

The body forces are $f = f_0 + \hat{f}$ with random perturbations \hat{f} . In the two cases, we minimize a weighted sum

$$(5.4) \quad \mathcal{J}(\Omega) := \widetilde{\mathcal{M}}(\Omega) + \delta\sqrt{\widetilde{\mathcal{V}}(\Omega)}$$

of the approximate mean value and standard deviation of \mathcal{C} with a weighting parameter $\delta \geq 0$.

First, we deal with the optimization of a bridge - see Figure 8 for details of the test case. The bridge is clamped on its lower-left corner, and its vertical displacement is prevented on the lower-right corner. Surface loads are neglected (i.e. $g = 0$), and the unperturbed body forces $f_0 = (0, -10)$ are applied on the red region of the lower part. Perturbations \hat{f} read:

$$(5.5) \quad \hat{f}(x, \omega) = \sum_{i=1}^2 f_i(x)\xi_i(\omega),$$

where ξ_1, ξ_2 are uncorrelated, centered and normalized random variables (i.e. (2.4) holds), f_1, f_2 are equal to $(0, -m)$ and concentrated on the blue regions. Several optimal shapes are computed with the algorithm described in Section 5.2.1, associated to different values of the parameters δ, m . In all the cases, a target volume $V_T = 0.75$ is imposed thanks to an Augmented Lagrangian algorithm, and 300 iterations are performed on a mesh composed of 9205 vertices (and about twice as many triangles). Each computation takes about 14 min., and the resulting optimal shapes are displayed on Figure 9 for $\delta = 0$ (no variance), and on Figure 10 for $\delta = 3$ (the objective function is a combination of the mean and variance), while the convergence histories are reported on Figure 11. As a reference, the optimal shape without uncertainties is displayed on Figure 8 (right). Note that the two small bumps on the horizontal lower bar in Figure 8 (right) correspond to the two non-optimizable regions associated to the perturbations (in blue on Figure 8 left). The designs at the bottom of Figure 9 are very similar to those obtained in [4] for multiple load compliance minimization, which is not a surprise in light of Example 5 and Remark 17 (namely, minimizing $\widetilde{\mathcal{M}}(\Omega)$ is exactly solving the multiple load problem).

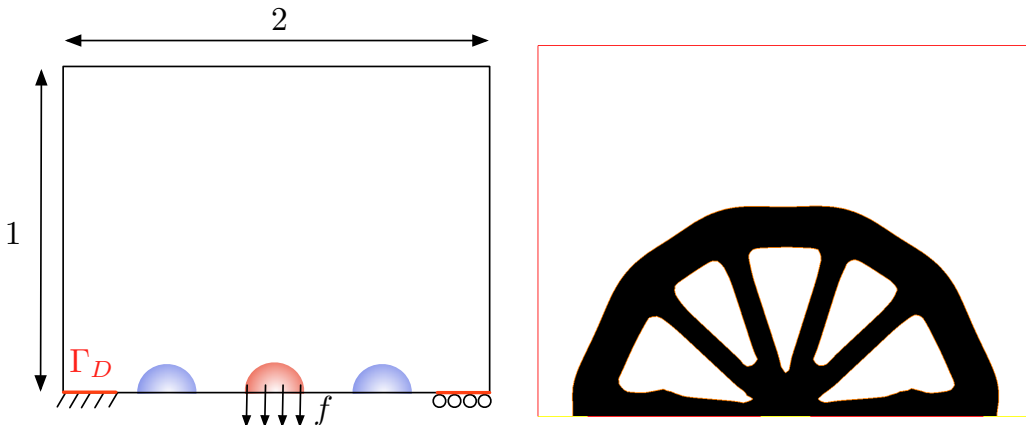


FIGURE 8. Section 5.2.2: (left) description of the bridge test case, (right) optimal shape in the unperturbed situation.

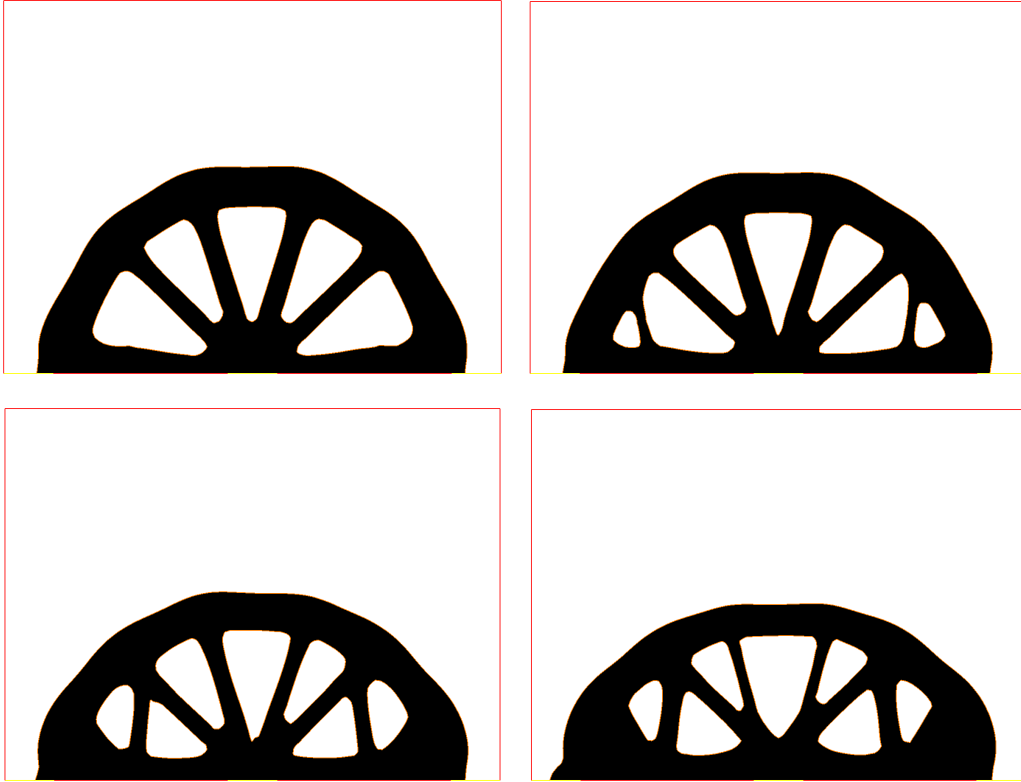


FIGURE 9. Section 5.2.2, bridge test case: optimal shapes for $\delta = 0$ and (from the left to the right, top to bottom) $m = 1, 2, 5, 10$.

It is interesting to compare the previous optimal designs for the minimization of (5.4) with the ones obtained in the worst-case scenario of vertical perturbations of amplitude m , that is, to the corresponding optimal shapes with respect to the functional:

$$(5.6) \quad \mathcal{J}(\Omega) = \sup_{\|\hat{f}\|_{L^2(\Omega)^d} \leq m} \mathcal{C}(\Omega, f_0 + \hat{f}).$$

In our previous work [2], we proposed a linearization method for approximating such worst-case objective functions. The main idea is to perform a first-order expansion of $\hat{f} \mapsto \mathcal{C}(\Omega, f_0 + \hat{f})$ (see the first-order terms in (4.5)) before taking the supremum in (5.6), which yields an explicit approximate worst-case functional $\tilde{\mathcal{J}}(\Omega)$. For the sake of comparison, we computed the optimal shapes for the linearized worst-case functional $\tilde{\mathcal{J}}$, associated to the values $m = 1, 2, 5$ and 10 , under the same volume constraint $V_T = 0.75$ as above. The resulting shapes are displayed in Figure 12. Moreover, Table 1 collects the values of the sole compliance of the optimal shapes obtained in the probabilistic and worst-case settings. Understandably enough, they reveal that performing shape optimization with a worst-case approach is more ‘pessimistic’ than doing so by taking into account the statistics of the expected perturbations, when available.

Remark 19. We take this opportunity to explain a fundamental difference between the linearized worst-case design approach of our previous work [2] and the present setting. In the linearized worst-case design framework, the worst-case loading \hat{f} is explicitly given in terms of the state u and the adjoint p . For a symmetric test case as the bridge here, it implies that the worst-case loading is symmetric if the design is symmetric too. However, in the present probabilistic framework, even if the problem is simplified by making a second-order Taylor expansion of the objective function, there are realizations of the uncertain loads which are not symmetric. On the bridge test case we intuitively expect that ‘bad’ loading perturbations are not

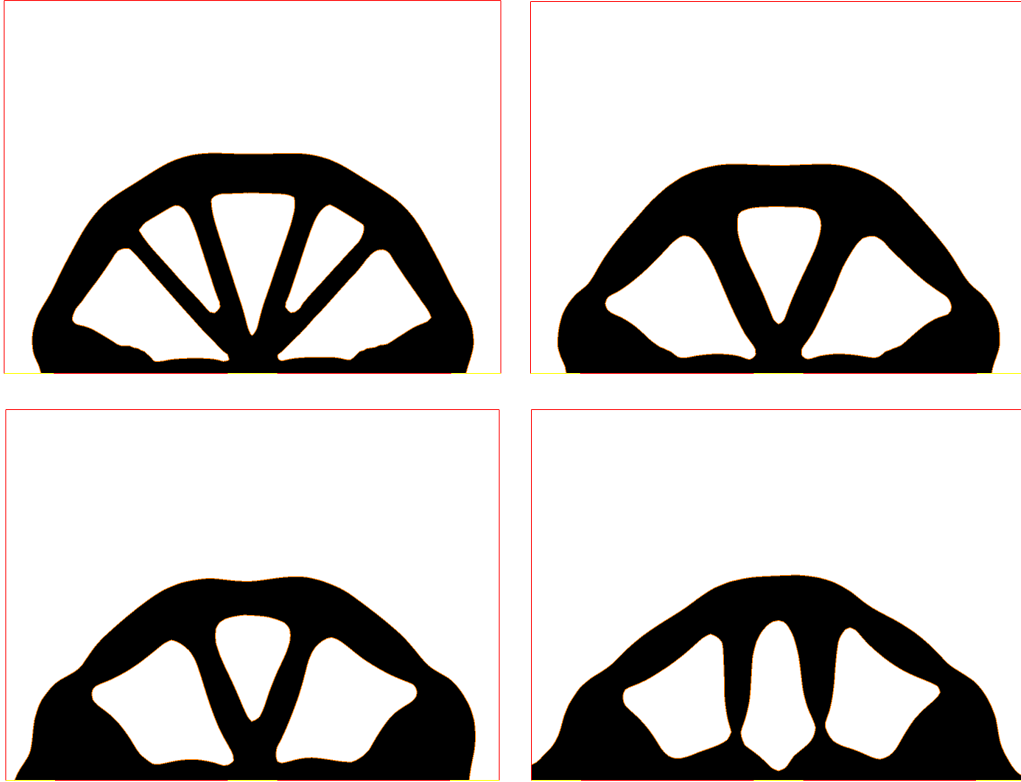


FIGURE 10. Section 5.2.2, bridge test case: optimal shapes for $\delta = 3$ and (from the left to the right, top to bottom) $m = 1, 2, 5, 10$.

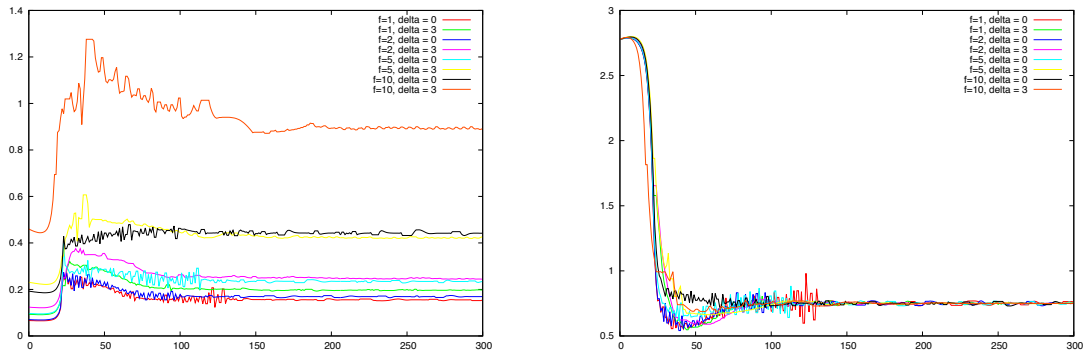


FIGURE 11. Section 5.2.2, bridge test case: convergence histories for the objective function (left), and the volume (right).

symmetric. Therefore, it is no surprise that the results of our present probabilistic approach on Figure 9 ‘look nicer’ than those of the linearized worst-case approach in Figure 12.

Our second example is a short cantilever example, as depicted on Figure 13: it is clamped on its left-hand side, and vertical body forces $f_0 = (0, -100)$ are applied on the red spot, in the middle of the right-hand side. Perturbations \hat{f} of the form (5.5) are expected, where the functions f_1, f_2 are supported on the two blue

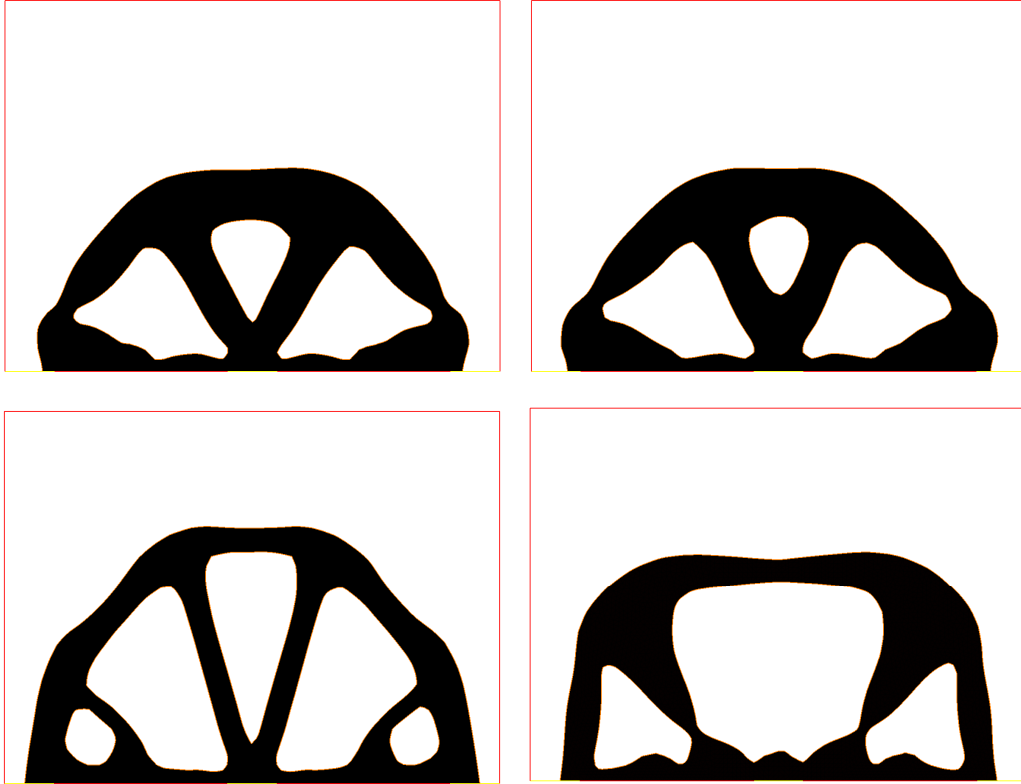


FIGURE 12. Section 5.2.2, bridge test case: optimal shapes for the linearized worst-case design approach with $m = 1, 2, 5, 10$ (from left to right, top to bottom).

	$m = 0$	$m = 1$	$m = 2$	$m = 5$	$m = 10$
Probabilistic setting $\delta = 0$	0.1479	0.1493	0.1523	0.1586	0.1733
Probabilistic setting $\delta = 3$	0.1479	0.1669	0.1969	0.2369	0.3843
Worst-case setting	0.1479	0.1944	0.2095	0.2456	0.4193

TABLE 1. Section 5.2.2, bridge test case: values of the compliance for the optimal shapes in the probabilistic and worst-case settings.

spots, and are *horizontal*, of the form $(-m, 0)$. A target volume $V_T = 0.45$ is imposed, and 200 iterations of the aforementioned Augmented Lagrangian algorithm are run for several values of the parameters δ and m , on a mesh composed of 5151 vertices. The optimal shapes and the convergence histories are displayed on Figures 14 and 15. These designs are in the same spirit than those obtained in [26] for the worst-case setting.

5.2.3. Optimization of the compliance of the frequency response of a bridge.

Let us turn to an illustration of Section 4.4 where vibrating loads are imposed with an uncertain frequency. A bridge, with boundary conditions as reported in Figure 16 (left) and volume constraint $V_T = 0.185$, is first optimized for maximizing its first fundamental frequency (in the absence of any load). For this goal we use the method described in [4]. The fundamental frequency of the resulting structure is $\xi^* \approx 4.24$ and the corresponding shape is displayed on Figure 16 (right). The computational mesh is here composed of 4068 vertices.

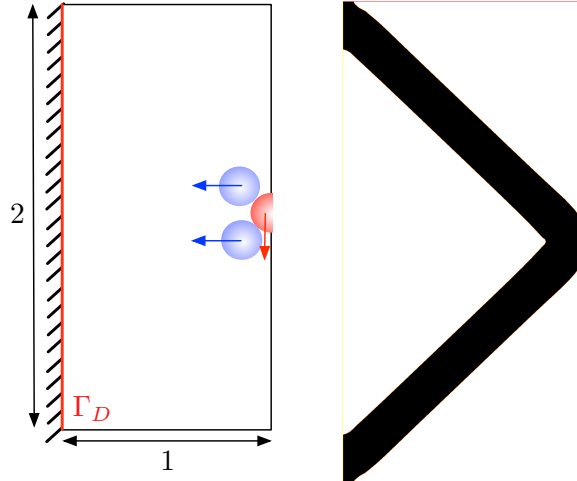


FIGURE 13. *Section 5.2.2: (left) setting of the short cantilever test case; (right) optimal shape without perturbations*

In a second step the bridge is submitted to time-harmonic surface loads, applied on the upper side, with modulus $g = (0, -1)$, and whose frequency ξ takes random, uniformly distributed values in $(\xi_0 - m, \xi_0 + m)$, where $\xi_0 = 2 < \xi^*$, and m is small. This models, for instance, the random passing of pedestrians or vehicles on the bridge. In this second step, we minimize the mean value $\widetilde{\mathcal{M}}(\Omega)$ of the compliance of the bridge given by (4.12). We start from an initial design which is the optimal shape for the first eigenvalue maximization obtained in Figure 16 (right).

We perform several computations of the ‘optimal’ shape of the bridge with respect to $\widetilde{\mathcal{M}}(\Omega)$, under the volume constraint $V_T = 0.185$, associated to several values of the parameter m . Each calculation takes about 4 min. (for 200 iterations) and the results are displayed on Figures 17.

Of course, the first frequency of shapes decreases during the optimization process, but we checked that this decrease is not too dramatic (the first eigenvalue varies between 3.65 and 2.89). In particular, the fundamental frequency of the bridge stays above the expected imposed frequency ξ_0 in all cases.

5.2.4. *Minimization of a least-square criterion under material uncertainties.*

We now illustrate the setting of Section 4.3 by designing a gripping mechanism, as represented on Figure 18: the considered shapes are clamped on a region Γ_D of their left-hand side, and an input force $g = (0.1, 0)$ is applied on another region Γ_N . To obtain a deformation which closes the ‘jaws’ of the gripping mechanism (the blue rectangles), we consider the cost function

$$\mathcal{C}(\Omega, E) = \int_{\Omega} k(x) |u_{\Omega, E} - u_0|^2 dx,$$

where $u_{\Omega, E}$ is the elastic displacement of Ω , solution to (4.1), and k is the characteristic function of the blue area, where the displacement of the optimal shape is expected to get close to the target u_0 , which equals $(0, -0.2)$ on the upper jaw, and $(0, 0.2)$ on the lower jaw.

Random perturbations \widehat{E} occur on the Young’s modulus E of the elastic material, which has the structure $E = E_0 + E$. The statistics of these perturbations are assumed to be known through the correlation function:

$$\text{Cor}(\widehat{E})(x, y) = \beta^2 e^{-\frac{|x-y|}{d}},$$

where β is a parameter quantifying the magnitude of perturbations, and the characteristic length d is set to 0.1. A Karhunen-Loève decomposition of \widehat{E} is performed (see [10] for an overview of the numerical methods

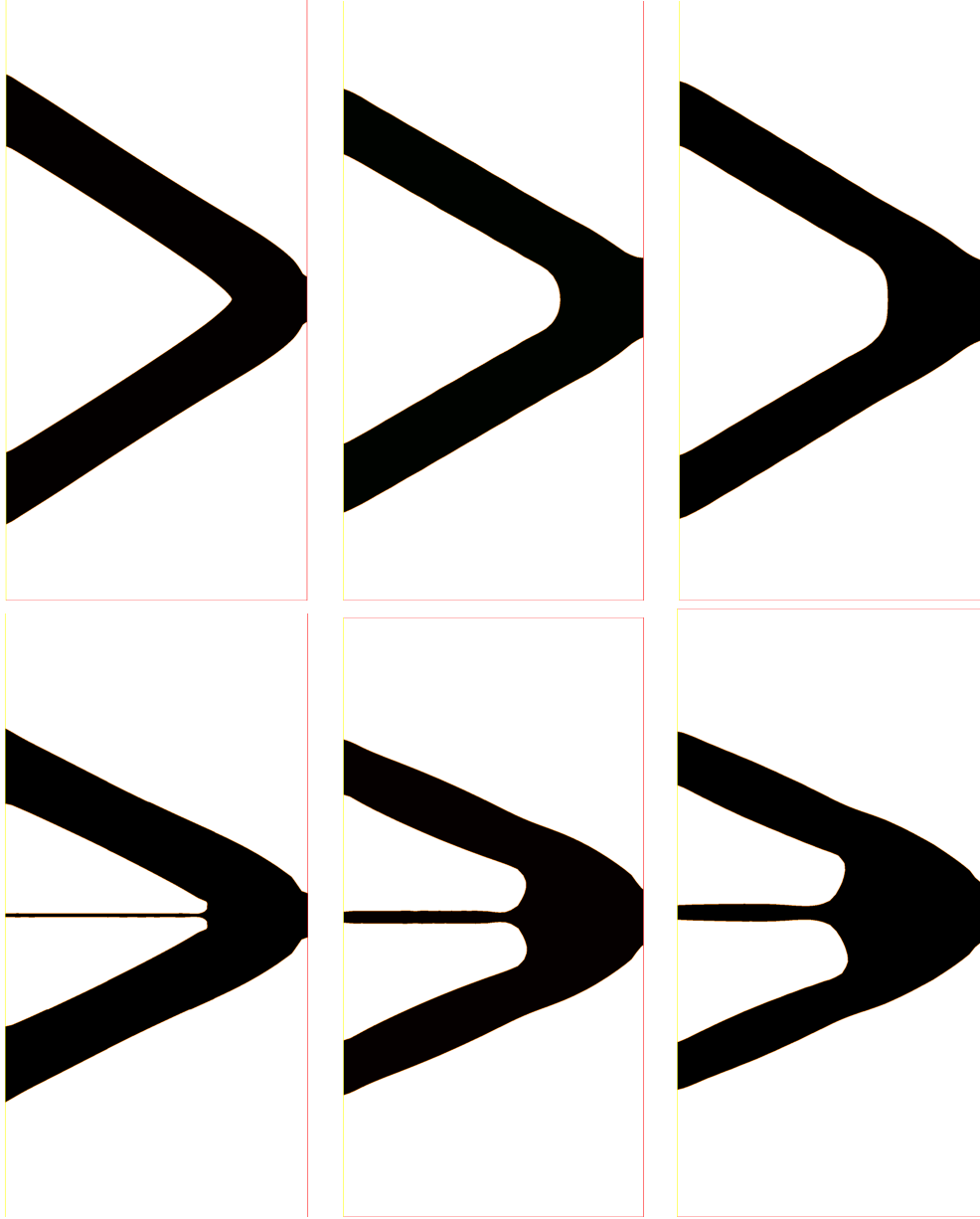


FIGURE 14. Section 5.2.2: optimal shapes obtained in the short cantilever test case. The upper row corresponds to the value $m = 50$, and the lower one to $m = 100$; then, from the left to the right, $\delta = 0, 2, 3$.

to carry out this step), then truncated after its first three terms, so that \widehat{E} takes the form

$$\widehat{E}(x) = \sum_{i=1}^3 E_i(x) \xi_i(\omega),$$

where the E_i are deterministic functions, and the ξ_i are uncorrelated, centered and normalized random variables.

We minimize the objective function $\widetilde{\mathcal{M}}(\Omega)$ which is the approximate mean value of the cost \mathcal{C} (see Section 4.3). Several computations are performed for different values of the parameter β , and the results are displayed on Figure 19 (recall that we plot the level set function which may be disconnected at the hinge's locations,

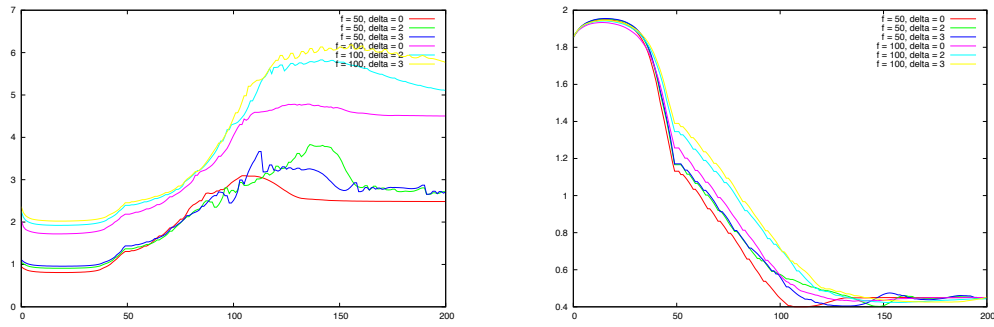


FIGURE 15. Section 5.2.2: convergence histories for the objective function (left), and the volume (right) in the short cantilever test-case.

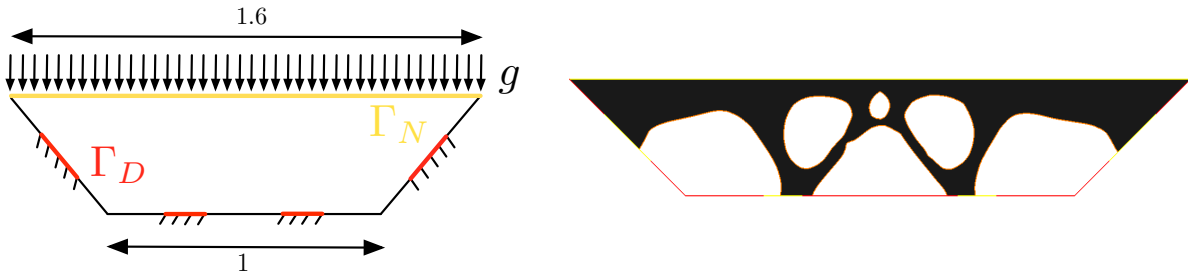


FIGURE 16. Section 5.2.3, bridge with an uncertain frequency load: (left) details of the test-case, (right) initial shape.

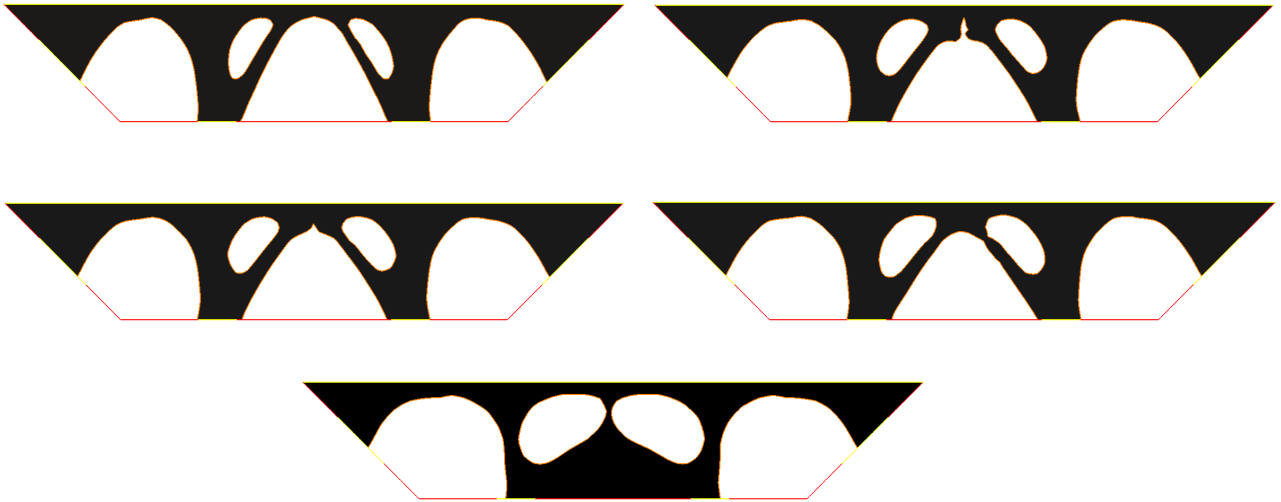


FIGURE 17. Section 5.2.3: optimal shapes of a bridge when perturbations are expected over the frequency regime, associated to the parameter (from the left to the right) $m = 0, 0.45, 0.6, 0.75, 0.765$. A target volume $V_T = 0.185$ is imposed.

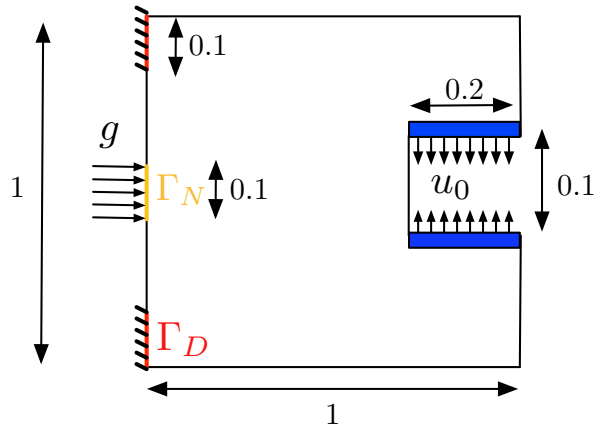


FIGURE 18. *Setting of the gripping mechanism example of Section 5.2.4*

but the material density is not). Note that, owing to the great numerical sensitivity of the cost functional at stake, each optimization is performed in two steps so to help the optimization process: a first one with a coefficient for the ersatz material equal to 10^{-2} , and a second one where this coefficient is decreased to 10^{-3} . On a different note, while it is a priori not necessary, a slight volume constraint is imposed to the shapes (via the addition to $\tilde{\mathcal{M}}(\Omega)$ of a term of the form $\ell \text{Vol}(\Omega)$, with a fixed Lagrange multiplier ℓ), to help in removing the small islands of unnecessary matter. As can be expected, for larger β (meaning more uncertainties on the Young's modulus), the resulting optimal shapes have thicker hinges and are therefore more robust.

5.2.5. *Minimization of the stress of an L-shaped beam under geometric perturbations.*

Our last example fits into the context of Section 4.5. We minimize the stress distribution of an L-shaped beam (see Figure 20 for details) by considering the cost function:

$$\mathcal{C}(\Omega) = \int_{\Omega} \|\sigma(u_{\Omega})\|^p dx,$$

with $p = 5$. In the above formula, the notation $\|\cdot\|$ refers to the Frobenius norm of matrices.

Random perturbations over the geometries of shapes occur on a subdomain D_p of the computational domain D (grayed area on Figure 20). We choose to have geometric fluctuations only in the lower part of the domain in order that they have more impact on the resulting optimal truss structures. The results are different and less ‘spectacular’ (see the supplementary material file for details) when we rather take $D_p = D$. The random perturbations are defined by (4.14), namely are normal to the boundary and proportional to a random field $v(x, \omega)$ which admits the following correlation function:

$$(5.7) \quad \forall x, y \in D_p, \quad \text{Cor}(v)(x, y) = e^{-\frac{|x-y|}{d}},$$

with characteristic length $d = 0.1$. In order to approximate $v(x, \omega)$ by a random field with the familiar structure $v \approx \sum_{i=1}^N v_i \xi_i$, a Karhunen-Loève expansion of this field is performed, and truncated: $N = 5$ eigenfunctions v_i are retained, which are displayed on Figure 21, and the corresponding random variables ξ_i are uncorrelated, centered and normalized.

We minimize the following objective function

$$(5.8) \quad \mathcal{J}(\Omega) = \mathcal{C}(\Omega) + \delta \sqrt{\tilde{\mathcal{V}}(\Omega)}$$

of the unperturbed cost functional $\mathcal{C}(\Omega)$ and the approximate standard deviation $\sqrt{\tilde{\mathcal{V}}(\Omega)}$ defined in (4.23). We cannot replace the unperturbed cost $\mathcal{C}(\Omega)$ by the mean value $\tilde{\mathcal{M}}(\Omega)$ as we did in other previous settings

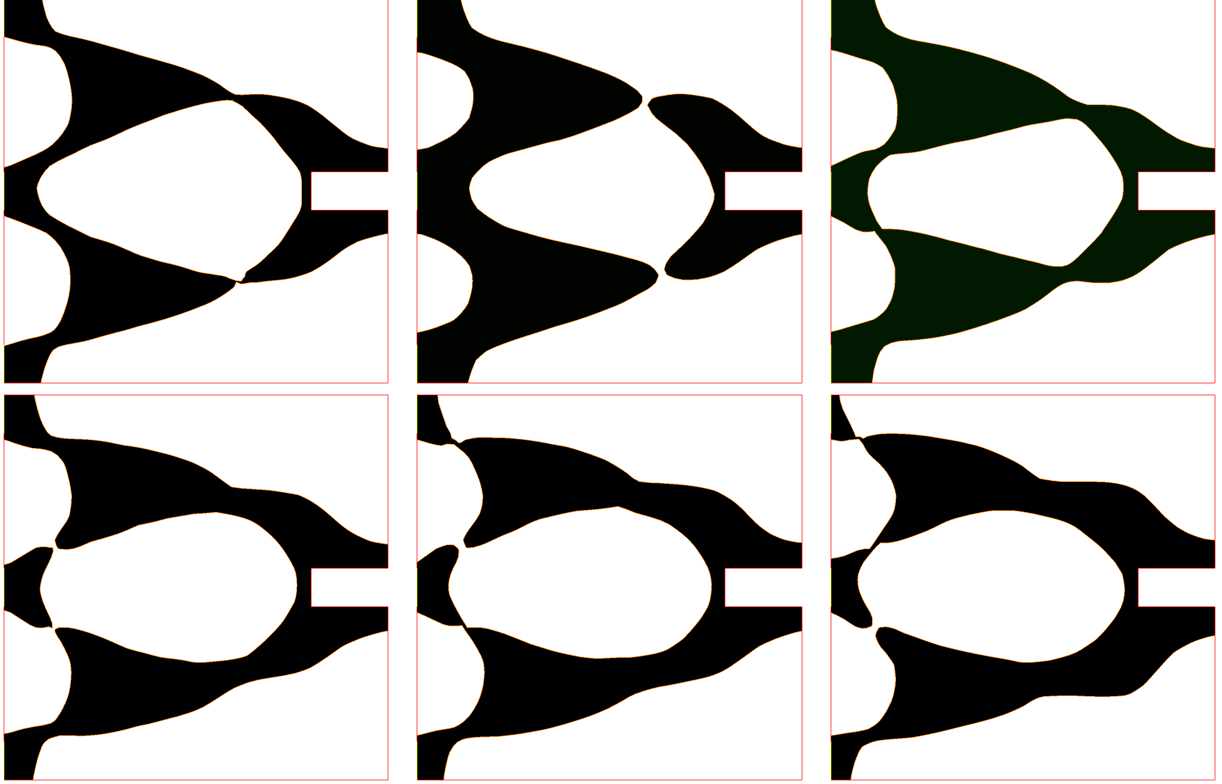


FIGURE 19. *Optimal shapes in the test case of section of Section 5.2.4, associated to values of β (from left to right, top to bottom) 0, 0.5, 1, 1.5, 2, 2.5.*

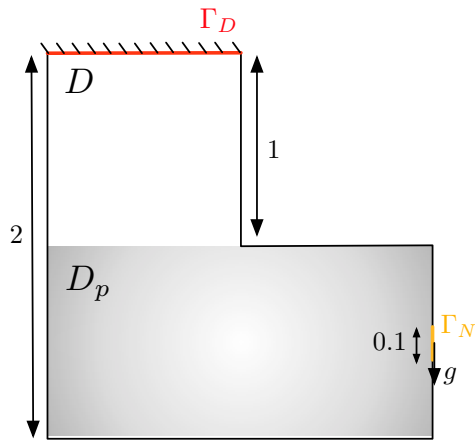


FIGURE 20. *Section 5.2.5: details of the L-shaped beam test-case.*

because, as explained in Section 5.2.5, the approximate mean value involves second-order shape derivatives. Therefore its optimization would require to evaluate a third-order shape derivative, a very unusual object. Indeed, apart from their intrinsic complexity, third-order shape derivatives feature high order geometric quantities (like the shape derivative of the mean curvature) which are quite delicate to compute for a non-parametric geometry. We did not venture in implementing third-order shape derivatives and we content ourselves with our simpler objective function (5.8). A volume constraint $V_T = 0.8$ is imposed on shapes, and

several results are displayed in Figure 22, associated to different values of the parameter δ . See also Figure 23 for the associated convergence histories. We check that, indeed for larger values of δ , the design is more robust to shape variations since it features more bars or thicker bars.

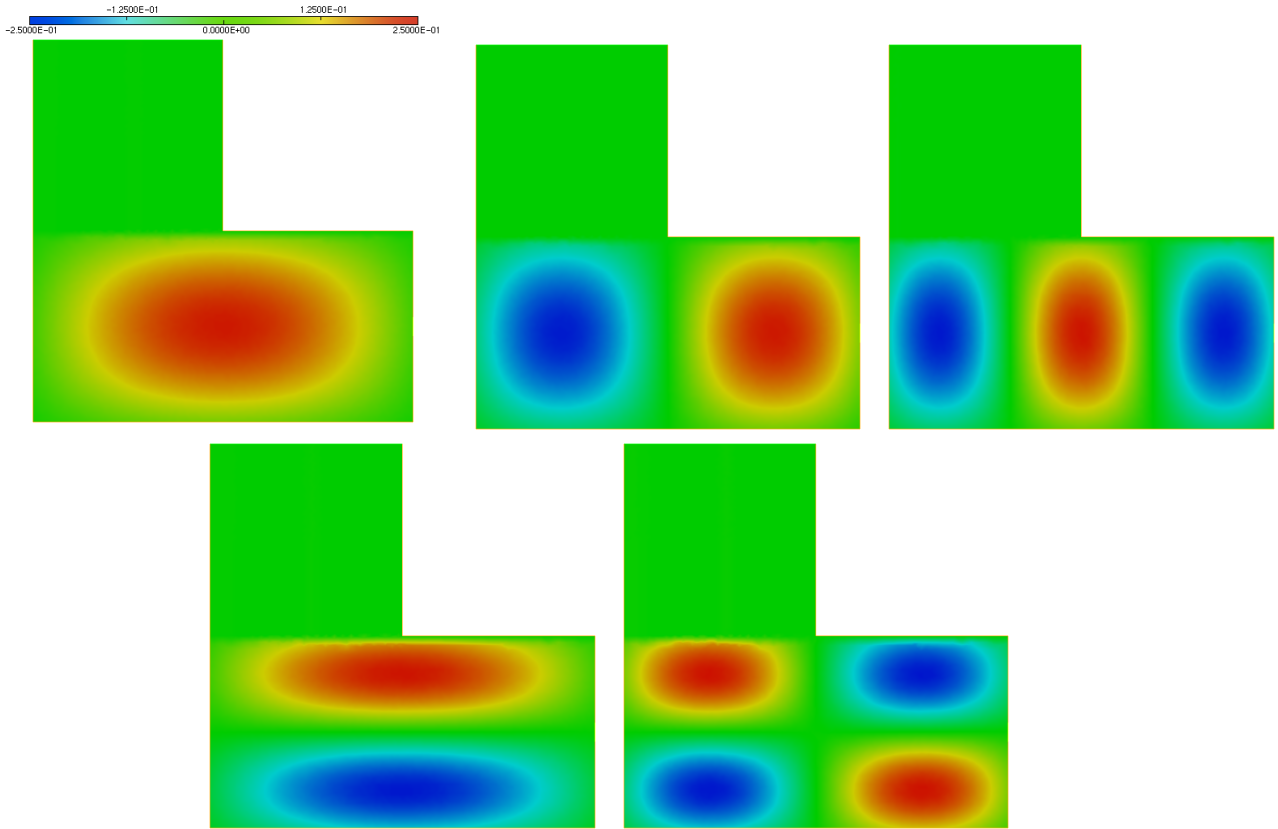


FIGURE 21. Section 5.2.5: plots of the first five eigenfunctions v_i of the correlation (5.7), retained in the approximation of the random perturbation field $v(x, \omega)$. The common scale to the five plots is displayed on the first one.

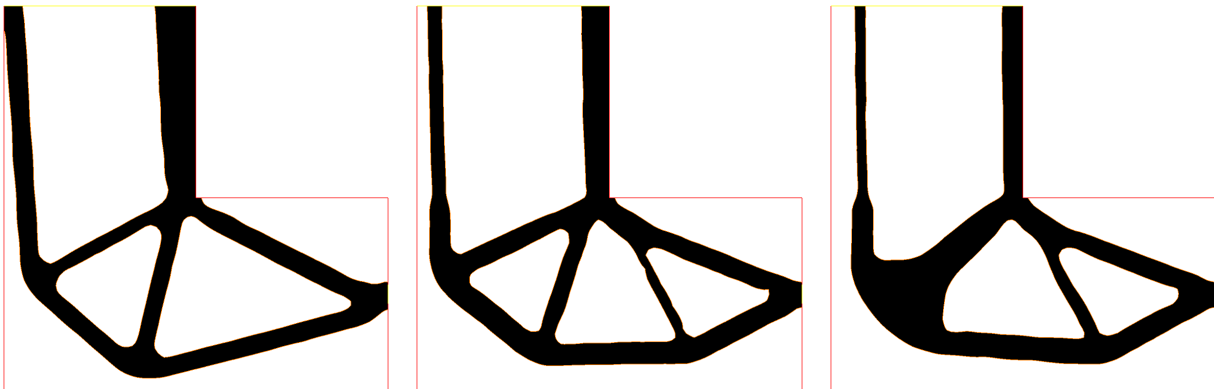


FIGURE 22. Section 5.2.5: optimal shapes in the minimization of the objective function (5.8), where the parameter δ equals (from the left to the right) 0, 0.5, 2.

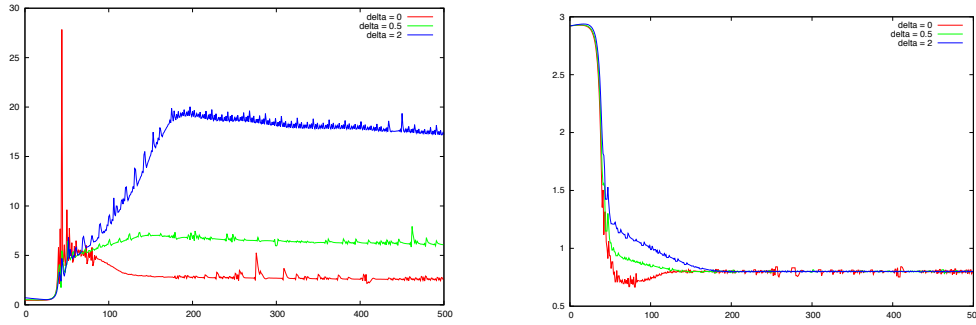


FIGURE 23. Section 5.2.5, L -beam test case: convergence history for the objective function (5.8) (left) and the volume (right), associated to values $\delta = 0, 0.5, 2$.

Acknowledgements. This work has partially been supported by the RODIN project (FUI AAP 13). G. Allaire is a member of the DEFI project at INRIA Saclay Ile-de-France. Part of this work was carried out during a one year visit by C. Dapogny to Rutgers University. He would like to thank the Department of Mathematics and Michael Vogelius for the hospitality extended, and to acknowledge partial support from NSF grant DMS 1211330.

APPENDIX A. ON SECOND-ORDER SHAPE DERIVATIVES

In this appendix, we collect some definitions and results about second-order shape derivatives, and notably the technical details of the proof of Theorem 18. Note that the related terminology is not uniform in the literature; in this article, we follow the definitions in [29, 44].

A.1. Second-order shape derivatives.

Definition 3. For a given $k \geq 1$, a functional $J(\Omega)$ is twice shape differentiable at $\Omega \subset \mathbb{R}^d$ if the underlying mapping $\mathcal{C}^{k,\infty}(\mathbb{R}^d, \mathbb{R}^d) \ni \theta \mapsto J((I + \theta)(\Omega))$ is twice Fréchet-differentiable at $\theta = 0$. The symmetric bilinear form over $\mathcal{C}^{k,\infty}(\mathbb{R}^d, \mathbb{R}^d)$ corresponding to the second variation of this functional is called the shape Hessian of J at Ω , and is denoted as: $(\theta, \xi) \mapsto J''(\Omega)(\theta, \xi)$, so that the following asymptotic expansion holds:

$$J((I + \theta)(\Omega)) = J(\Omega) + J'(\Omega)(\theta) + \frac{1}{2}J''(\Omega)(\theta, \theta) + o(\|\theta\|_{\mathcal{C}^{k,\infty}(\mathbb{R}^d, \mathbb{R}^d)}^2).$$

Remark 20. The notion of shape Hessian contains a subtlety; indeed, contrary to the situation in vector spaces, it does not hold that the shape Hessian $J''(\Omega)(\theta, \xi)$ of J at Ω coincides with $(J')'(\Omega)(\theta)(\xi)$, the derivative at Ω , in the direction ξ , of the first-derivative function $\Omega \mapsto J'(\Omega)(\theta)$, evaluated in the fixed direction θ (the last quantity being actually easier to calculate in practice). According to [44], under mild regularity assumptions on the shape Ω and the vector fields θ, ξ , the relation between these functions is actually

$$(A.1) \quad J''(\Omega)(\theta, \xi) = (J')'(\Omega)(\theta)(\xi) - J'(\Omega)(\nabla\theta \cdot \xi).$$

A.2. Proof of Theorem 18.

First, we need the following technical lemma, which is a slight generalization of Lemma 14 in [2], and whose proof is outlined for the sake of convenience.

Lemma 22.

(1) The functional of the domain $\mathcal{C}(\Omega)$ is shape differentiable at any $\Omega \in \mathcal{U}_{ad}$, and its shape derivative reads:

$$\forall \theta \in \Theta_{ad}, \quad \mathcal{C}'(\Omega)(\theta) = \int_{\Gamma} (j(u_{\Omega}) + Ae(u_{\Omega}) : e(p_{\Omega}) - f \cdot p_{\Omega}) \theta \cdot n \, ds,$$

where p_{Ω} is the adjoint state defined by the system (4.16).

(2) Let $\ell : \mathbb{R}_u^d \times \mathbb{R}_p^d \times \mathbb{R}_e \rightarrow \mathbb{R}$ be a smooth enough function which vanishes in a neighborhood of $\Gamma_D \cup \Gamma_N$, and consider the functional $L(\Omega)$:

$$L(\Omega) = \int_{\Gamma} \ell(u_{\Omega}, p_{\Omega}, Ae(u_{\Omega}) : e(p_{\Omega})) \, ds,$$

where p_{Ω} is defined by system (4.16). Then L is shape differentiable and its shape derivative reads:

$$\forall \theta \in \Theta_{ad}, \quad L'(\Omega)(\theta) = \int_{\Gamma} \mathcal{D}(u_{\Omega}, p_{\Omega}, q_{\Omega}, z_{\Omega}) \theta \cdot n \, ds,$$

with

$$\mathcal{D}(u_{\Omega}, p_{\Omega}, q_{\Omega}, z_{\Omega}) = \left(\frac{\partial}{\partial n} + \kappa \right) \left(\ell(u_{\Omega}, \sigma(u_{\Omega})_{\tau\tau} : e(p_{\Omega})_{\tau\tau}) \right) + Ae(p_{\Omega}) : e(q_{\Omega}) + Ae(u_{\Omega}) : e(z_{\Omega}) - f \cdot z_{\Omega},$$

and the second and third adjoint states $q_{\Omega}, z_{\Omega} \in H_{\Gamma_D}^1(\Omega)^d$ are respectively defined as the unique solutions to:

$$\begin{cases} -\operatorname{div}(Ae(q)) = 0 & \text{in } \Omega \\ q = 0 & \text{on } \Gamma_D \\ Ae(q)n = 0 & \text{on } \Gamma_N \\ Ae(q)n = -\nabla_p \ell(u_{\Omega}, p_{\Omega}, Ae(u_{\Omega}) : e(p_{\Omega})) \\ \quad + \operatorname{div}_{\Gamma} \left(\frac{\partial \ell}{\partial e}(u_{\Omega}, p_{\Omega}, Ae(u_{\Omega}) : e(p_{\Omega})) (\sigma(u_{\Omega}))_{\tau\tau} \right) & \text{on } \Gamma \end{cases},$$

and:

$$(A.2) \quad \begin{cases} -\operatorname{div}(Ae(z)) = -\nabla^2 j(u_{\Omega}) q_{\Omega} & \text{in } \Omega \\ z = 0 & \text{on } \Gamma_D \\ Ae(z)n = 0 & \text{on } \Gamma_N \\ Ae(z)n = -\nabla_u \ell(u_{\Omega}, p_{\Omega}, Ae(u_{\Omega}) : e(p_{\Omega})) \\ \quad + \operatorname{div}_{\Gamma} \left(\frac{\partial \ell}{\partial e}(u_{\Omega}, p_{\Omega}, Ae(u_{\Omega}) : e(p_{\Omega})) (\sigma(p_{\Omega}))_{\tau\tau} \right) & \text{on } \Gamma \end{cases}.$$

(3) Let $\ell : \mathbb{R}_u^d \times \mathbb{R}_p^d \times \mathbb{R}_e$ be a smooth enough function, $\theta \in \Theta_{ad}$ be fixed, and consider the functional $L_{\theta}(\Omega)$ defined by:

$$L_{\theta}(\Omega) = \int_{\Gamma} \ell(u_{\Omega}, p_{\Omega}, Ae(u_{\Omega}) : e(p_{\Omega})) \theta \cdot n_{\Omega} \, ds,$$

where $n = n_{\Omega}$ is the exterior unit normal of Ω , u_{Ω} and p_{Ω} are defined by (4.1) and (4.16). Then $L_{\theta}(\Omega)$ is shape differentiable and:

$$\forall \xi \in \Theta_{ad}, \quad L'_{\theta}(\Omega)(\xi) = \int_{\Gamma} \mathcal{D}_{\theta}(u_{\Omega}, p_{\Omega}, q_{\Omega}(\theta), z_{\Omega}(\theta))(\xi) \, ds,$$

where the integrand factor reads:

$$\begin{aligned} \mathcal{D}_{\theta}(u_{\Omega}, p_{\Omega}, q_{\Omega}(\theta), z_{\Omega}(\theta))(\xi) &= \frac{\partial}{\partial n} (\ell(u_{\Omega}, p_{\Omega}, Ae(u_{\Omega}) : e(p_{\Omega})) \theta \cdot n) (\xi \cdot n) - \ell(u_{\Omega}, p_{\Omega}, Ae(u_{\Omega}) : e(p_{\Omega})) [\theta]_{\Gamma} \cdot \nabla_{\Gamma}(\xi \cdot n) \\ &\quad + \kappa \ell(u_{\Omega}, p_{\Omega}, Ae(u_{\Omega}) : e(p_{\Omega})) (\theta \cdot n) (\xi \cdot n) + Ae(u_{\Omega}) : e(z_{\Omega}(\theta)) (\xi \cdot n) \\ &\quad + Ae(p_{\Omega}) : e(q_{\Omega}(\theta)) (\xi \cdot n) - f \cdot z_{\Omega}(\theta) (\xi \cdot n) + \nabla j(u_{\Omega}) \cdot q_{\Omega}(\theta) (\xi \cdot n), \end{aligned}$$

and the adjoint states $q_{\Omega}(\theta)$ and $z_{\Omega}(\theta)$ are respectively defined by the systems:

$$(A.3) \quad \begin{cases} -\operatorname{div}(Ae(q)) = 0 & \text{in } \Omega \\ q = 0 & \text{on } \Gamma_D \\ Ae(q)n = 0 & \text{on } \Gamma_N \\ Ae(q)n = -\nabla_p \ell(u_{\Omega}, p_{\Omega}, (Ae(p_{\Omega}))_{\tau\tau} : e(u)_{\tau\tau}) (\theta \cdot n) \\ \quad + \operatorname{div}_{\Gamma} \left(\frac{\partial \mathcal{L}}{\partial e}(u_{\Omega}, p_{\Omega}, (Ae(p_{\Omega}))_{\tau\tau} : e(u_{\Omega})_{\tau\tau}) (\theta \cdot n) (Ae(u_{\Omega}))_{\tau\tau} \right) & \text{on } \Gamma \end{cases}.$$

$$(A.4) \quad \begin{cases} -\operatorname{div}(Ae(z)) &= -\nabla^2 j(u_\Omega) q_\Omega(\theta) && \text{in } \Omega \\ z &= 0 && \text{on } \Gamma_D \\ Ae(z)n &= 0 && \text{on } \Gamma_N \\ Ae(z)n &= \begin{array}{l} -\nabla_u \ell(u_\Omega, p_\Omega, (Ae(p_\Omega))_{\tau\tau} : e(u)_{\tau\tau}) (\theta \cdot n) \\ + \operatorname{div}_\Gamma \left(\frac{\partial \mathcal{L}}{\partial e}(u_\Omega, p_\Omega, (Ae(p_\Omega))_{\tau\tau} : e(u_\Omega)_{\tau\tau}) (\theta \cdot n) (Ae(p_\Omega))_{\tau\tau} \right) \end{array} && \text{on } \Gamma \end{cases} .$$

Proof. (1): It is a very classical result in shape optimization; see for instance [6], Thm. 7.

(2): See [2], Lemma 4.2 (or the following point for a similar proof in a slightly more difficult context).

(3): The proof is essentially that of Lemma 14 in [2], and we briefly recall the argument for the sake of convenience. Again, the shape differentiability of L_θ at $\Omega \in \mathcal{U}_{ad}$ stems from an avatar of Lemma 1 in the present context. In order to calculate the associated shape derivative, we rely on C ea's method [12]. Consider the Lagrangian function $\mathcal{L} : \mathcal{U}_{ad} \times (H^2(\mathbb{R}^d)^d \cap H_{\Gamma_D}^1(\mathbb{R}^d)^d)^4 \rightarrow \mathbb{R}$, defined by:

$$\begin{aligned} \mathcal{L}(\Omega, u, p, q, z) &= \int_\Gamma \ell(u, p, Ae(u) : e(p)) \theta \cdot n \, ds + \int_\Omega Ae(u) : e(z) \, dx - \int_\Omega f \cdot z \, dx - \int_{\Gamma_N} g \cdot z \, ds \\ &\quad + \int_\Omega Ae(p) : e(q) \, dx + \int_\Omega \nabla j(u) \cdot q \, dx, \end{aligned}$$

which incorporates as constraints both variational formulations for u_Ω and p_Ω . Notice also that the first integral in the right-hand side of the previous formula makes sense because of the choice of $H^2(\mathbb{R}^d) \cap H_{\Gamma_D}^1(\mathbb{R}^d)$ as the definition space for u, p (thus q, z). For a given shape $\Omega \in \mathcal{U}_{ad}$, we look for the critical points $(u, p, q, z) \in (H^2(\mathbb{R}^d) \cap H_{\Gamma_D}^1(\mathbb{R}^d))^4$ of $\mathcal{L}(\Omega, \cdot, \cdot, \cdot, \cdot)$;

- Canceling the partial derivative of \mathcal{L} with respect to z leads to the fact that:

$$\forall \widehat{z} \in H^2(\mathbb{R}^d)^d \cap H_{\Gamma_D}^1(\mathbb{R}^d)^d, \quad \int_\Omega Ae(u) : e(\widehat{z}) \, dx - \int_\Omega f \cdot \widehat{z} \, dx - \int_{\Gamma_N} g \cdot \widehat{z} \, ds;$$

since by density of $H^2(\mathbb{R}^d)$ in $H^1(\mathbb{R}^d)$, the above formula actually holds for any $\widehat{z} \in H_{\Gamma_D}^1(\mathbb{R}^d)^d$, u turns out to be nothing else than u_Ω , the unique solution to the system (4.1).

- Similarly, canceling the partial derivative of \mathcal{L} with respect to q yields:

$$\forall \widehat{q} \in H^2(\mathbb{R}^d) \cap H_{\Gamma_D}^1(\mathbb{R}^d), \quad \int_\Omega Ae(p) : e(\widehat{q}) \, dx + \int_\Omega \nabla j(u) \cdot \widehat{q} \, dx;$$

since $u = u_\Omega$, the same argument as above allows to conclude that $p = p_\Omega$, the solution to (4.16).

- The study of the derivative of \mathcal{L} with respect to u involves a slightly more subtle argument; indeed, at this point, we know that the critical point (u, p, q, z) of interest is such that $u = u_\Omega$ and $p = p_\Omega$. Hence, $Ae(u)n = Ae(p)n = 0$ on the free boundary Γ of $\partial\Omega$, outside which $\theta = 0$. Hence, for any $\widehat{u} \in H^2(\mathbb{R}^d)^d \cap H_{\Gamma_D}^1(\mathbb{R}^d)^d$, one has:

$$Ae(\widehat{u}) : e(p) = Ae(p) : e(\widehat{u}) = (Ae(p))_{\tau\tau} : e(\widehat{u})_{\tau\tau} \text{ a.e. on } \Gamma.$$

Consequently, the partial derivative $\frac{\partial \mathcal{L}}{\partial u}$ at (u, p, q, z) reads, for any $\widehat{u} \in H^2(\mathbb{R}^d)^d \cap H_{\Gamma_D}^1(\mathbb{R}^d)^d$:

$$\begin{aligned} \frac{\partial \mathcal{L}}{\partial u}(\Omega, u, p, q, z)(\widehat{u}) &= \int_\Omega Ae(z) : e(\widehat{u}) \, dx + \int_\Gamma \nabla_u \ell(u, p, (Ae(p))_{\tau\tau} : e(u)_{\tau\tau}) \cdot \widehat{u} (\theta \cdot n) \, ds \\ &\quad + \int_\Gamma \frac{\partial \mathcal{L}}{\partial e}(u, p, (Ae(p))_{\tau\tau} : e(u)_{\tau\tau}) (Ae(p))_{\tau\tau} : e(\widehat{u})_{\tau\tau} (\theta \cdot n) \, ds \\ &= \int_\Omega Ae(z) : e(\widehat{u}) \, dx + \int_\Gamma \nabla_u \ell(u, p, (Ae(p))_{\tau\tau} : e(u)_{\tau\tau}) \cdot \widehat{u} (\theta \cdot n) \, ds \\ &\quad - \int_\Gamma \operatorname{div}_\Gamma \left(\frac{\partial \mathcal{L}}{\partial e}(u, p, (Ae(p))_{\tau\tau} : e(u)_{\tau\tau}) (\theta \cdot n) (Ae(p))_{\tau\tau} \right) \cdot \widehat{u} \, ds, \end{aligned}$$

where an integration by parts formula on Co-dimension 1 submanifolds was used from the first line to the second one (see [22], Prop. 5.3 and 5.4). Under the last form, the equation $\frac{\partial \mathcal{L}}{\partial u}(u, p, q, z)(\widehat{u}) = 0$, which holds for $\widehat{u} \in H^2(\mathbb{R}^d)^d \cap H_{\Gamma_D}^1(\mathbb{R}^d)^d$ extends, by density, to $\widehat{u} \in H_{\Gamma_D}^1(\mathbb{R}^d)^d$, and leads to the fact that $z = z_\Omega(\theta)$, defined by (A.4).

- Using the same argument for the partial derivative $\frac{\partial \mathcal{L}}{\partial p}$, evaluated at (u, p, q, z) , we obtain that $q = q_\Omega(\theta)$, defined by (A.3).

Eventually, we observe that, for any $\widehat{q}, \widehat{z} \in H^2(\mathbb{R}^d)^d \cap H_{\Gamma_D}^1(\mathbb{R}^d)^d$, the following identity holds:

$$L_\theta(\Omega) = \mathcal{L}(\Omega, u_\Omega, p_\Omega, \widehat{q}, \widehat{z}).$$

Differentiating this expression with respect to Ω in an arbitrary direction $\xi \in \Theta_{ad}$, and evaluating at $\widehat{q} = q_\Omega(\theta)$ and $\widehat{z} = z_\Omega(\theta)$ yield:

$$L'_\theta(\Omega)(\xi) = \frac{\partial \mathcal{L}}{\partial \Omega}(\Omega, u_\Omega, p_\Omega, q_\Omega(\theta), z_\Omega(\theta))(\xi).$$

The result now stems from a straightforward, yet tedious calculation, involving the shape derivative of the normal vector (see e.g. [35] on this issue). \square

Proof of Theorem 18. The expression of the shape derivative of $\mathcal{C}(\Omega)$ is just Lemma 22, (1). As for the shape Hessian, Lemma 22 (3) yields, for any $\theta, \xi \in \Theta_{ad}$:

$$(\mathcal{C}')'(\Omega)(\theta)(\xi) = \int_{\Gamma} \mathcal{D}_\theta(u_\Omega, p_\Omega, q_\Omega(\theta \cdot n), z_\Omega(\theta \cdot n))(\xi \cdot n) ds,$$

where the integrand factor is defined as:

$$\begin{aligned} \mathcal{D}_\theta(u_\Omega, p_\Omega, q_\Omega(\theta \cdot n), z_\Omega(\theta \cdot n))(\xi \cdot n) &= \left(\frac{\partial}{\partial n} + \kappa \right) ((j(u_\Omega) + Ae(u_\Omega) : e(p_\Omega) - f \cdot p_\Omega) \theta \cdot n) (\xi \cdot n) \\ &\quad - (j(u_\Omega) + Ae(u_\Omega) : e(p_\Omega) - f \cdot p_\Omega) \theta_\Gamma \cdot \nabla_\Gamma(\xi \cdot n) + Ae(u_\Omega) : e(z_\Omega(\theta \cdot n)) (\xi \cdot n) \\ &\quad + Ae(p_\Omega) : e(q_\Omega(\theta \cdot n))(\xi \cdot n) - f \cdot z_\Omega(\theta \cdot n) (\xi \cdot n) + \nabla j(u_\Omega) \cdot q_\Omega(\theta \cdot n) (\xi \cdot n), \end{aligned}$$

and the adjoint states q_Ω and z_Ω are given by (4.18) and (4.19). The above expression for $(\mathcal{C}')'(\Omega)(\theta)(\xi)$ then rewrites:

$$\begin{aligned} (\mathcal{C}')'(\Omega)(\theta)(\xi) &= \int_{\Gamma} \left(\frac{\partial}{\partial n} + \kappa \right) (j(u_\Omega) + Ae(u_\Omega) : e(p_\Omega) \theta \cdot n) (\xi \cdot n) ds \\ &\quad - \int_{\Gamma} (j(u_\Omega) + Ae(u_\Omega) : e(p_\Omega) - f \cdot p_\Omega) \theta_\Gamma \cdot \nabla_\Gamma(\xi \cdot n) ds - \int_{\Omega} \nabla^2 j(u_\Omega)(q_\Omega(\theta \cdot n), q_\Omega(\xi \cdot n)) dx \\ &\quad - \int_{\Omega} (Ae(q_\Omega(\theta \cdot n)) : e(z_\Omega(\xi \cdot n)) + Ae(q_\Omega(\xi \cdot n)) : e(z_\Omega(\theta \cdot n))) dx. \end{aligned}$$

Now, using the relation (A.1) between $(\mathcal{C}')'(\Omega)(\theta)(\xi)$ and $\mathcal{C}''(\Omega)(\theta)(\xi)$ and calculating:

$$\begin{aligned} \frac{\partial}{\partial n}(\theta \cdot n) \xi \cdot n - \theta_\Gamma \cdot \nabla_\Gamma(\xi \cdot n) - (\nabla \theta \xi) \cdot n &= (\nabla \theta^T n) \cdot n (\xi \cdot n) - \theta_\Gamma \cdot \nabla_\Gamma(\xi \cdot n) - (\nabla \theta \xi) \cdot n \\ &= (\nabla \theta^T n) \cdot ((\xi \cdot n)n - \xi) - \theta_\Gamma \cdot \nabla_\Gamma(\xi \cdot n) \quad , \\ &= -\xi_\Gamma \cdot (\nabla \theta^T n) - \theta_\Gamma \cdot \nabla_\Gamma(\xi \cdot n) \end{aligned}$$

and

$$\begin{aligned} \xi_\Gamma \cdot \nabla_\Gamma(\theta \cdot n) &= \xi_\Gamma \cdot (\nabla(\theta \cdot n) - (\nabla(\theta \cdot n) \cdot n)n) \\ &= \xi_\Gamma \cdot (\nabla \theta^T n + \nabla n^T \theta - ((\nabla \theta^T n) \cdot n)n) \quad , \\ &= \xi_\Gamma \cdot (\nabla \theta^T n) + (\nabla n^T \theta)_\Gamma \cdot \xi_\Gamma \end{aligned}$$

we end up with the desired formula. \square

REFERENCES

- [1] G. ALLAIRE, *Conception optimale de structures, Mathématiques et Applications 58, Springer, Heidelberg* (2006).
- [2] G. ALLAIRE AND C. DAPOGNY, *A linearized approach to worst-case design in parametric and geometric shape optimization*, M3AS Vol. 24, No. 11 (2014) 2199-2257.
- [3] G. ALLAIRE AND C. DAPOGNY, *A deterministic approximation method in shape optimization under random uncertainties: supplementary material*, submitted, (2015).
- [4] G. ALLAIRE AND F. JOUVE, *A level-set method for vibration and multiple loads structural optimization*, Comput. Meths. Appl. Mech. Engrg., 194, (2005), pp. 3269–3290.
- [5] G. ALLAIRE, F. JOUVE, *Minimum stress optimal design with the level set method*, Engineering Analysis with Boundary Elements **32**, pp. 909–918 (2008).
- [6] G. ALLAIRE AND F. JOUVE AND A.M. TOADER, *Structural optimization using shape sensitivity analysis and a level-set method*, J. Comput. Phys., 194 (2004) pp. 363–393.
- [7] S. AMSTUTZ AND M. CILIGOT-TRAVAIN, *A notion of compliance robustness in topology optimization*, accepted for publication in ESAIM: Control, Optimization and Calculus of Variations, (2014).
- [8] I. BABUŠKA, F. NOBILE AND R. TEMPONE, *A stochastic collocation method for elliptic partial differential equations with random input data*, SIAM. J. Numer. Anal., Vol 45, No. 3, (2007), pp. 1005–1034.
- [9] M. BENDSOE, O. SIGMUND, *Topology Optimization. Theory, Methods, and Applications*, Springer Verlag, New York (2003).

- [10] W. BETZ, I. PAPAIOANNOU AND D. STRAUB , *Numerical methods for the discretization of random fields by means of the KarhunenLoève expansion*, Comput. Meths. Appl. Mech. Engrg., 271, (2014), pp. 109–129.
- [11] C. BUI, C. DAPOGNY AND P. FREY, *An accurate anisotropic adaptation method for solving the level set advection equation*, Int. J. Numer. Methods in Fluids, Volume 70, Issue 7, pp. 899–922 (2012).
- [12] J. CÉA , *Conception optimale ou identification de formes, calcul rapide de la dérivée directionnelle de la fonction coût*, Math. Model. Num. 20, 3 (1986), pp. 371–420.
- [13] S. CHEN, W. CHEN AND S. LEE , *Level set based robust shape and topology optimization under random field uncertainties*, Struct Multidisc Optim, 44, 1 (2010), pp. 507–524.
- [14] S. CHEN AND W. CHEN , *A new level-set based approach to shape and topology optimization under geometric uncertainty*, Struct Multidisc Optim, 44, 1 (2011), pp. 1–18.
- [15] A. CHERKAEV AND E. CHERKAEVA , *Principal Compliance and Robust Optimal Design*, Journal of Elasticity, 72 (2003), pp.71–98.
- [16] A. CHKIFA, A. COHEN AND C. SCHWAB, *Breaking the curse of dimensionality in sparse polynomial approximation of parametric PDEs*, Journal de Mathématiques Pures et Appliquées, 103, 2 (2015), pp. 400–428.
- [17] S.-K. CHOI, R. GRANDHI, AND R. A. CANFIELD , *Reliability-based Structural Design*, Springer, (2007).
- [18] P.G. CIARLET, *Mathematical Elasticity, vol I: Three Dimensional Elasticity*, North Holland Publishing Company (1988).
- [19] S. CONTI, H. HELD, M. PACH, M. RUMPF, AND R. SCHULTZ , *Shape optimization under uncertainty - a stochastic programming approach*, SIAM J. Optim, 19, 4 (2009), pp. 1610–1632.
- [20] M. DAMBRINE, H. HARBRECHT AND B. PUIG , *Computing quantities of interest for random domains with second order shape sensitivity analysis*, Institute of Mathematics, University of Basel, Rheinsprung 21, CH - 4051 Basel Switzerland, Preprint No 2014-13 (2014), 18 pp.
- [21] M. DAMBRINE, C. DAPOGNY AND H. HARBRECHT, *Shape optimization for quadratic functionals and states with random right-hand sides*, submitted (2015).
- [22] C. DAPOGNY, *Shape optimization, level set methods on unstructured meshes and mesh evolution*, PhD Thesis of University Pierre et Marie Curie (2013), available at: <http://tel.archives-ouvertes.fr/tel-00916224>.
- [23] C. DAPOGNY AND P. FREY, *Computation of the signed distance function to a discrete contour on adapted triangulation*, Calcolo, Volume 49, Issue 3, pp. 193-219 (2012).
- [24] M.C. DELFOUR AND J.-P. ZOLESIO, *Shapes and Geometries: Metrics, Analysis, Differential Calculus, and Optimization*, SIAM, Philadelphia 2nd ed. (2011).
- [25] P.D. DUNNING AND H.A. KIM, *Robust Topology Optimization: Minimization of Expected and Variance of Compliance*, AIAA Journal, Vol. 51, No. 11 (2013), pp. 2656–2664.
- [26] F. DE GOURNAY, G. ALLAIRE AND F. JOUVE , *Shape and topology optimization of the robust compliance via the level set method*, ESAIM: Control, Optimization and Calculus of Variations, 14, (2008), pp. 43–70.
- [27] X. GUO, W. BAI AND W. ZHANG , *Confidence extremal structural response analysis of truss structures under static load uncertainty via SDP relaxation*, Computers and Structures, 87, (2009) pp. 246–253.
- [28] F. HECHT, *New development in FreeFem++*, J. Numer. Math. 20 (2012), no. 3-4, pp. 251–265.
- [29] A. HENROT AND M. PIERRE, *Variation et optimisation de formes, une analyse géométrique*, Mathématiques et Applications 48, Springer, Heidelberg, (2005).
- [30] B. S. LAZAROV, M. SCHEVENELS AND O. SIGMUND, *Topology optimization with geometric uncertainties by perturbation techniques*, Int. J. Numer. Meth. Engng., 90 (2012), pp. 1321–1336.
- [31] O. P. LE MAITRE AND O. M. KNIO, *Spectral Methods for Uncertainty Quantification, with Applications to Computational Fluid Dynamics*, Springer, (2010).
- [32] M. LOEVE, *Probability Theory*, Vol. II, Graduate texts in mathematics, 4th ed., Springer-Verlag, (1977).
- [33] J. MARTÍNEZ-FRUTOS, M. KESSLER AND F. PERIAGO, *Robust optimal shape design for an elliptic PDE with uncertainty in its input data*, submitted (2015).
- [34] K. MAUTE, *Topology Optimization under uncertainty*, in Topology Optimization in Structural and Continuum Mechanics, CISM International Centre for Mechanical Sciences Volume 549, (2014), pp. 457–471.
- [35] F. MURAT AND J. SIMON, *Sur le contrôle par un domaine géométrique*, Technical Report RR-76015, Laboratoire d'Analyse Numérique (1976).
- [36] J. NOCEDAL, S.J. WRIGHT, *Numerical optimization*. Springer Science+ Business Media (2006).
- [37] S.J. OSHER AND J.A. SETHIAN, *Fronts propagating with curvature-dependent speed : Algorithms based on Hamilton-Jacobi formulations*, J. Comput. Phys., 79 (1988), pp. 12–49.
- [38] O. PIRONNEAU, F. HECHT, A. LE HYARIC, *FreeFem++ version 2.15-1*, <http://www.freefem.org/ff++/>.
- [39] G. ROZVANY, *Structural design via optimality criteria*, Kluwer Academic Publishers, Dordrecht (1989).
- [40] C. SCHILLINGS, S. SCHMIDT AND V. SCHULZ, *Efficient shape optimization for certain and uncertain aerodynamic design*, Computers & Fluids, Vol. 46, Issue 1, (2011), pp. 78–87.
- [41] V. SCHULZ AND C. SCHILLINGS, *Optimal Aerodynamic Design under Uncertainty*, Management and Minimisation of Uncertainties and Errors in Numerical Aerodynamics, ed. B. Eisefeld et al (Berlin: Springer-Verlag), (2013), pp. 297–338.
- [42] C. SCHWAB AND R. TODOR, *Karhunen-Loève approximation of random fields by generalized fast multipole methods*, J. Comput. Phys., 217 (2006) pp. 100–122.
- [43] O. SIGMUND, *On the design of compliant mechanisms using topology optimization*, Mech. Struct. Mach. **25**, pp. 493–524 (1997).

- [44] J. SIMON, *Second variation for domain optimization problems*, In Control and estimation of distributed parameter systems, F. Kappel, K. Kunish et W. Schappacher éd., International Series of Numerical Mathematics, no 91, Birkhäuser (1989), pp. 361–378.
- [45] J. SOKOŁOWSKI AND J.-P. ZOLESIO, *Introduction to shape optimization: shape sensitivity analysis*, Springer Series in Computational Mathematics, Vol. 10, Springer, Berlin, (1992).
- [46] M. Y. WANG, X. WANG AND D. GUO, *A level set method for structural topology optimization*, Comput. Methods. Appl. Mech. Engrg, 192, (2003), pp. 227-246.